A Hydrogeochemical Investigation of Metalliferous Coal Pile Runoff and Its Interactions with Soil and Groundwater

by

Michael Alan Anderson

Dissertation submitted to the Faculty of the
Virginia Polytechnic Institute and State University
in partial fulfillment of the requirements for the degree of
Doctor of Philosophy
in
Crop and Soil Environmental Sciences

APPROVED:

Lucian W. Zelazny, Co-chair

Paul M. Bertsch, Co-chair

David C. Martens

W. Lee Daniels

John G. Dillard

May, 1990

Blacksburg, Virginia

A Hydrogeochemical Investigation of Metalliferous Coal Pile Runoff and Its Interactions with Soil and Groundwater

by

Michael Alan Anderson

Lucian W. Zelazny, Co-chair

Paul M. Bertsch, Co-chair

Crop and Soil Environmental Sciences

(ABSTRACT)

Highly acidic and metal-rich runoff from coal storage facilities can have a dramatic impact on local surface and ground water quality. In order to identify important reactions governing metal transport within subsurface environments subject to infiltration of coal pile runoff, samples of uncontaminated subsoil and aquifer materials adjacent to the D-Area coal stockpile runoff containment basin at the Department of Energy's Savannah River Site were collected and subjected to leaching with the acidic, metalliferous coal pile runoff. Columns were packed to bulk densities of 1.5 Mg m^{-3} and subjected to steady, saturated flows of 0.2 and 1.3 cm h^{-1}. Effluent was collected and multicomponent transport through the subsoil and aquifer materials evaluated. Observed transport was then related to soil chemical and mineralogical properties. Mass balance calculations, a sequential dissolution scheme in which column leaching was terminated and elements partitioned to aqueous, *M* NH_4Cl, and ammonium oxalate in the dark (Ox)-extractable phases, and mineralogical and surface chemical analyses were used to identify important chemical processes and mineralogical alterations.

Sulfate mobility was governed principally by ion exchange. Initial breakthrough of most elements was coincident with sulfate breakthrough and a result of the neces-

sary condition of electroneutrality within solution. Ion exchange was also important to the mobility of the alkaline earth and a number of the divalent first row transition metals, whereas precipitation-dissolution reactions regulated Fe(III) mobility. Coprecipitation with Fe apparently controlled Cr and Cu mobility. Prolonged leaching also resulted in a net export of Al and Si from the columns, gibbsite formation, destabilization of interstratified mica-vermiculite, increased 10 Å material, and apparent destabilization of crystalline Fe phases to an Ox-extractable phase. Reduction in Darcy velocity from 1.3 to 0.2 cm h^{-1} had little influence on observed transport of components subject to ion exchange, though did influence components regulated by precipitation-dissolution and/or specific adsorption reactions. Solubility relations based upon speciation of column effluent with MINTEQA2 were, in general, of little utility in describing element fluxes.

Acknowledgements

I would like to begin by thanking Dr. Paul Bertsch, Co-chairman, and the individual whose example has made this a goal and whose support has made it possible. I would also like to thank Dr. Lucian Zelazny, Co-chairman, for all his efforts and contributions. Gratitude is also due Drs. Lee Daniels, David Martens, and John Dillard for their unique contributions as members of my committee.

I would also like to thank the friends and acquaintances I have made while here at Virginia Tech, including Steve Feldman, Terence Johnson, Barry Stewart, David Ditsch, Paul Gassman, John Chermak, David Parker, and others.

Table of Contents

List of Illustrations

List of Tables

Chapter I

Introduction

Acid mine drainage has been recognized for some time as a serious threat to surface waters, capable of near sterilization of impacted waters. More recently, concerns have been expressed as to the potential impacts of acid mine drainage, and coal mining operations in general, on groundwater quality (NRC, 1981), and also the related influences that leachate and runoff from coal storage facilities may have on local ground and surface water quality (Davis and Boegly, 1981).

To assess the potential impacts of coal mining on groundwater resources, the U.S. Department of the Interior, Bureau of Mines supported a National Research Council Commission created to evaluate the relationships between coal mining and groundwater resources. The Committee on Groundwater Resources in Relation to Coal Mining was thus formed (NRC, 1981). In their report, the Committes's recommendations included further research on: water movement in the unsaturated zone of both undisturbed and relaimed lands; geochemical interactions between groundwater

and spoil material; and the potential of natural hydrogeologic processes in ameliorating adverse effects of coal mining operations. It was also noted that there exists a serious lack of adequately trained scientists evaluating the effects of coal mining and other energy development activites on groundwater and water quality (NRC,1981).

An issue which the Committe did not directly address but is intimately related with coal mining operations is the storage of coal by utilities and industries dependent upon the fossil fuel. Just as in the case of acid mine drainage, coal pile leachate can be highly acidic, and heavily laden with toxic metals and organics (Nichols, 1974). As a result, the same concerns regarding acid mine drainage can be expressed for coal stockpiles, with the further consideration that coal stockpiles are relatively abundant, not restricted to areas associated with mining operations, and often uncontrolled.

While the general chemistry of acid mine drainage and coal pile runoff is well established, natural geochemical attenuation processes remain incompletely understood. Alkaline neutralization reactions have been shown to effectively reduce the pernicious character of the metalliferous acid leachates (Wangen and Williams, 1982) and are frequently employed as a treatment of acid mine drainage prior to release to receiving streams. Similarly, Wangen and Jones (1984) demonstrated that carbonatic soils were highly effective at reducing acidity and retaining a number of elements when acidic leachate generated from coal minerals wastes was percolated through soil samples. A naturally acidic, non-carbonatic soil afforded relatively little attenuation, however (Wangen and Jones, 1984). Inasmuch as a significant portion of the U.S. coal reserves and coal stockpiles reside within moderately to highly weathered geologic regions with little carbonate alkalinity, direct neutralization of acid mine

drainage via carbonate dissolution may be of secondary importance relative to more complex and heterogeneous adsorption, dissolution and precipitation reactions.

The objectives of this research, then, were to edify current understanding of the environmental impacts of the energy industry by evaluating the hydrogeochemical interactions of acidic runoff from coal stockpiles with soil and groundwater, focusing on attenuation processes, differential transport of heavy metals through acid leachate-impacted non-carbonaceous soils, and the mineralogical alterations and precipitation reactions resulting from contact of acidic leachates with soils.

References

Davis, E. C., and W. J. Boegly. 1981. A review of water quality issues associated with coal storage. J. Environ. Qual. **10:** 127-133.

National Research Council, 1981. Coal mining and groundwater resources in the United States. National Academy Press, Washington, DC. 197 pp.

Nichols, C. R. 1974. Development document for the proposed effluent limitations, guidelines, and new source performance standards for the steam-electric power generating point source category. U.S. Environmental Protection Agency, Washington, DC. EPA-440/1-73-029. 132 pp.

Wangen, L. E., and J. M. Williams. 1982. Control by alkaline neutralization of trace elements in acidic coal cleaning waste leachates. J. Water Pollut. Contr. Fed. **54:** 1302-1310.

Wangen, L. E., and M. M. Jones. 1984. The attenuation of chemical elements in acidic leachates from coal mineral wastes by soils. Environ. Geol. Water. Sci. **6:** 161-170.

Chapter II

Literature Review

Sulfidic ores, predominated by pyrite (FeS_2), undergo oxidation when exposed to an atmospere with oxygen present, generating sulfuric acid and ferrous iron (Fe^{2+}) (Nordstrom et al., 1979; Nordstrom, 1982a; Vuorinen et al., 1983). Ferrous iron is then oxidized to the ferric form (Fe^{3+}), which, in turn, can be reduced by pyrite yielding additional Fe^{2+} and acidity; it is this oxidation to Fe^{3+} that is considered to be the rate-determining step in acid mine drainage formation (Singer and Stumm, 1970). The inorganic oxidation of Fe^{2+} to Fe^{3+} under acidic conditions is slow (e.g., $t_{1/2}$ at pH 3 is $\simeq$1000 days) (Singer and Stumm, 1970), but is accelerated 5 to 6 orders of magnitude over the inorganic rate through the microbial action of *Thiobacillus ferroxidans* (Nordstrom, 1982a; Singer and Stumm, 1970). Mining operations generate tremendous quantities of spoil materials; it has been estimated that mineral wastes from coal mining operations are generated at a rate near 100 million tons a year, with more that 3 billion tons produced by 1984 (Wangen and Jones, 1984). Such spoil materials are often high in pyritic minerals, which are in contact with atmosperic oxygen and

also subject to intrusion by water. The resultant leachates are often highly acidic, and heavily laden with dissolved Fe, aluminum (Al), manganese (Mn), and a host of associated heavy metals.

In addition to spoil production, coal mining operations also generate metalliferous acidic leachates and runoff from the coal stockpiled at utilities and industries, thus creating additional water quality concerns (Davis and Boegly, 1981). The National Coal Association estimated that there were 128 million metric tons of coal in storage in 1978, with that amount predicted to rise to 680 million metric tons by the the year 2000 (Davis and Boegly, 1981). Swift (1985) summarized the chemical composition of coal pile leachates from a number of studies and found a very high degree of similarity with acid mine drainage.

The interaction of these metalliferous acid leachates with more alkaline, natural soils and waters results in neutralization or dilution of acidity, resulting in precipitation of Fe and Al hydroxides, oxyhydroxides, and/or basic sulfates (Theobald et al., 1963; Brady et al., 1986; Nordstrom et al., 1979; Nordstrom, 1982a; Nordstrom, 1982b; Chapman et al., 1983; Wangen and Jones, 1984; Wangen and Williams, 1982; Jones, 1986; Foster et al., 1978), and sorption or coprecipitation of heavy metals to the freshly precipitated materials (Jones, 1986; Foster et al., 1978; Wangen and Williams, 1982; Chapman et al., 1983; Robinson, 1981). Sorption of trace metals to Fe-oxyhydroxides, particularly goethite (α-FeOOH), is a well-documented phenomenon (Benjamin and Leckie, 1981; Forbes et al., 1976; Theis and Richter, 1980; Kinniburgh et al., 1976).

The precipitates formed at confluences of metalliferous acid mine streams and natural surface waters are often X-ray amorphous; as a result, standard mineralogical

analyses have been frequently augmented by evaluation of saturation indices for various mineral phases (e.g., Chapman et al., 1983; Nordstrom, 1982b; Nordstrom et al., 1979). Sulfate is the principal anion in acidic leachates issuing from both mine tailings and spoils and from coal stockpiles. Thus, sulfate-solid phases are often presumed and/or identified as well as hydroxides and oxyhydroxides. Theobald et al. (1963) observed a sequence of colored precipitates of brown, pale brown, white, and black with increasing pH from ≃5 to 7-8 formed at the confluence of Deer Creek and the Snake River, following the order of hydrolysis of Fe, Al, and Mn. All of the precipitates were amorphous to X-ray and petrographic analysis. Sulfur analysis was only performed on the white precipitate, where a significant amount of SO_4 was reported, suggesting a basic Al-sulfate phase in addition to Al-hydroxide (Theobald et al., 1963). Nordstrom (1982b) outlined the stability relations in the $Al_2O_3 - SO_3 - H_2O$ system, noting that alunogen ($Al_2(SO_4)_3 \bullet 17\ H_2O$) is stable in aqueous solution only at pH < 0, jurbanite, $Al(SO_4)(OH) \bullet 5(H_2O)$ from pH < 0 to 3-5 depending upon sulfate activity; alunite, $KAl_3(SO_4)_2(OH)_6$, up to pH of 4-7, and gibbsite above these pH limits. Basaluminite, $Al_4(SO_4)(OH)_{10} \bullet 5\ H_2O$, is the kinetically favored precipitate, but is metastable to the other phases.

Similarly, a number of Fe-hydroxysulfate minerals may exist, depending upon conditions. Very highly concentrated acid mine waters can precipitate melanterite, $FeSO_4 \bullet H_2O$, which may subsequently oxidize to copiapite, $Fe^{2+}Fe^{3+}_4(SO_4)_6(OH)_2 \bullet 20H_2O$, or coquimbite, $Fe_2(SO_4)_3 \bullet 9H_2O$ (Nordstrom, 1982a). Potassium jarosite, $KFe_3(SO_4)_2(OH)_6$, has been identified in precipitates within acid mine drainage streams (Nordstrom, 1982a), cat clays, associated with pyrite veins, and in laboratory bacterial precipitates (Ivarson et al., 1982). Ross et al. (1982) also reported the occurrence of natrojarosite, the Na analog to jarosite, in significant quantities within a number of

Canadian acid sulfate soils. Potassium jarosite was found to form more rapidly in laboratory systems than natrojarosite, though Na-jarosite was often the dominant form identified with the soils (Ross et al., 1982). At pH values much above 3, amorphous ferric hydroxide is the likely phase (Nordstrom, 1982a).

Brady et al. (1986) isolated an ochreous precipitate from a stream receiving metalliferous acid mine drainage which was determined to consist primarily of goethite, with lesser amounts of ferrihydrite-like minerals. Despite XRD (X-ray diffraction) evidence for reasonably crystalline α-FeOOH as a major component to the material, an oxalate-to-dithionite soluble Fe ratio of 0.99 was found (Brady et al., 1986), suggesting extremely poor crystallinity (Schwertmann, 1964). Such high oxalate solubility is more typically observed only for ferrihydrite (Carlson and Schwertmann, 1981). Total S content of the precipitate was determined to be 3 percent, suggesting that adsorbed or coprecipitated sulfate may have inhibited crystallization and thus been responsible for the anomalously high oxalate solubility (Brady et al.,1986).

Brady et al. (1986) also evaluated the influence of sulfate on Fe-oxide formation in laboratory studies. Ferric nitrate solutions (0.02 *M*) were hydrolyzed in the absence and presence of sulfate, from 0 to 2000 mg/L. In all experiments in which the hydrolysis was conducted in the presence of sulfate, natrojarosite was the initial phase formed, though Nordstrom (1982a) suggested rather that a kinetic hindrance to jarosite formation may operate, serving to explain deviations between predicted mineralogies (based upon thermodynamic calculations) and those observed in many acid mine streams. Subsequent 30 day dialysis against pH 6 solutions containing either distilled water or sulfate at the same concentrations as in the original

hydrolyzate yielded variable results. In the absence of sulfate, ferrihydrite was formed, while modest levels of sulfate (250 -500 mg/L) yielded α-FeOOH mixed with another, poorly ordered Fe-oxide (Brady et al, 1986). With increased sulfate, evidence for α-FeOOH diminished, and at 2000 mg/L no evidence for goehtite was apparent; rather, poorly ordered ferrihydrite and feroxyhite predominated (Brady et al, 1986). Dialysis against sulfate yielded results similar to that obtained for distilled water-dialyzed samples except that stronger α-FeOOH diagnostics were observed.

As noted earlier, acid mine drainage and coal pile leachates are also generally highly enriched in heavy metals. Upon dilution or neutralization, these metals are typically associated with the precipitated Fe and Al phases (Jones, 1986; Foster et al., 1978; Chapman et al., 1983; Bradley and Lewin, 1982; Theobald et al., 1963). Jenne (1968) emphasized the importance of hydrous oxides in controlling trace metal concentrations in soils and water. Considerable work has been done evaluating trace metal and also anion sorption to hydrous oxides (e.g., Benjamin and Leckie, 1981; Kinniburgh and Jackson, 1982; Harrison and Berkheiser, 1982; Millward and Moore, 1982; Parfitt and Smith, 1978; Parfitt and Russell, 1977; Pierce and Moore, 1982; Sigg and Stumm, 1981; Dyck, 1968; Hem, 1977; Rao Gadde and Laitinen, 1974). Most work has been done on model systems however, with well-characterized solid phases and relatively simple solution chemistries; as a result direct extrapolation to complex acid mine drainage or coal pile leachate systems is tenuous at best.

Another factor influencing the overall environmental impacts of metalliferous acid mine drainage and coal pile leachates is related to its mode of migration in the environment. Confluence of metalliferous acid streams with natural higher pH surface waters can often be adequately described by simple flow measurements coupled with

suitable chemical and mineralogical analyses. Chapman et al. (1983) described a method (congruent element analysis) in which conservative components within acid mine drainage were identified and then used to index removal processes and plume migration within two streams in Australia. A similar approach was used by Bencala et al. (1987) in studying the confluence of the Snake River with Deer Creek (previously discussed with reference to the work of Theobold et al., 1963).

While the impacts of acid mine drainage on surface waters are often apparent enough (e.g., flocculent, highly colored precipitates coating the streambed, noticeably sterile lakes and stream reaches), the influence on subsurface waters is less obvious and less well-understood (NRC, 1981). Subsurface generation of acidic waters, and contaminant plume migration through soils and other geologic materials are under the control of transport processes, which in turn affect the nature and extent of subsequent geochemical reactions. Both macropore and micropore, or Darcy, flow can occur within soils. Root and earthworm channels and ped faces in highly structured soils can all serve to rapidly conduct water under periods of high precipitation inputs (relative to Darcy flow) within the vadose zone (Buoma and Wosten, 1979; Ehler, 1975); similarly, fractures and contacts within subsurface geologic strata may be responsible for the bulk of water movement within the phreatic zone under certain conditions.

Consequences of water movement in vadose zone macropores were reviewed by Thomas and Phillips (1979) and more recently by Beven and Germann (1982). The rapid movement of potentially large volumes of water via macropores serves to reduce interaction with the soil matrix, thereby substantially reducing the opportunity for geochemical attenuation processes. Cozzarelli et al. (1987) demostrated this

general phenomenon in a study of Al mobility in a forested watershed in Virginia. Zero tension lysimeters were used to collect macropore soil water, which was found to have undergone less extensive neutralization and Al immobilization than micropore water collected from tension lysimeters (Cozzarelli et al, 1987).

Reaction kinetics, then, also serve to influence transport; high interstitial flow velocities within porous media, as may be found in macropore or fractured flow regimes, may exert a hydrologic control on natural geochemical attenuation processes, violating the so-called local equilibrium assumption (LEA) (e.g., Whiffin and Bahr, 1985; Goltz and Roberts, 1986). A ratio of reaction rate to fluid velocity (the Damkohler number) in excess of 10 indicates reasonable validity of the local equilibrium assumption for that reaction (Dria et al., 1987). James and Rubin (1979) evaluated the applicability of the LEA to the transport through soils of solutes affected by ion exchange and observed apparent breakdown of the LEA for Ca self-exchange in Delhi and Oakley sands at Darcy velocities greater than approximately 0.6 cm/h. However, they noted that under conditions where the hydrodynamic dispersion coefficient is approximately equivalent to the molecular diffusion coefficient in the soil the LEA applies (James and Rubin, 1979). Lai and Jurinak (1971) also noted some evidence for breakdown of the LEA for cation exchange in miscible displacement studies through soil columns.

Transport of components within metalliferous acid leachates through soil and groundwater systems can be expected to involve a number of chemical reactions, including ion exchange, specific adsorption and precipitation. As a result, efforts to evaluate and model such complicated systems are still needed, though some progress is being made (Dria et al, 1987; Willis and Rubin, 1987). Observation of ap-

parent precipitation of Fe- and Al-oxyhydroxides and sorption of trace metals were followed by dissolution of the solid phases resulting in release of previously sorbed trace metals when acid coal mineral waste water was percolated through soils (Wangen and Jones, 1984), consistent with the theory presented by Dria et al. (1987).

References

Bencala, K. E., D. M. McKnight, and G. W. Zellweger. 1987. Evaluation of natural tracers in an acidic and metal-rich stream. Water Resour. Res. **23** :827-836.

Benjamin, M. M., and J. O. Leckie. 1981. Multiple-site adsorption of Cd, Cu, Zn, and Pb on amorphous iron oxyhydroxide. J. Coll. Interface Sci. **79:** 209-221.

Beven, K., and P. Germann. 1982. Macropores and water flow in soils. Water Resour. Res. **18:** 1311-1325.

Bradley, S. B., and J. Lewin. 1982 Transport of heavy metals on suspended sediments under high flow conditions in a mineralized region of Wales. Environ. Pollut. **4:** 257-267.

Brady, K. S., J. M. Bigham, W. F. Jaynes, and T. J. Logan. 1986. Influence of sulfate on Fe-oxide formation: comparisons with a stream receiving acid mine drainage. Clays Clay Miner. **34:** 266-274.

Buoma, J., and J. H. M. Wosten. 1979. Flow patterns during extended saturated flow in two undisturbed swelling clay soils with different macrostructures. Soil Sci. Soc. Am. J. **43:** 16-22.

Carlson, L., and U. Schwertmann. 1981. Natural ferrihydrites in surface deposits from Finland and their association with silica. Geochim. Cosmochim. Acta **45:** 421-429.

Caruccio, F. T., and G. Geidel. 1978. Geochemical factors affecting coal mine drainage quality. In F. W. Schalles and P. Sutton (ed.). Reclamation of drastically disturbed lands. pp. 129-148. Am. Soc. of Agron., Madison, WI.

Chapman, B. M., D. R. Jones, and R. F. Jung. 1983. Processes controlling metal ion attenuation in acid mine drainage streams. Geochim. Cosmochim. Acta **47:** 1957-1973.

Cozzarelli, I. M., J. S. Herman, and R. A. Parnell. 1987. The mobilization of aluminum in a natural soil system: effects of hydrologic pathways. Water Resour. Res. **23:** 859-874.

Davis, E. C., and W. J. Boegly. 1981. A review of water quality issues associated with coal storage. J. Environ. Qual. **10:** 127-133.

Dria, M. A., L. Bryant, R. S. Scheichter, and L. W. Lake. 1987. Interacting precipitation/dissolution waves: the movement of inorganic contaminants in groundwater. Water Resour. Res. **23:** 2076-2090.

Dyck, W. 1968. Adsorption and coprecipitation of silver on hydrous ferric oxide. Can. J. Chem. **46:** 1441-1444.

Ehlers, W. 1975. Observations on earthworm channels and infiltration on tilled and untilled loess soil. Soil Sci. **119:** 242-248.

Forbes, E. A., A. M. Posner, and J. P. Quirk. 1976. The specific adsorption of divalent Cd, Co, Cu, Pb, and Zn on goethite. J. Soil Sci. **27:** 1654-1666.

Foster, P., D. T. E. Hunt, and A. W. Morris. 1978. Metals in an acid mine stream and estuary. Sci. Total Environ. **9:** 75-86.

Goltz, M. N., and P. V. Roberts. 1986. Interpreting organic solute data from a field experiment using physical nonequilibrium models. J. Contam. Hydrol. **1:** 77-93.

Harrison, J. B., and V. E. Berkheiser, 1982. Anion interactions with freshly prepared hydrous iron oxides. Clays Clay Miner. **30:** 97-102.

Hem, J. D. 1977. Reactions of metal ions at surfaces of hydrous iron oxide. Geochim. Cosmochim. Acta **41:** 527-538.

Jackson, M. L., C. H. Lim, and L. W. Zelazny. 1986. Oxides, hydroxides, and aluminosilicates. In A. Klute (ed.) Methods of soil analysis, Part I. Agron. **9:** 101-142. Am. Soc. of Agron., Madison, WI.

James, R. V., and J. Rubin. 1979. Applicability of the local equilbrium assumption to transport through soils of solutes affected by ion exchange. In E. A. Jenne (ed.) Chemical modeling in aqueous systems: Speciation, sorption, solubility, and kinetics. ACS Symp. Ser. **93:** 225-235. ACS, Washington, DC.

Jenne, E. A. 1968. Controls on Mn, Fe, Co, Ni, Cu, and Zn concentrations in soils and water: the significant role of hydrous Mn and Fe oxides. In R. F. Gould (ed.) Trace inorganics in water, Adv. Chem. Ser. **73:** 337-387, ACS, Washington, DC.

Jones, K. C. 1986. The distribution and partitioning of silver and other heavy metals in sediments associated with an acid mine drainage stream. Environ. Pollut. (Ser. B) **12:** 249-263.

Kinniburgh, D. G., M. L. Jackson, and J. K. Syers. 1976. Adsorption of alkaline earth, transition, and heavy metal cations by hydrous oxide gels of iron and aluminum. Soil Sci. Soc. Am. J. **40:** 796-799.

Kinniburgh, D. G., and M. L. Jackson. 1982. Concentration and pH dependence of calcium and zinc adsorption by iron hydrous oxide gel. Soil Sci. Soc. Am. J. **46:** 56-61.

Lai, S., and J. J. Jurinak. 1971. Numerical approximation of cation exchange in miscible displacement through soil columns. Soil Sci. Soc. Am. Proc. **35:** 894-899.

May, H. M., D.G. Kinniburgh, P. A. Helmke, and M. L. Jackson. 1986. Aqueous dissolution, solubilities, and thermodynamic stabilities of common aluminosilicate clay minerals: kaolinite and smectites. Geochim. Cosmochim. Acta **50:** 1667-1677.

Millward, G. E., and R. M. Moore. 1982. The adsorption of Cu, Mn, and Zn by iron oxyhydroxide in model estuarine solutions. Water Res. **16:** 981-985.

Nordstrom, D. K., E. A. Jenne, and J. W. Ball. 1979. Redox equilibria of iron in acid mine waters. In E. A. Jenne (ed.) Chemical modeling in aqueous systems: speciation, sorption, solubility, and kinetics. ACS Symp. Ser. **93:** 51-79. ACS, Washington, DC.

Nordstrom, D. K. 1982a. Aqueous pyrite oxidation and the consequent formation of secondary iron minerals. In J. A. Kittrick, D. S. Fanning, and L. R. Hossner (ed.) Acid sulfate weathering. Soil Sci. Soc. of Am. Spec. Publ. **10:** 37-56. Soil Science Society of America, Madison, WI.

Nordstrom, D. K. 1982b. The effect of sulfate on aluminum concentrations in natural waters: some stability relations in the system $Al_2O_3 - SO_3 - H_2O$ at 298 K. Geochim. Cosmochim. Acta **46:** 681-692.

Parfitt, R. L., and J. D. Russel. 1977. Adsorption on hydrous oxides. IV. Mechanisms of adsorption of various ions on goethite. Soil Sci. J. **28:** 297-305.

Parfitt, R. L., and R. St. C. Smith. 1978. The mechanism of sulfate adsorption on iron oxides. Soil Sci. Soc. Am. J. **42:** 48-50.

Pierce, M. L., and C. B. Moore. 1982. Adsorption of arsenite and arsenate on amorphous iron hydroxide. Water Res. **16:** 1247-1253.

Rao Gadde, R., and H. A. Laitinen. 1974. Studies of heavy metal adsorption by hydrous iron and manganese oxides. Anal. Chem. **46:** 2022-2026.

Robinson, G. D. 1981. Adsorption of Cu, Zn, and Pb near sulfide deposits by hydrous manganese-iron oxide coatings on stream alluvium. Chem. Geol. **33:** 65-79.

Ross, G. J., K. C. Ivarson, and N. M. Miles. 1982. Microbial formation of basic ferric sulfates in laboratory systems and in soils. In J. A. Kittrick, D. S. Fanning, and

L. R. Hossner (ed.) Acid sulfate weathering. Soil Sci. Soc. Am. Spec. Publ. **10:** 77-94. Soil Science Society of America, Madison, WI.

Schwertmann, U. 1964. Differenzierung der Eisenoxide des Boden durch photochemische Extrakition mit saurer Ammoniumoxalat - Losung. Z. Pfanzenern. Dung Bodenkunde **105:** 194-202.

Sigg, L., and W. Stumm. 1981. The interaction of anions and weak acids with the hydrous goethite (α —FeOOH) surface. Coll. Sur. **2:** 101-117.

Singer, P. C., and W. Stumm. 1970. Acidic mine drainage: the rate-determining step. Science **167:** 1121-1123.

Swift, M. C. 1985. Effects of coal pile runoff on stream quality and macro-invertebrate communities. Water Resour. Res. **21:** 449-457.

Theis, T. L., and R. O. Richter. 1980. Adsorption reactions of nickel species at oxide surfaces. In M. C. Kavanough and J. O. Leckie (ed.) Particulates in water. Adv. in Chem. Ser. **189:** 73-96. ACS, Washington, DC.

Theobald, P. K., H. W. Lakin, and D. B. Hawkins. 1963. The precipitation of aluminum, iron and manganese at the junction of Deer Creek with the Snake River in Summit County, Colorado. Geochim. Cosmochim. Acta **27:** 121-132.

Thomas, G. W., and R. E. Phillips. 1979. Consequences of water movement in macropores. J. Environ. Qual. **8:** 149-152.

Vuorinen, A., P. Hiltunen, J. C. Hsu, and O. H. Tuovinen. 1983. Solubilization and speciation of iron during pyrite oxidation by *Thiobacillus ferroxidans*. Geomicrobiol. J. **3:** 95-120.

Wangen, L. E., and J. M. Williams. 1982. Control by alkaline neutralization of trace elements in acidic coal cleaning waste leachates. J. Water Pollut. Contr. Fed. **54:** 1302-1310.

Wangen, L. E., and M. M. Jones. 1984. The attenuation of chemical elements in acidic leachates from coal mineral wastes by soils. Environ. Geol. Water. Sci. **6:** 161-170.

Whiffin, R. B., and J. M. Bahr. 1985. Assessment of purge well effectiveness for aquifer decontamination. In Proceedings of the fourth national symposium on aquifer restoration and groundwater monitoring. national well association, Worthington, OH.

Willis, C, and J. Rubin. 1987. Transport of reacting solutes subject to a moving dissolution boundary: numerical methods and solutions. Water Resour. Res. **23:** 1561-1574.

Chapter III

Observed Component Transport

Abstract

Runoff from coal stockpiled at industrial facilities is generally very acidic and highly enriched in metals. As a result, the storage of coal can pose a serious threat to local surface and groundwater. To edify our understanding of the geochemical processes pursuant with the infiltration of this acidic, metal-rich runoff through soil and aquifer materials, samples from a subsoil-aquifer unit adjacent to a coal stockpile near Aiken, South Carolina were leached with coal pile runoff under steady saturated flow conditions. Mobility of a number of important components within coal pile runoff were determined and related to aqueous and soil chemical and mineralogical properties. Initial appearance of components in column effluent was governed by sulfate mobility via the necessary condition of electroneutrality in solution. Displacement of native soil cations and chromatographic effects resulted in peak effluent concentrations well

in excess of influent concentrations. Beryllium, Co, Li, Mn, Na, Ni, and Zn movement through the soil columns was rapid (peak effluent concentrations moving at 0.25 to 1 times the groundwater velocity) and controlled by ion exchange. Potassium movement was considerably slower than that for Na, apparently a result of sorption to high selectivity sites within 2:1 minerals. Absence of Fe in column effluent until pH less than 3 was noted, indicating transport governed by precipitation/dissolution. Peak Cr and Cu effluent concentrations occurred later than that for other transition metals and were also coincident with reduction in effluent pH below 3. Speciation of column effluent indicated supersaturation with respect to a series of jarosites, Si concentrations in equilibrium with respect to an amorphous SiO_2 phase, and Al concentrations tending to follow that based upon equilibrium with jurbanite.

Introduction

Analogous to acid mine drainage, the storage of coal also results in the generation of highly acidic, metalliferous leachate through oxidation of sulfidic ores present in coal as impurities (Davis and Boegly, 1981; Swift, 1985). Additional water quality concerns with regard to coal storage include the fact that coal stockpiles are relatively abundant, not restricted to areas associated with mining operations, and often uncontrolled.

The interaction of these metalliferous acid leachates with more alkaline surface waters results in neutralization or dilution of acidity, precipitation of Fe and Al

hydroxides, oxyhydroxides, and/or basic sulfates (Theobald et al., 1963; Brady et al., 1986; Nordstrom et al., 1979; Nordstrom, 1982a), and sorption or coprecipitation of heavy metals to the freshly precipitated materials (Chapman et al., 1983; Wangen and Williams, 1982; Jones, 1986; Foster et al., 1978; Robinson, 1981). Wangen and Jones (1982) evaluated the capacity of a number of different soils to neutralize coal mineral waste leachate and found that carbonate content governed acidity and thus also metal concentrations of soil column effluent. A naturally acidic soil, with no free carbonates present, afforded little attenuation (Wangen and Jones, 1982). Inasmuch as a significant portion of the U.S. coal reserves and coal stockpiles reside within moderately to highly weathered geologic regions with little carbonate alkalinity, an evaluation of the mobility of components within coal pile runoff upon infiltration of this highly acidic effluent through a weathered, naturally acidic subsoil-aquifer unit was undertaken.

Materials and Methods

Study Site

Soil samples were collected from a site immediately adjacent to the D-Area coal pile runoff containment basin within the Department of Energy's Savannah River Site near Aiken, South Carolina (Figure 1). The coal stockpile is 3.6 ha in areal extent, containing ≃131,000 metric tons of low-S (1-2 %) coal, and the basin ≃5.1 ha with a volume

capacity $\simeq 3.8 \times 10^{10}$ L. Monitoring wells indicate significant degradation of groundwater downgradient of the coal pile and basin (toward Beaver Dam Creek) (Figure 1, inset).

Soils

The basin was created by excavation and removal of the surficial 1-2 m of soil (Fuquay, a thermic, sandy, kaolinitic Plinthic Paleudult). Soil samples were collected by augering adjacent to the basin, with samples collected every 25 cm until the sandy, unconfined aquifer was reached (1.25 m). Bulk densities were determined on samples extruded from cores of known volume (Blake and Hartge, 1986). The samples were weighed prior and subsequent to oven drying to 105 °C. Bulk densities were taken as the oven dry weight divided by core volume. Porosities were calculated from the bulk densities assuming a particle density of 2.65 Mg m^{-3} (Danielson and Sutherland, 1986). Particle size distributions were determined via a modified pipette method (Miller and Miller, 1987). Bulk soil samples were air-dried, and passed through a 2 mm sieve. Soil pH was determined on 1:1 soil:water equilibrations (McLean, 1986). Non-crystalline and free oxide contents of triplicated 1 g (oven dry weight basis) subsamples were estimated via the 4 h ammonium-oxalate in the dark (Ox) and dithionite-citrate-bicarbonate (DCB) procedures, respectively (Jackson, et al., 1986). Soil organic matter contents were determined using the Walkley-Black method (Allison, 1965). Cation exchange capacities of the whole soil were determined by summation of native cations exchanged from triplicate 5 g oven dry weight basis subsamples with three 30 min extractions of *M* NH_4Cl.

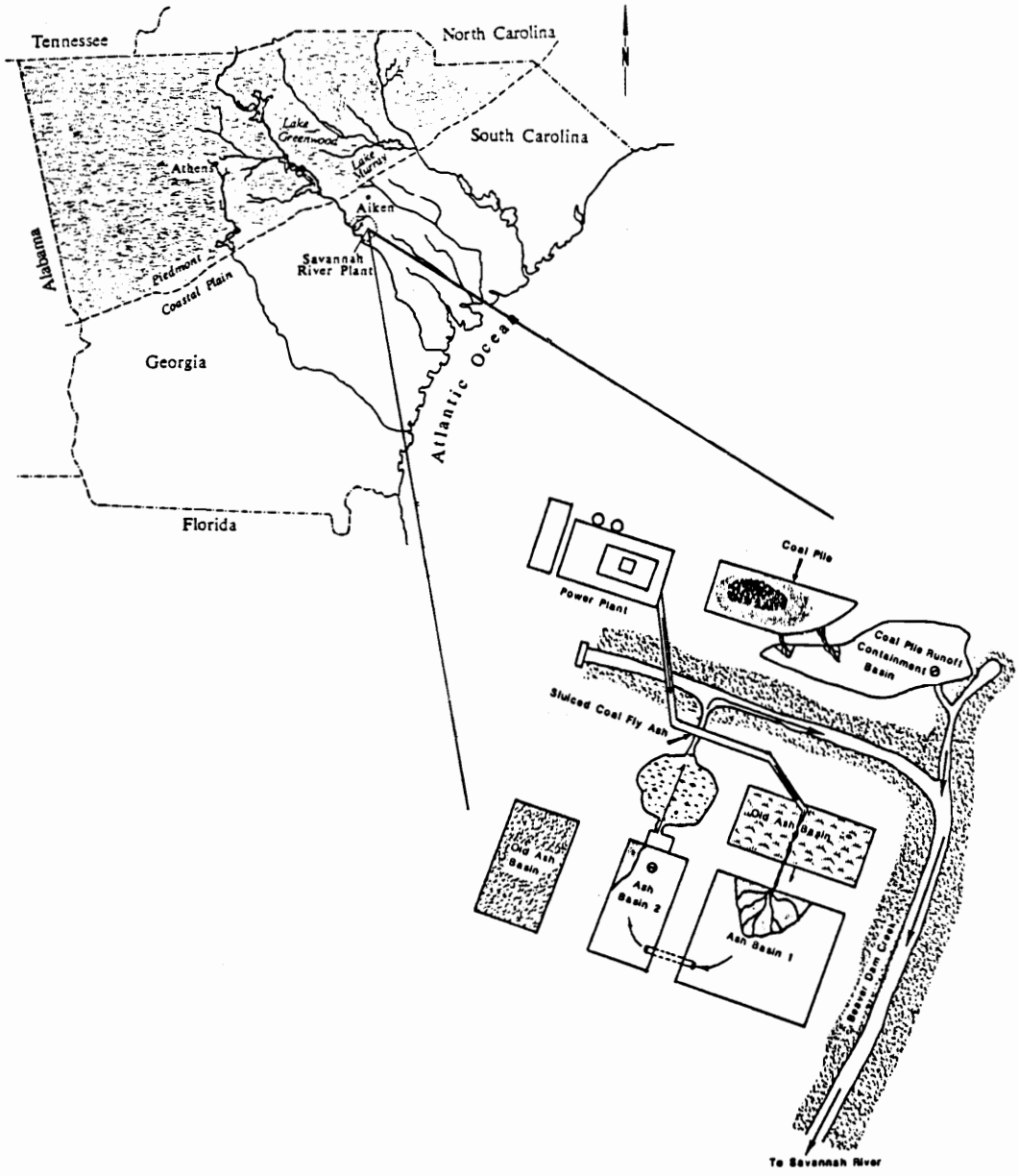

Figure 1. Study site.

Mineralogy

Silt and clay-sized materials were separated from whole soils after Fe removal by DCB (Jackson et al., 1986) via wet sieving and centrifugation (Whittig and Allardice, 1986). A tile mounting technique (Rich and Barnhisel, 1977) was used to prepare oriented clay mounts with Mg and K saturations. A clean, flat ceramic tile was placed in the suction apparatus and a clay suspension containing ≃250 mg sample was pipetted onto the tile. After free water has been drawn through the tile, 5 mL of *M* KCl was added. The process was repeated a total of 5 times, then washed in a similar fashion with Milli-Q deionized water (5 times). Analogously, Mg-saturated tiles were also prepared using 0.5 *M* $MgCl_2$, followed by one wash with 5 mL 20 % glycerol solution after the fifth water wash (Mg-gly).

The mounts were then X-rayed with a Diano X-ray spectrometer from 2-32 °2θ at a step speed of 0.075 °2θ/4 s. A Cu source was used (λ = 1.542 Å). The Mg-gly tile mounts were X-rayed at room temperature and after heating to 110 °C and the K-saturated tile mounts at room temperature and after heating to 110, 300, and 550 °C. Powder mounts of the silt fractions were prepared by packing oven-dry samples into a powder holder with a spatula. Five mg samples from the K-saturated tile mounts were removed for analysis by differential scanning calorimetry. The sample was placed in a gold pan and heated to 625 °C at a rate of 20 °C/min with a DuPont 1090 Thermal Analyzer.

Column Leaching Experiments

Air-dried, < 2 mm soils were packed into 25 cm x 2.54 cm columns to a uniform bulk density of 1.50 Mg m^{-3} . Columns were then wet from the bottom with Milli-Q water supplied at a constant flow equivalent to a Darcy velocity (q) of 1.3 cm h^{-1} via a Dionex APM pump module. Once steady saturated flow had been attained, the columns were allowed to equilibrate overnight. Coal pile runoff collected from the basin was then supplied and the columns leached under steady saturated flow (q = 1.3 cm h^{-1}). Effluent was collected via an LKB linear fraction collector. Column dispersivities were determined via pulse injections equivalent to approximately one pore volume of 5 *mM* LiBr followed by Milli-Q water. Breakthrough data were then analyzed via the parameter estimation method of Parker and van Genucthen (1984).

Analytical

Hydrogen ion activites of the soil:water extracts and column effluent fractions were determined using a GK2401C combined glass-calomel electrode and a Radiometer PHM 84 pH meter. Bromide concentrations were determined using a Fisher 13-620-520 Br^- ion specific electrode and a Radiometer K401 reference electrode. Effluent fractions and extracts were analyzed for total dissolved major and trace element concentrations via inductively coupled plasma emission spectroscopy(ICPES). Sulfate analysis was performed using a Dionex System 2010i ion chromatograph (IC). Ferrous iron concentrations were determined via the o-phenanthroline method (APHA, 1976).

Speciation

Analytical speciation of elements was limited to S and Fe. Excellent agreement between total S via ICPES and S concentrations as SO_4^{2-} via IC was obtained (< 1 % deviation); as a result, all S was considered as SO_4^{2-} (Table 1). The distribution of Fe between the Fe^{2+} and Fe^{3+} forms was determined from the o-phenanthroline determined Fe^{2+} with Fe^{3+} taken as the difference between ICPES total Fe and Fe^{2+}. For thermodynamic equilibrium speciation calculations, the valence of remaining elements was assigned assuming forms common to those elements under typical environmental conditions (Table 1), though subsequent discussions will exclude reference to particular valence states except where explicitly determined. Equilibrium speciation of the coal pile runoff and column effluent was calculated via EPA's MINTEQA2 geochemical equilibrium model (Brown and Allison, 1987). The reader is referred to that work for a list of the thermodynamic constants used for these calculations.

Results

Coal Pile Runoff

The coal pile runoff was highly acidic, with considerable dissolved SO_4^{2-} , Fe^{3+}, and Al contents (Table 1). The runoff also possessed high levels of alkaline earth and transition metals and other elements (Table 1).

Soils

The subsoil overlying the unconfined aquifer is characteristic of soils of the generally highly weathered Coastal Plain region. The soils are of naturally low pH, modest cation exchange capacities with a predominance of exchangeable Al, and of coarse texture (Table 2). The soils also possessed very low organic matter contents (< 0.15 %). The bulk density for the first sampling depth (0 - 0.25 m beneath basin surface, or $\simeq$2 -2.25 m below natural soil surface was 1.53 Mg m^{-3}. A saturated hydraulic conductivity of $\simeq$1 cm h^{-1} was estimated from particle size and bulk density data via SOILPROP (Mishra and Parker, 1989).

The subsoil was found to vary significantly with respect to solid phase composition over the relatively narrow depth to water table. Ammonium oxalate-extractable Al and Si varied only moderately, and tended to be greatest for the 0.25 - 1.25 m depth, while Ox-extractable Fe was highest at a depth of 0.75 - 1.25 m, which corresponds to the zone adjacent to the existing (at time of sampling) water table (Table 3). Seasonal fluctuations in the water table likely resulted in an enrichment of relatively poorly crystalline Fe oxide phases at this depth. DCB-extractable Fe was also greatest for this depth interval, which supports the notion of deposition-dissolution of Fe during seasonal water table fluctuations. The presence of Al within the reductant-soluble DCB Fe fraction suggests a coprecipitation reaction. A relatively constant mole ratio of DCB-extractable Al to Fe (0.15, 0.16, 0.17, and 0.13 for the 0 - 0.25, 0.25 - 0.75, 0.75 - 1.25, and 1.25 - 1.40 m depths, respectively) was noted. The occurrence of natural Al-substituted goethites, often approaching 30 %, has been well-documented (Norrish and Taylor, 1961). Ratios of Ox to DCB-extractable Fe are often used as an index of the overall crystallinity of soil Fe phases. Consistent with the proposed role of the

Table 1. Coal pile runoff composition.

Component	Concentration (mg/L)†
pH	2.13
Al^{3+}	101.0
Be^{2+}	0.055
Ca^{2+}	83.62
Co^{2+}	0.461
Cr^{3+}	0.010
Cu^{2+}	0.262
Fe^{2+}	4.70
Fe^{3+}	119.5
K^{+}	1.668
Li^{+}	0.232
Mg^{2+}	62.17
Mn^{2+}	7.302
Na^{+}	11.52
Ni^{2+}	0.878
H_4SiO_4	69.44
SO_4	2024
Sr^{2+}	0.791
Zn^{2+}	2.392

† except pH

Table 2. Selected soil properties.

Depth	pH_{H_2O}†	CEC‡	Base Saturation	Particle Size Distribution		
				Sand	Silt	Clay
m		$cmol_c\ kg^{-1}$	%	------- % -------		
0.00 - 0.25	4.93	4.43	15.3	78	2	20
0.25 - 0.75	4.96	6.82	16.1	75	5	20
0.75 - 1.25	5.06	3.71	21.1	81	6	13
1.25 - 1.40	5.12	2.15	11.3	88	2	10

† 1:1 soil:water

‡ $\sum$ Exchangeable bases + Al^{3+}

fluctuating water table in regulating overall crystallinity of the Fe phases, a significant increase in Ox/DCB Fe was noted for the lower two sampling depths (Table 3).

The mineralogical composition was also found to vary with depth. Quartz comprised the major component within the subsoil, accounting for all sand and silt-sized material, and tended to increase with depth (Table 4). Kaolinite, a common 1:1 weathering product of 2:1 phyllosilicate minerals and a dominant mineral within the highly weathered Piedmont and Coastal Plain provinces, was the next most abundant mineral for all depths. Smectite was greatest within the first sampling depth and decreased with depth. Mica, vermiculite, hydroxy-interlayered vermiculite, and interstratified mica-vermiculite were also present in varying quantities within the subsoil (Table 4). A trace of gibbsite was observed for the first sampling depth, evidence for most intense weathering and desilication at this first depth. Talc was also present within the aquifer material.

Results from the transport studies are presented using reduced values for time, or equivalently, as the number of pore volumes supplied to the columns. Reduced concentrations, C/C_0, where C is the effluent concentration relative to that of the influent (C_0), are used when different C_0 values are plotted on the same figure. Reproducibility of columns and column effluent concentration histories was very good. For example, duplicated columns of the 0.25 - 0.75 m material yielded fitted dispersion coefficients of 2.00 and 2.02 cm^2/h as well as very similar column effluent concentrations histories (e.g., Figure 2).

pH

Hydrogen ion activities as a function of eluted pore volumes exhibited similar relative

Table 3. Sequential extraction results.

Depth	Ox			DCB†		Ox/Ox + DCB
	Al	Fe	Si	Al	Fe	Fe
m	%			%		
0.00 - 0.25	0.022	0.028	0.005	0.036	0.477	0.06
0.25 - 0.75	0.033	0.054	0.007	0.062	0.826	0.06
0.75 - 1.25	0.033	0.085	0.006	0.075	0.910	0.09
1.25 - 1.40	0.025	0.029	0.006	0.020	0.295	0.09

† Following Ox treatment

Table 4. Soil mineralogical properties (on whole soil basis).

Depth	Q	K	M	S	V	HIV	M-V	G	T
m			---------- % ----------						
0.00 - 0.25	80	12.8	1.0	4.8	Tr	0.3	1.1	Tr	ND
0.25 - 0.75	80	13.2	1.2	3.4	Tr	Tr	2.2	ND	ND
0.75 - 1.25	87	6.3	0.9	3.3	0.2	Tr	2.3	ND	ND
1.25 - 1.40	90	5.1	0.4	1.5	0.2	Tr	2.0	ND	0.9

where Q = quartz, K = kaolinite, M = mica, S = smectite, V = vermiculite, HIV = hydroxy-interlayered vermiculite, M-V = interstratified mica-vermiculite, G = gibbsite, and T = talc. Tr = trace and ND = none detected.

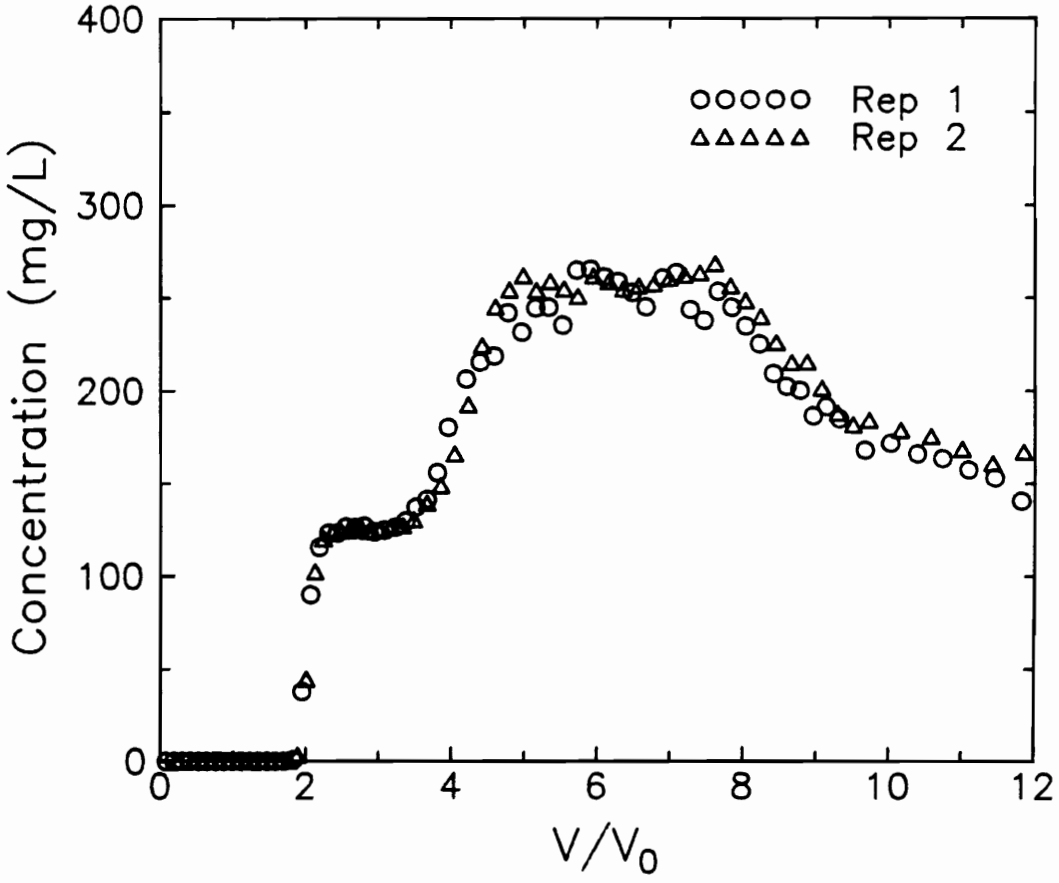

Figure 2. Column effluent concentration vs. reduced time (replicated 0.25 - 0.75 m material): Al.

trends for all four soil depths (Figure 3). The pH was essentially constant as the initial volume of equilibrated de-ionized water was displaced. At varying subsequent pore volumes, a slight rise in pH was observed, immediately followed by a rapid decrease in pH to ≃3.7. Apparent buffering reactions served to maintain solution pH at approximately 3.5 for volumes and times which were depth-specific, followed by a second region of relatively rapid increase in hydrogen ion activites (Figure 3). The initial rapid decrease in pH would be expected to occur at $V/V_0 \simeq 1$ if no retardation or reaction occurred. As breakthrough occurred between 1.3 and 2 pore volumes, some mechanism resulting in retardation was occurring.

One notes the necessary condition of electroneutrality in solution, and previous observations for significant adsorption of sulfate to soil and soil components (Singh, 1984; Sigg and Stumm, 1980; Aylmore et al., 1967) and precipitation of basic Al and Fe sulfates (Nordstrom, 1982). Breakthrough of sulfate was coincident with the initial reduction in pH to ≃3.5 (Figure 4). To further evaluate this relationship between anion mobility and breakthrough of protons, equivalent pH solutions containing only sulfate or nitrate were compared with the coal pile runoff (Figure 5). Breakthrough of protons occurred most rapidly when the counter ion was nitrate, which could be expected to interact less extensively than sulfate with the soil surface, followed relatively closely by the runoff solution, with breakthrough of protons and sulfate for the pH 2.13 H_2SO_4 solution not occurring until ≃4 pore volumes. The differences in pH and sulfate breakthrough behavior for the runoff and H_2SO_4 solution appear to be principally due to the ≃4x greater sulfate concentration in the coal pile runoff.

Though the metals associated with the runoff would be expected to complex to varying degrees with sulfate, and thus reduce its interactions with the soil surface and

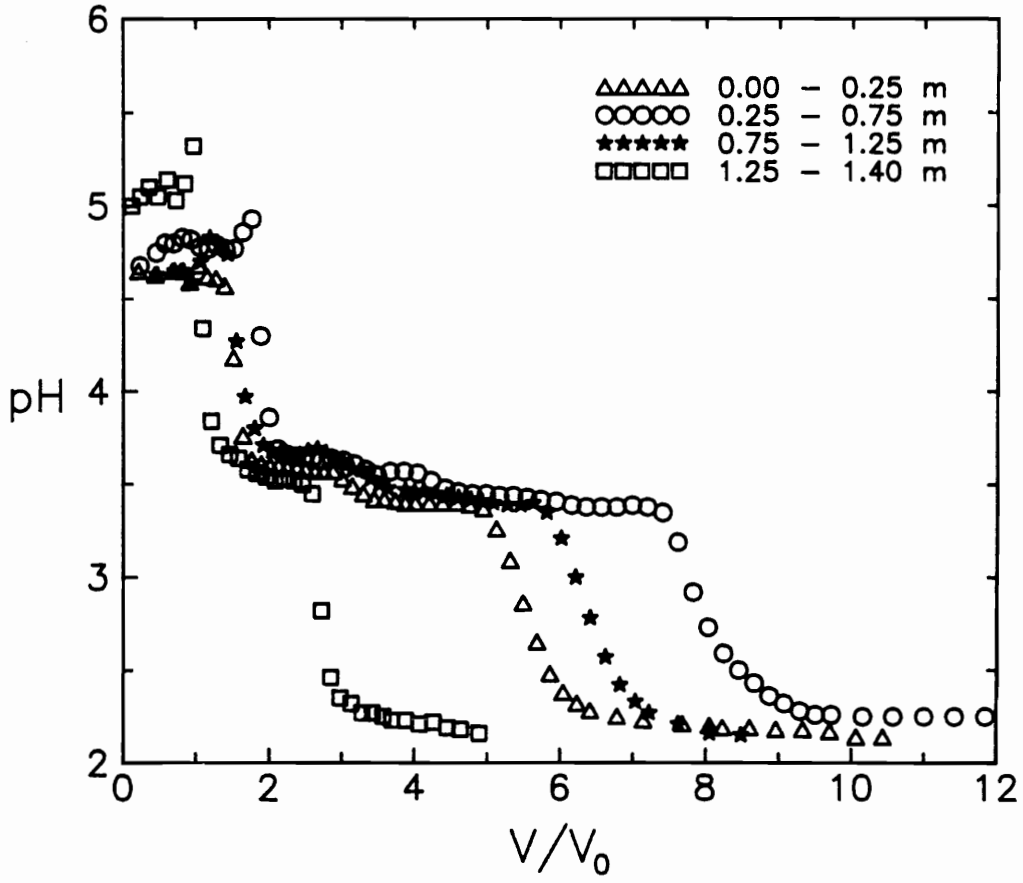

Figure 3. Column effluent concentration vs. reduced time: pH.

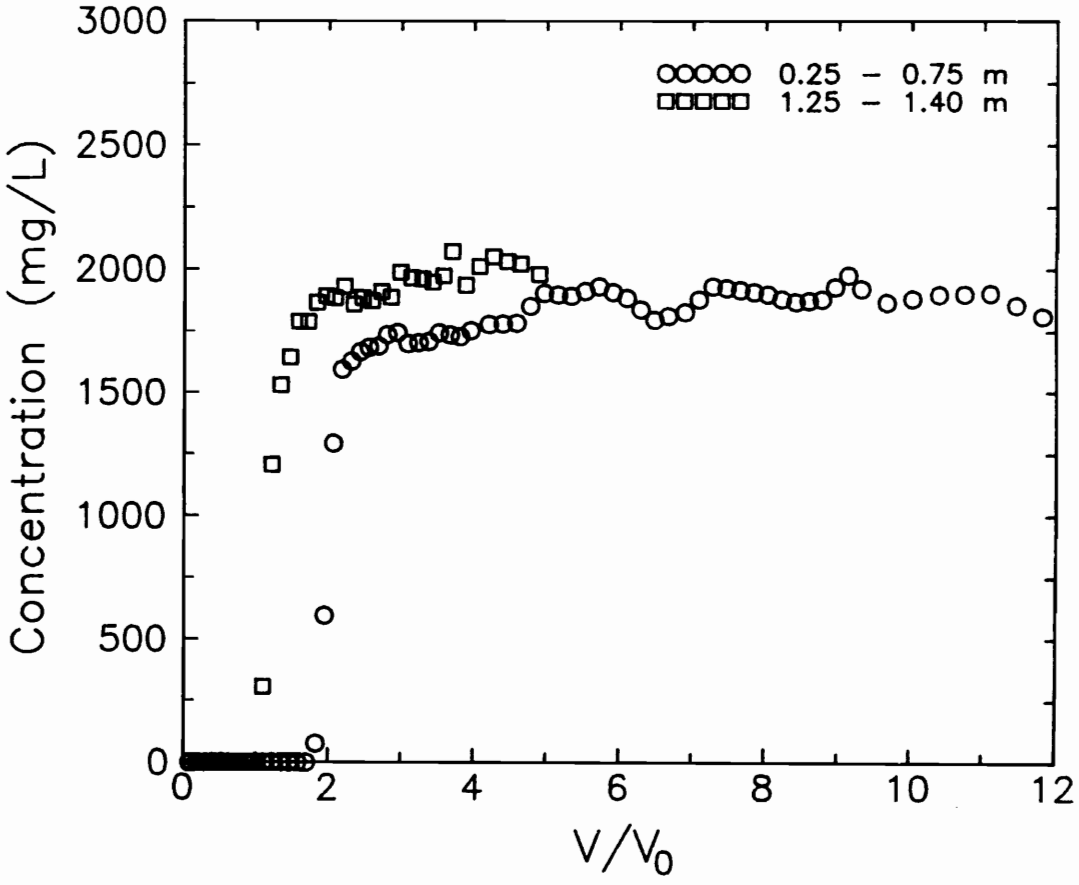

Figure 4. Column effluent concentration vs. reduced time: sulfate.

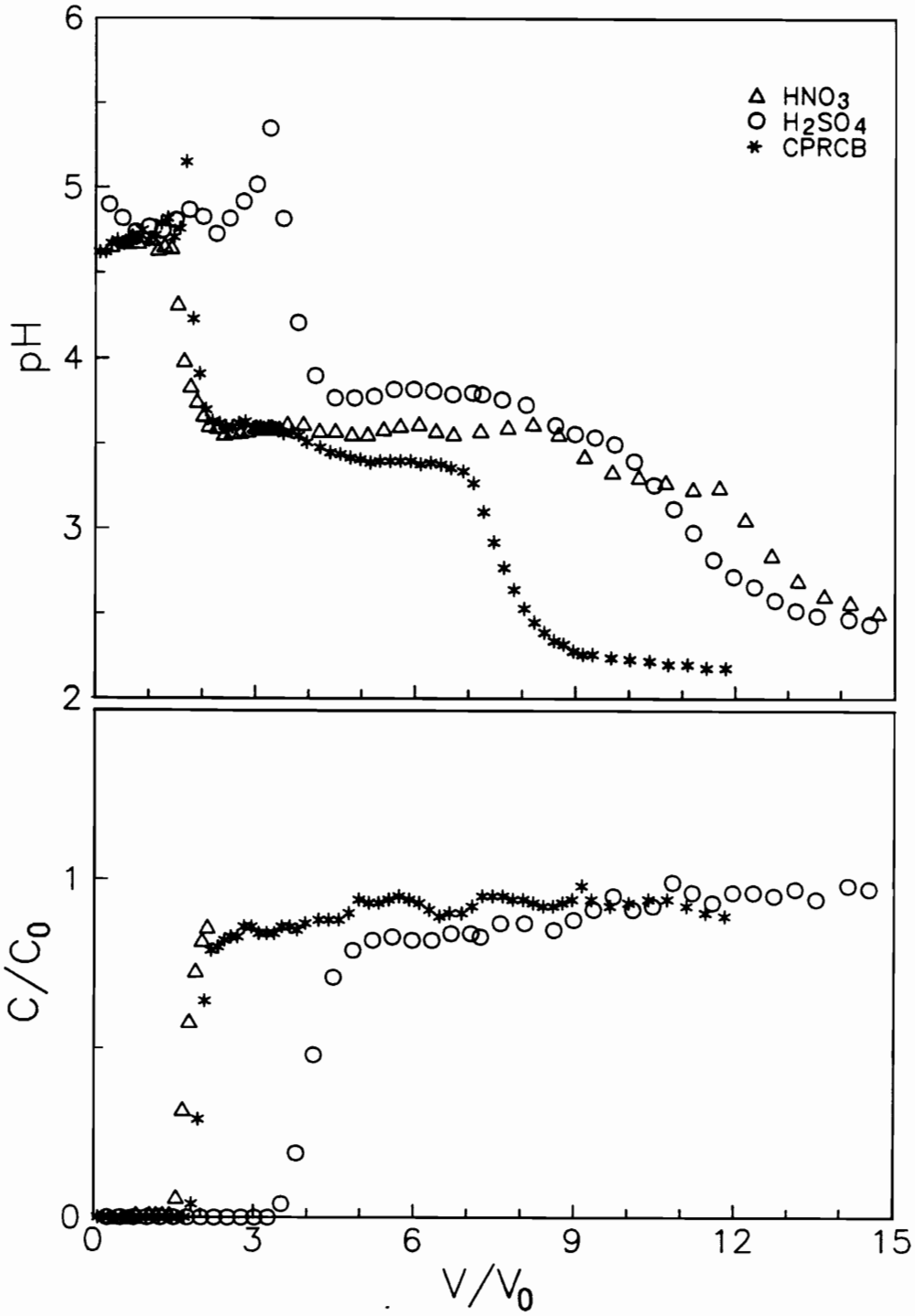

Figure 5. Column effluent concentration vs. reduced time for runoff (CPRCB) and equivalent pH nitric and sulfuric acid influent solutions (0.25-0.75 m material).

hasten transport through the soil, MINTEQA2 calculations indicate that approximately 31 % of the sulfate would be complexed with metals at its influent pH. If one allows the remaining sulfate (48.4 % as SO_4^{2-} and 20.1 % as HSO_4^-) to participate in sorption reactions, the active sulfate concentration would remain ≃3x as great as that for the pH 2.13 H_2SO_4 solution and may fill available sorption sites more rapidly (the magnitude of which is in relative agreement with observed sulfate breakthrough). It appears then, that sorption reactions are governing sulfate mobility and, through the condition of electroneutrality in solution, also cation migration through the soil.

The next feature on the proton breakthrough curves for these various soil depths is the plateau at pH ≃3.5 (Figure 3). Relatively little buffer capacity was noted for the aquifer material while the 0.25 - 0.75 m depth possessed appreciable buffering. A number of reactions can be invoked to account for this buffering, including dissolution of various oxyhydroxides and/or interlayer materials, protonation of edge sites of phyllosilicates, and proton exchange. An evaluation of the various baseline chemical and mineralogical data for these soils fails to identify a single factor apparently responsible for the observed buffering. Neither Ox nor DCB-extractable Al, Fe, or Si follows observed buffering. Whole-soil kaolinite contents and CEC values qualitatively tend to follow the observed trend, though a direct relation is lacking. Proton exchange may be in part responsible for the observed buffering, though the high concentration of di- and trivalent metal ions in solution should minimize adsorption of protons except for selective edge sites. Specific adsorption of sulfate may result in pH buffering due to displacement of surface hydroxyls (Rajan, 1978), and accounts for the slight increase in pH preceding the initial reduction in pH (Figure 3) though little sulfate removal from solution (i.e., $C/C_0 \simeq 1$) was observed over this buffer region (Figure 4). It thus appears that a complex array of coupled surface re-

actions, rather than a single, well-defined reaction, is responsible for the observed buffering. Titration of whole soil samples suspended in deionized water underestimated buffer capacity by ≃40 %, likely due in part to the rapid rate of titration relative to the leaching experiments (≃28 min titration).

Comparison of the runoff and pH 2.13 H_2SO_4 solution breakthrough curves (Figure 5) reveal another reaction occurring within the soil column. For an equivalent hydrogen ion activity in the influent solution, the soil is able to sustain greater leaching volumes before descending to the plateau region ≃pH 3.5 and also to near influent pH when only protons and sulfate are present. The hydrolysis of Fe(III) would impart additional acidity to the solution (Baes and Mesmer, 1976), and thus the runoff possesses greater overall acidity. If one allows all the Fe(III) in solution to hydrolyze, an additional proton loading nearly equivalent to the measured H^+ activity would result. That the observed buffer region for the CPRCB leached column is ≃two-thirds that of the pH 2.13 H_2SO_4 leached column under equivalent flux rates suggests that the Fe(III) is not hydrolyzing to $Fe(OH)_3$ but to a lower hydroxyl content phase.

Major Elements

Breakthrough of Al was observed concurrent with the breakthrough of sulfate and the initial reduction in pH for the different soil materials (Figure 6). Peak concentrations in the effluents from the different materials tended to be related to the CEC and native exchangeable Al contents (Table 5), with peak effluent Al concentration for the low Al content-low CEC aquifer material (1.25 -1.40 m depth) observed after only ≃2.5 pore volumes, while peak Al concentration in the high Al-high CEC 0.25 -0.75 m subsoil occurred at $V/V_0 \simeq 6$ (Figure 6). Native exchangeable Al (Table 5), and not an amorphous Al solid phase (Table 3) appears to be a primary source for the initial high

Al concentrations in solution, and a result of exchange by cations in the runoff. An interesting and important observation, one can expect Al concentrations several times that of the runoff to follow the sulfate plume in coal pile runoff-contaminated acid soil sites. This is, thus, the parallel phenomenon to the so-called "hardness halo" noted for groundwater contaminated by municipal landfills in the Midwest (Cartwright et al., 1977).

Iron was retained to a large extent by materials from all depths (Figure 7). Coincident with the decline in pH from the buffer region near pH 3.5 toward that of the influent pH (2.13), Fe was observed in the effluent (Figure 7). Low pH would be necessary to keep Fe(III) (the principal form of Fe in the runoff, Table 1) from hydrolyzing and precipitating as a hydroxo- or basic sulfate phase. As discussed in the previous section, it appears that the Fe is precipitating to a basic sulfate phase with an OH/Fe mole ratio near 2. This precipitated phase could also be expected to undergo dissolution as the soil buffer capacity is exhausted and the ambient pH descends toward that of the influent; thus Fe iron breakthrough behavior is one of coupled precipitation-dissolution.

Silicon was observed to break through and peak in effluent concentration (Figure 8) immediately preceding the initial drop in pH and the breakthrough of sulfate (Figure 4). A relatively high Si effluent concentration (Figure 8) was maintained during the observed pH buffer regions (Figure 3) which implies a role in the buffering reactions for these soils. Barnhisel and Rotromel (1974) subjected kaolinite and illite clay minerals to simulated acid mine drainage solutions and concluded that the mode of attack on both clays occurred at the edges, releasing Al and Si, and also Fe and K in the case of the illite, and suggested that phyllosilicate dissolution is the probable

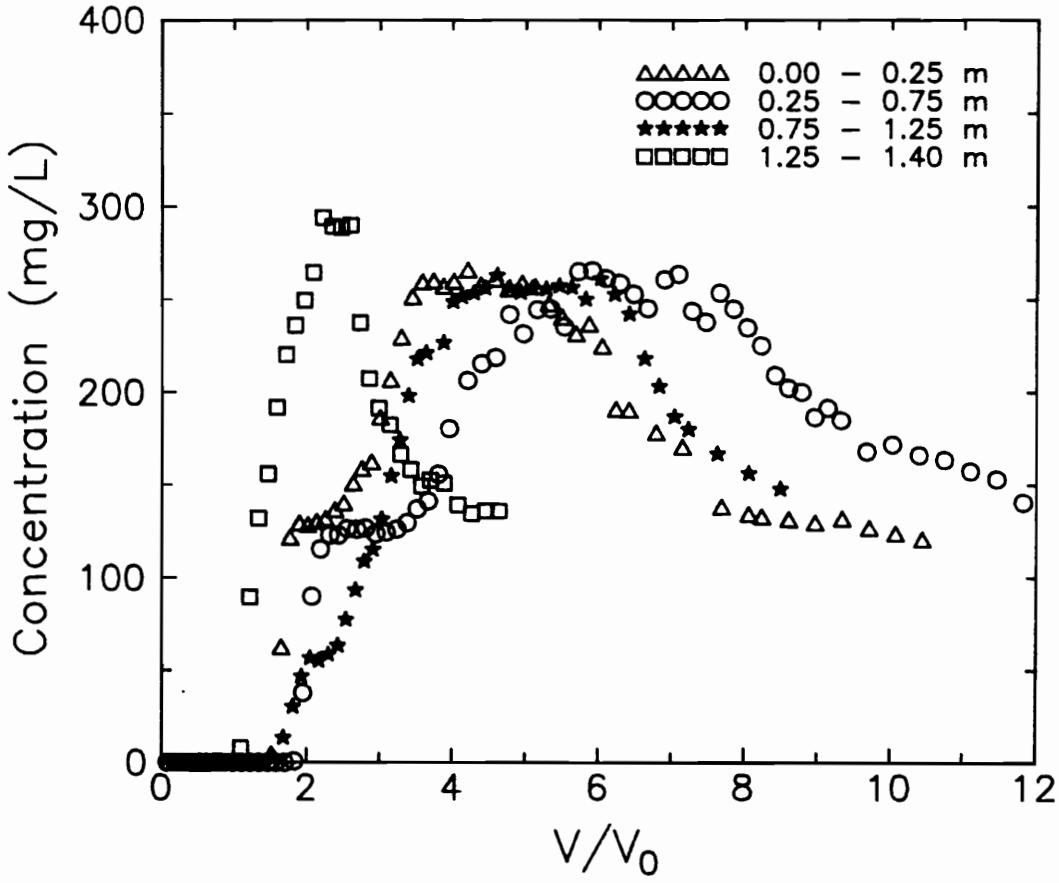

Figure 6. Column effluent concentration vs. reduced time: Al.

Table 5. Exchange phase composition.

Depth m	Al	Ca	Mg	Na	K	Be	Co	Cr	Cu	Li	Mn	Ni	Si	Sr	Zn
	---------- $mmol_c\ kg^{-1}$ ----------					---------- $\mu g\ g^{-1}$ ----------									
0.00 - 0.25	37.52	1.08	5.27	0.23	0.24	ND	ND	ND	0.05	ND	0.2	ND	10.3	0.75	0.02
0.25 - 0.75	57.77	1.28	8.62	0.18	0.38	0.01	ND	ND	0.34	0.04	0.2	ND	22.0	1.10	ND
0.75 - 1.25	29.29	1.99	5.20	0.36	0.30	ND	ND	ND	0.21	ND	0.3	ND	14.1	0.79	ND
1.25 - 1.40	19.07	ND	1.61	0.20	0.64	ND	ND	ND	0.02	ND	ND	0.05	4.6	ND	1.77

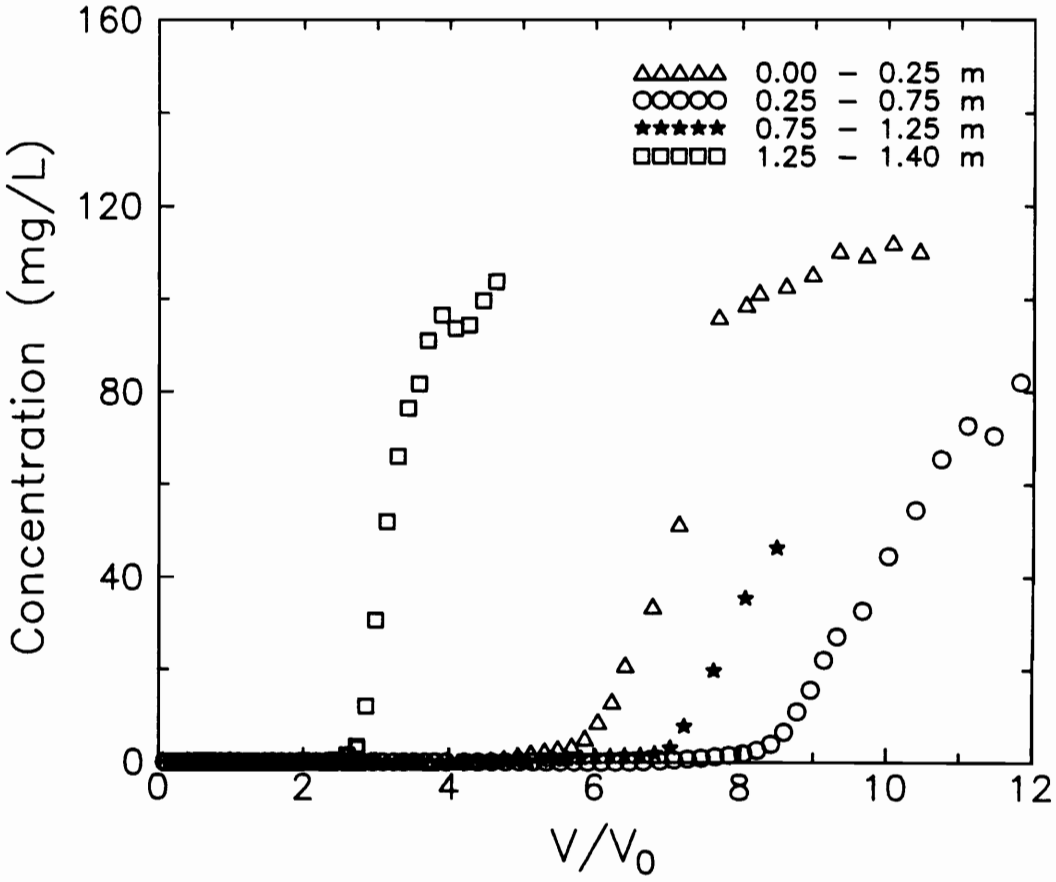

Figure 7. Column effluent concentration vs. reduced time: Fe.

source of Si and also Al in coal spoil solutions. Filipek et al. (1987) similarly suggested that the dissolution of phyllosilicate minerals was the principal source of Si found in acid mine drainage.

Alkali Metals

Breakthrough curves of potassium (K), lithium (Li), sodium (Na), and for the four sample depths are provided in Figures 9-11. One notices quite disparate behavior for these three alkali metals. Though a considerable amount of scatter in the data was found, peak K concentrations tend to occur later in the leaching process for samples with higher CEC values (Figure 9). Unlike that noted for Al, however, no relationship between native exchange phase K content and elution profile intensity was apparent (e.g., the aquifer sample had the highest exchangeable K level (Table 5) though greatest eluted K was noted for the 0.75-1.25 m sample) (Figure 9). The K-bearing phyllosilicate minerals present within these materials (Table 4) may be an additional source of K to solution.

A general lack of detectable exchange phase Li (Table 5) apparently resulted in the absence of a pronounced effluent peak noted for other elements (Figure 10), with breakthrough again concurrent with that of sulfate (Figure 4). Rather only subtle peaks at $\simeq$2 and 4 pore volumes for the 0.25-0.75 and 1.25-1.40 m samples were noted, with column effluent Li concentrations then corresponding to approximately that of the influent (Figure 10). Native exchangeable Li for Coastal Plain soils is generally very low, on the order of 1 μmol kg^{-1} (Anderson et al., 1988).

Sodium breakthrough is rapid and sharp (Figure 11), quickly returning to a concentration near that of the influent (Table 1), and provides an interesting contrast to that

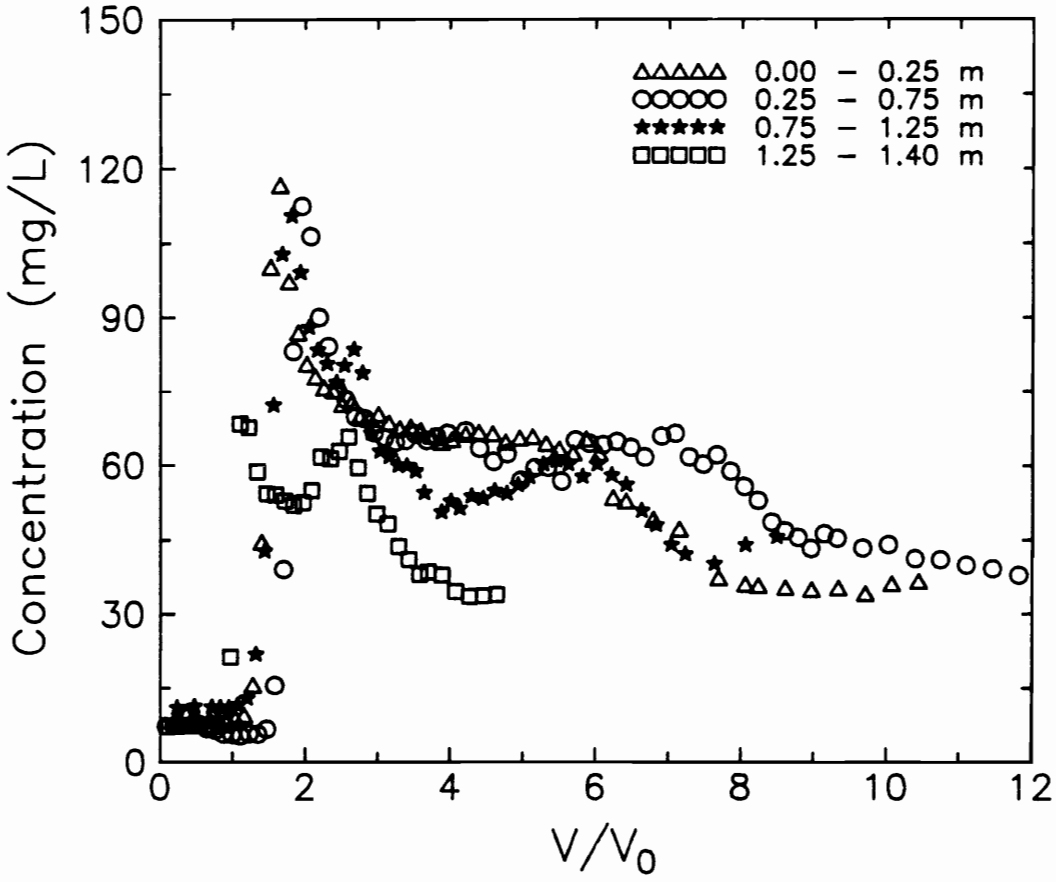

Figure 8. Column effluent concentration vs. reduced time: Si.

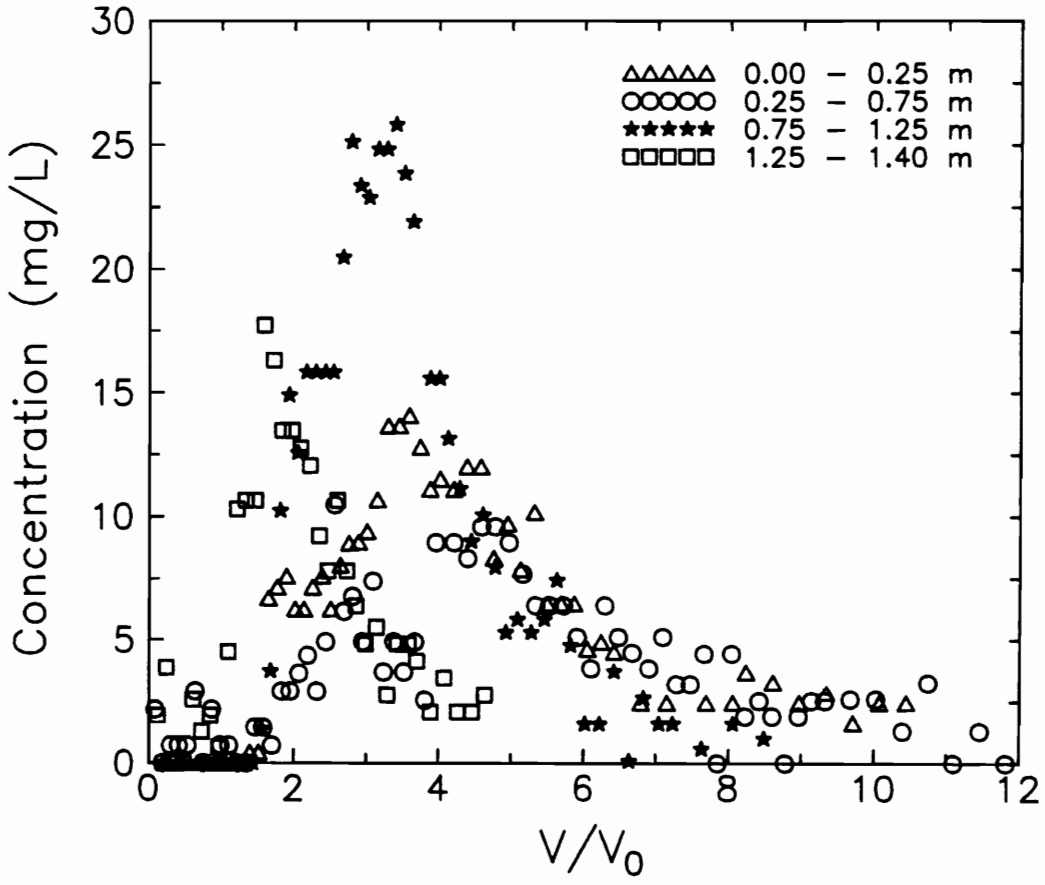

Figure 9. Column effluent concentration vs. reduced time: K.

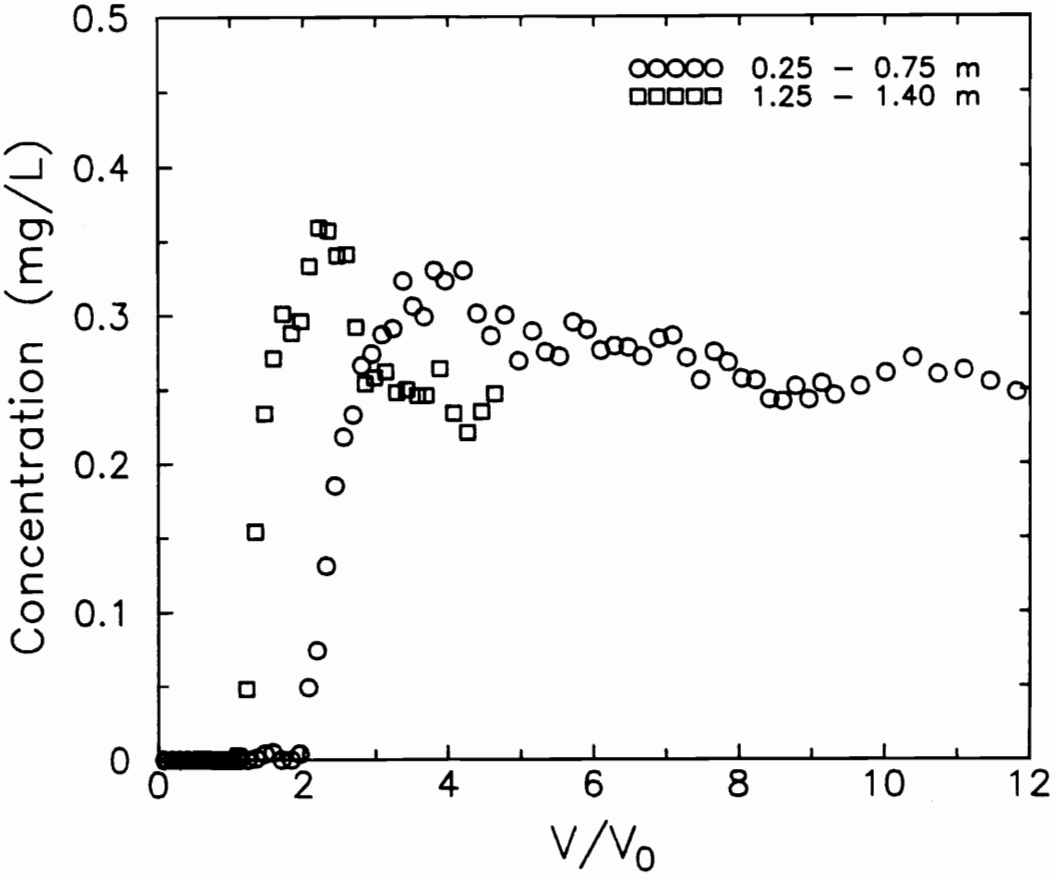

Figure 10. Column effluent concentration vs. reduced time: Li.

of K (Figure 9). Both Na and K are relatively minor components of the exchange phase of the samples (Table 5), and monovalent. Yet the K peak for all samples is retarded and also greatly broadened relative to Na (Figures 9 and 11). Considerable research has established, however, that a number of 2:1 clay minerals have a high selectivity for K over other common soil cations (Sposito, 1984). Due to its low hydration energy and size, which allows it to fit easily into hexagonal holes within Si tetrahedral layers (Sposito, 1984), K can participate in fixation reactions with certain 2:1 phyllosilicate minerals (e.g., vermiculite) found within these materials (Table 4). The observed retardation of K relative to Na thus appears to be a result of K sorption to these highly K-selective sites, though precipitation within an alunite or jarosite phase can not be discounted.

Alkaline Earth Metals

Breakthrough for all the alkaline earth metals (Figures 12-15) commences coincident with the breakthrough of sulfate (Figure 4) and the initial decline in pH (Figure 3). Initial breakthrough was related to the presence of native exchangeable metals, the magnitude of which descends in the order Mg > Ca > Sr > Be (Table 5).

While exchangeable Ca and Mg is a commmon feature of soils, reports of native exchangeable Sr and Be are less frequent. Exchangeable Be within Coastal Plain soils has been reported to be particularly low, on the order of 0.1 $\mu mol_c\, kg^{-1}$ (Anderson et al., 1990). Hydrolysis and precipitation of Be would not be expected under the pH and concentrations in these experiments (Baes and Mesmer, 1976). Peak effluent concentrations of Ca (Figure 13) and Mg (Figure 14) follow the general trend noted for Al (Figure 6), with peak concentration and retardation being related to CEC (Table 2) and exchange phase content (Table 5). For example, the highest

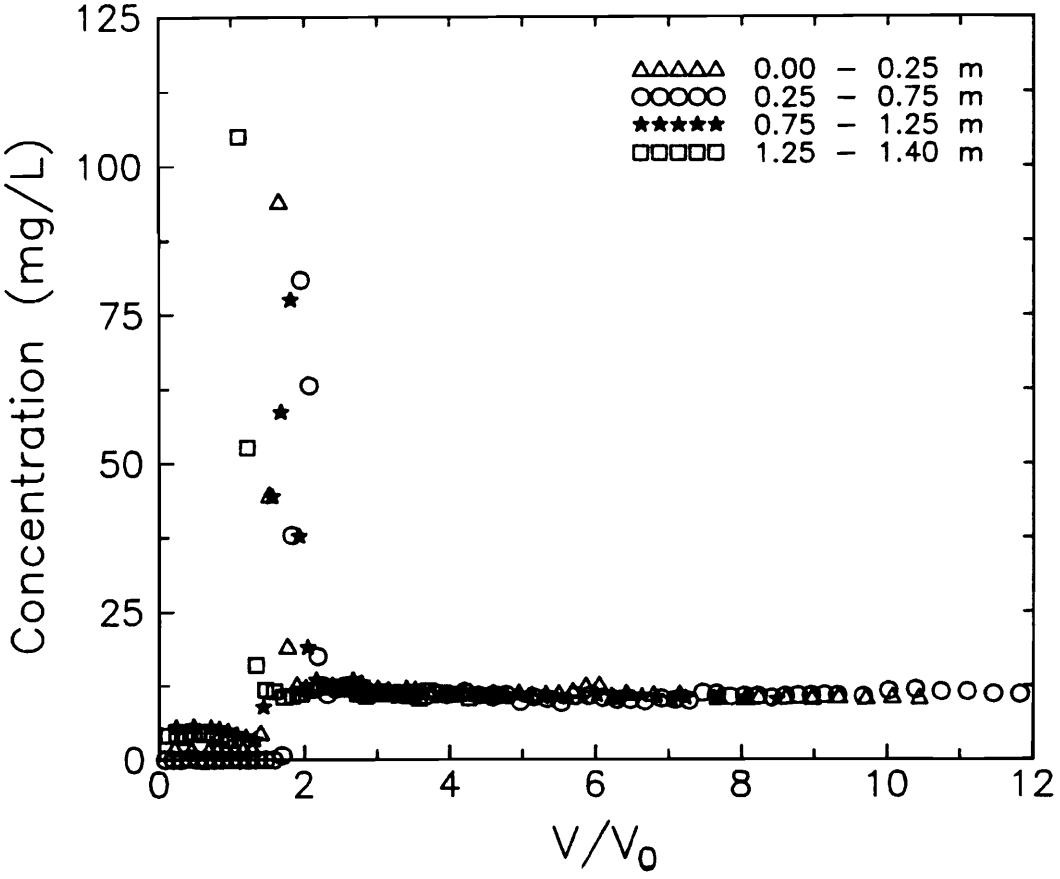

Figure 11. Column effluent concentration vs. reduced time: Na.

exchange phase Ca content of the 0.75-1.25 m sample resulted in the greatest peak concentration and peak intensity, while the peak Ca concentration occurred latest for the highest CEC 0.25-0.75 m depth (Figure 13). Strontium exhibited similar trends to Ca and Mg, though two peaks in the breakthrough curve were noted for the 0.25-0.75 m sample (Figure 15). This depth possessed the highest native exchangeable Sr as well as the highest CEC. Apparently these factors resulted in a chromatographic separation and elution of Sr in two chromatographic waves (Figure 15).

Transition Metals

The breakthrough of Ni, Zn, Co, and Mn all tend to follow one another very closely for a given material (Figures 16-19). As with other elements, initial appearance in the effluent was related to sulfate mobility, while peak concentrations tended to be retarded to a degree related to CEC, with peak concentrations occurring at the shortest pore volumes for the lowest CEC aquifer material and longest for the highest CEC 0.25-0.75 m sample (Figures 16-19). This observation was tested more rigorously by a simple statistical analysis in which CEC, Ox-Fe, and DCB-Fe contents were regressed against the V/V_0 at which peak effluent concentrations were noted. Notwithstanding the small sample size (only two degrees of freedom), CEC was the only soil property which had a significant correlation with observed peak effluent transition metal concentrations ($r = 0.94$, significant at 0.10). Oxalate and DCB-extractable Fe yielded non-significant correlation coefficients of 0.40 and 0.75, respectively, when regressed against V/V_0. This suggests that ion exchange is the principal reaction governing transport of these metals for these soils leached with coal pile runoff. Thus, though specific adsorption to native Fe phases is a well-established mechanism for removal of trace metals from solution (Jenne, 1968), neither sorption to native Fe phases nor coprecipitation with freshly precipitating phases

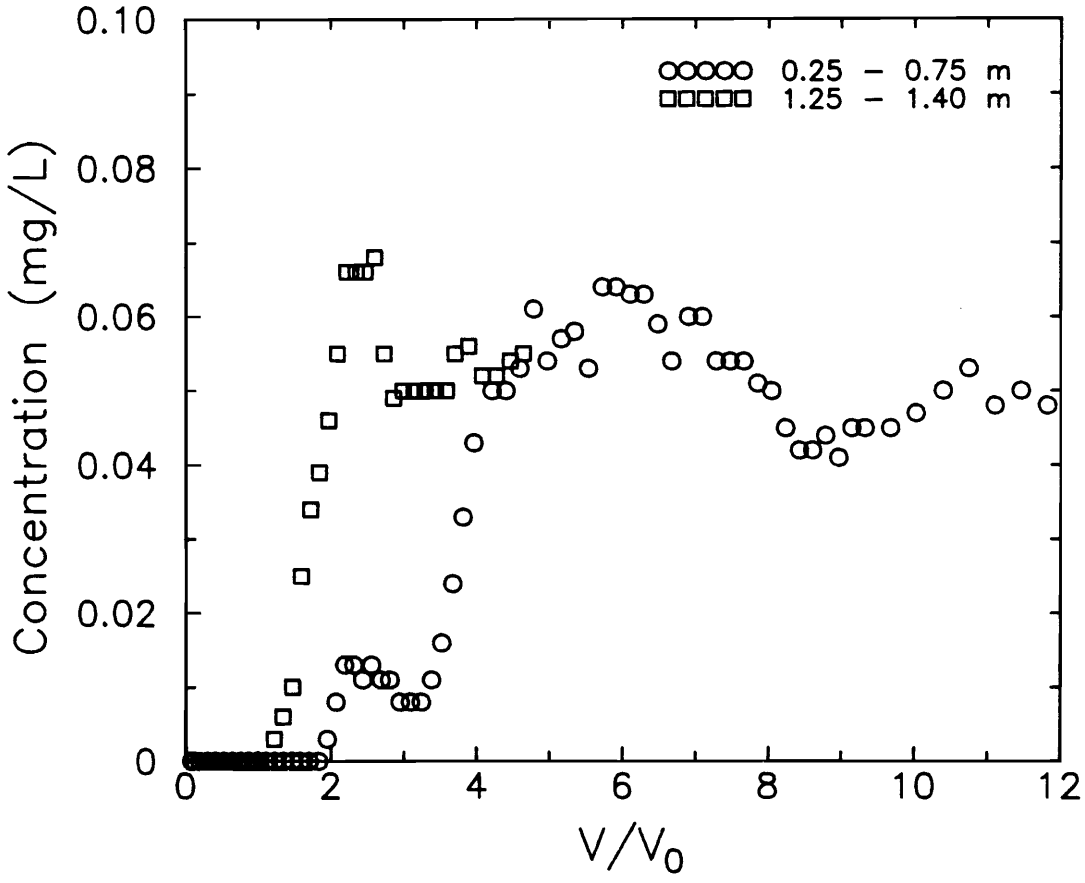

Figure 12. Column effluent concentration vs. reduced time: Be.

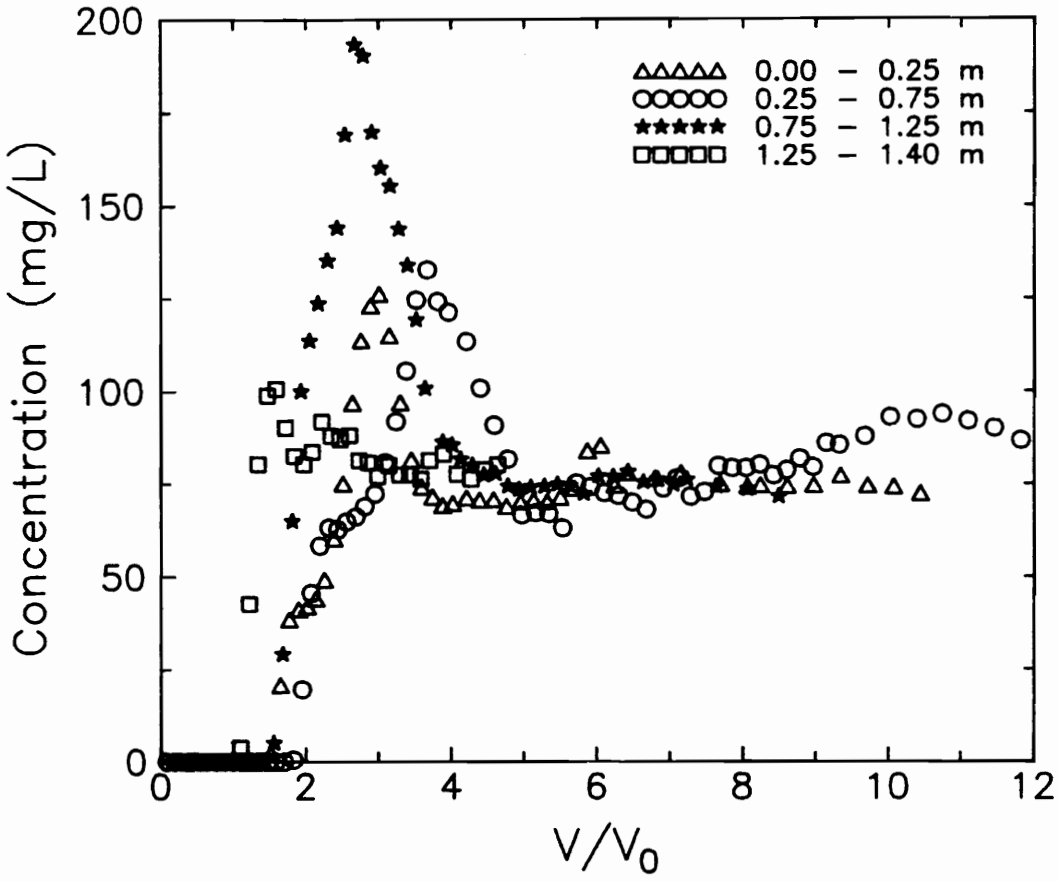

Figure 13. Column effluent concentration vs. reduced time: Ca.

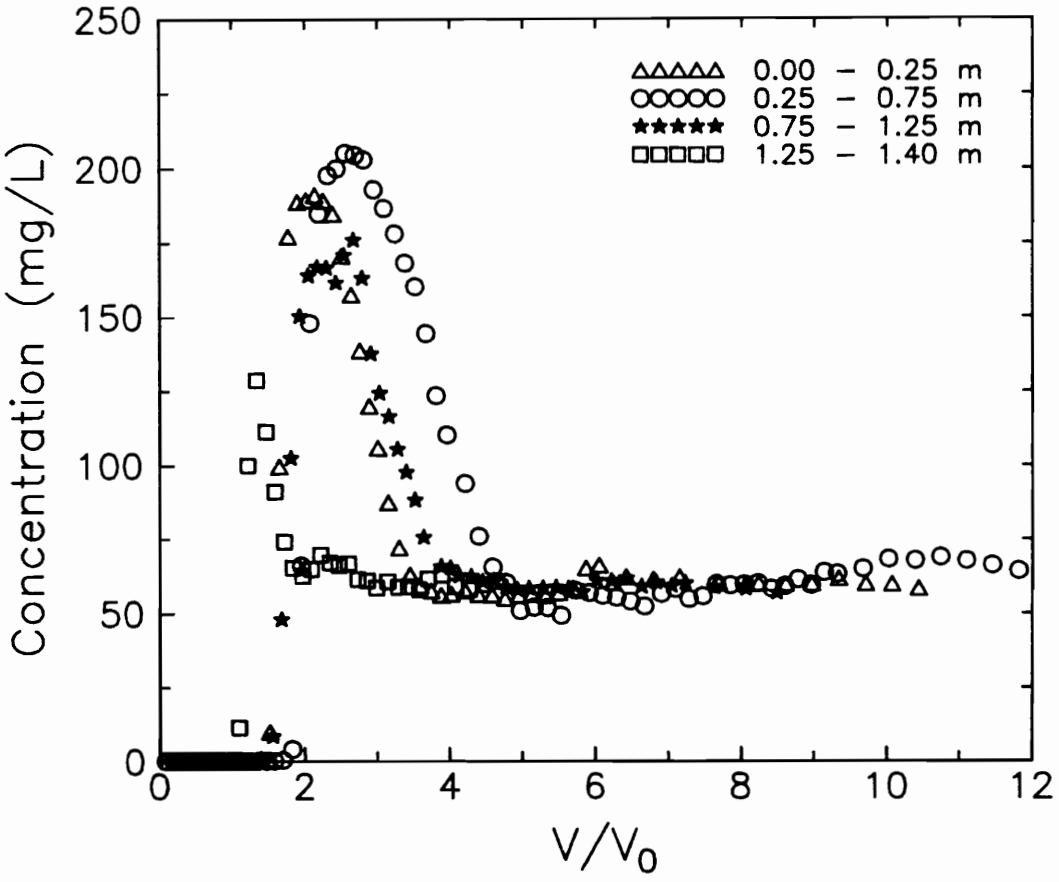

Figure 14. Column effluent concentration vs. reduced time: Mg.

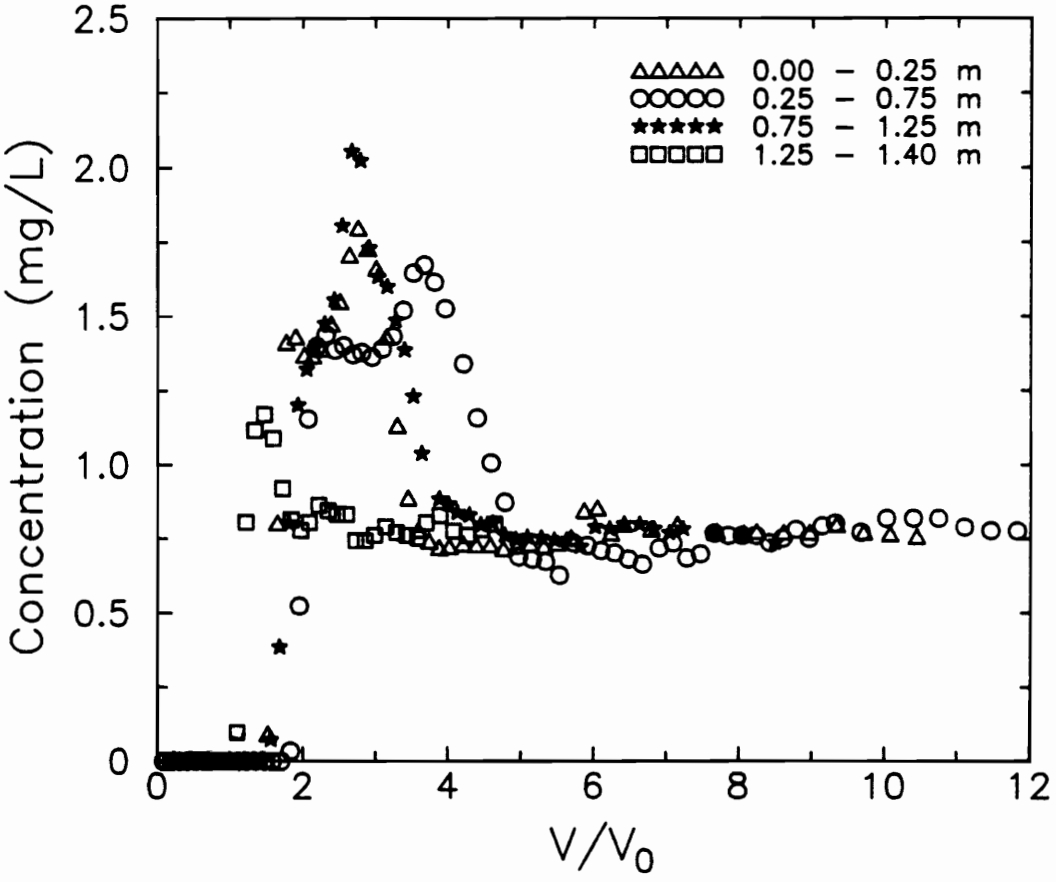

Figure 15. Column effluent concentration vs. reduced time: Sr.

wholly regulates Ni, Zn, Co, and Mn activities in solution. Additionally, pH-adsorption edges for these metals with ferric hydroxides tend to be above the native soil pH, and well above the pH range encountered during much of the leaching experiments (Benjamin and Leckie, 1981; Forbes et al., 1976). Considering the 0.25-0.75 m sample, one notices that the peak metal concentrations coincide with the second peak in the breakthrough curve for Sr (Figure 15). Apparently the lack of significant exchangeable transition metal contents (Table 5) results in the reduction or absence of the first peak at $\simeq$ 2.2 pore volumes most apparent for Sr.

Unlike the previous transition metals, Cr and Cu exhibited quite different breakthrough behavior (Figures 20 and 21, respectively). While limited amounts tended to break through with the other transition metals, peak concentrations occurred much later, and approximately coincided with the descent in pH from 3.5 toward the influent pH of 2.13, with peak Cr (Figure 20)lagging slightly behind that of Cu (Figure 21). It thus appears that Cr and Cu mobility is regulated by a mechanism different than that of the other transition metals examined. The pH dependence implies a precipitation-dissolution, coprecipitation, or specific adsorption-desorption reaction.

Influence of Flow Rate on Observed Transport

To ascertain the influence of flow rate on the breakthrough behavior of elements, the aquifer material was also leached under steady saturated flow at a Darcy velocity of 0.2 cm/h. Selected results are presented in Figures 22-25. Hydrogen ion activity as a function of eluted pore volumes exhibitted similar behavior to that at q = 1.3 cm/h at short V/V_0, though deviated at higher pore volumes (Figure 22). Decreasing q re-

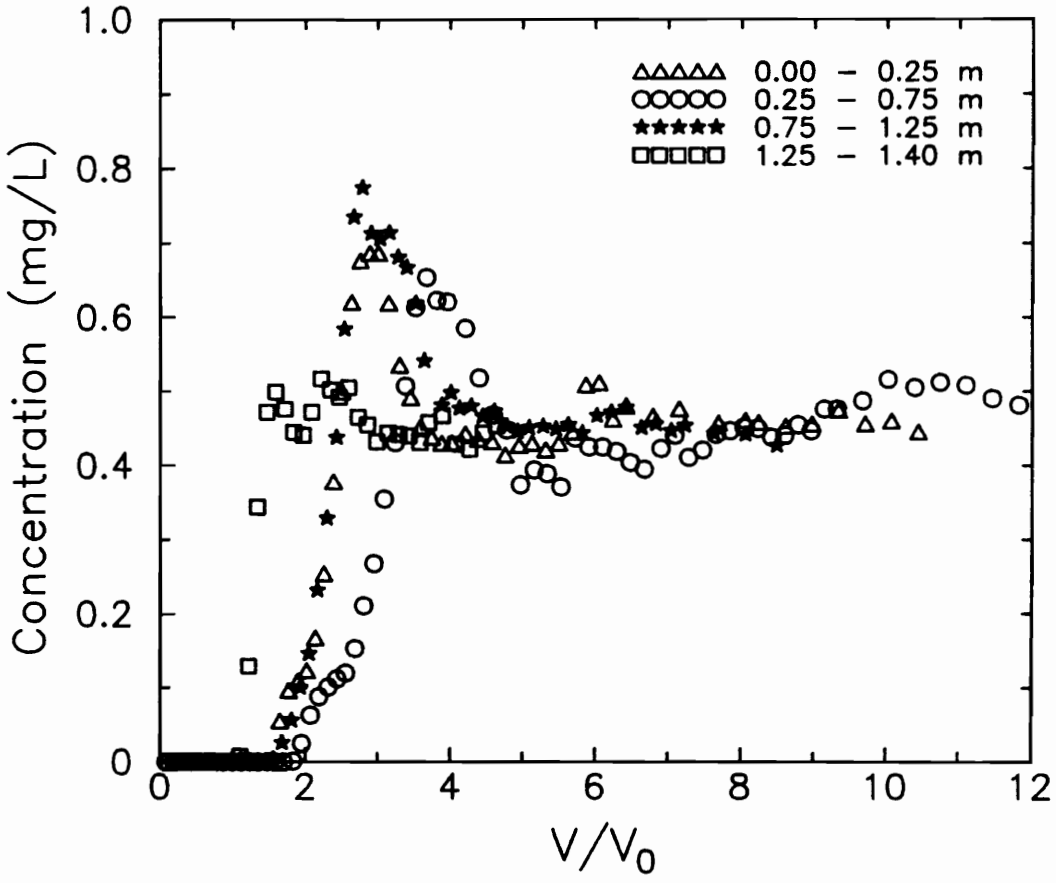

Figure 16. Column effluent concentration vs. reduced time: Co.

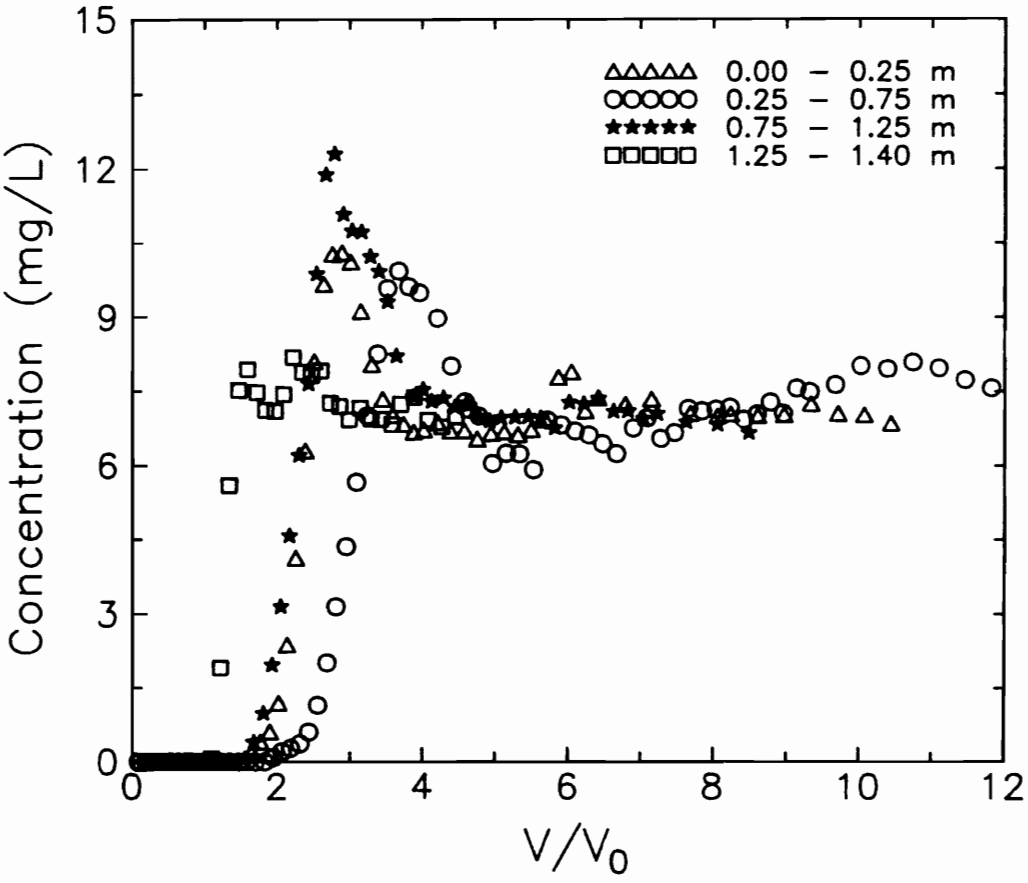

Figure 17. Column effluent concentration vs. reduced time: Mn.

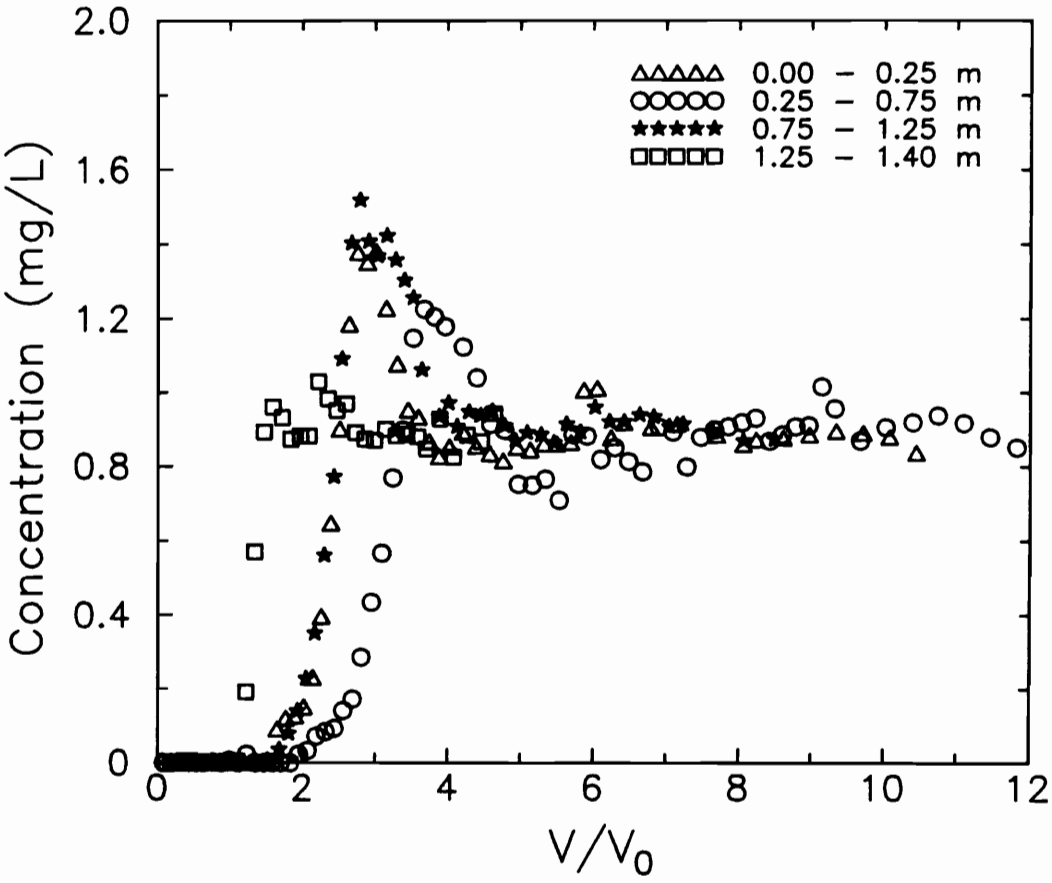

Figure 18. Column effluent concentration vs. reduced time: Ni.

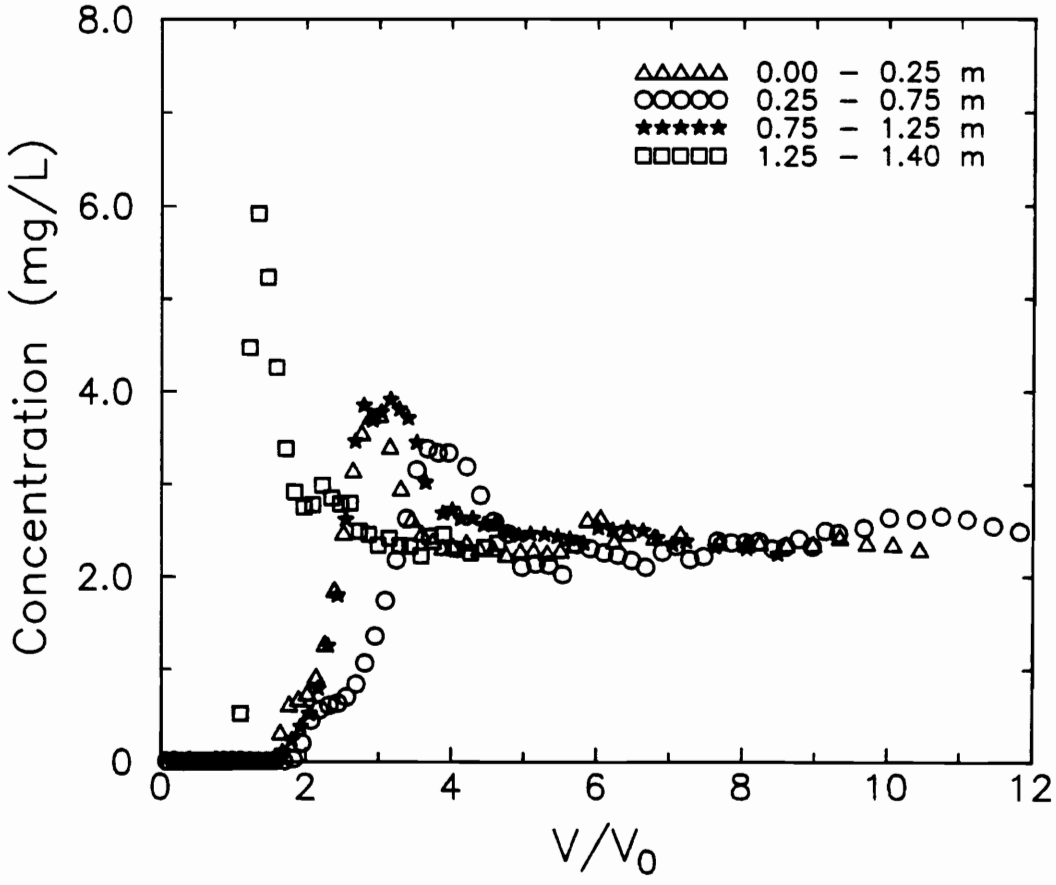

Figure 19. Column effluent concentration vs. reduced time: Zn.

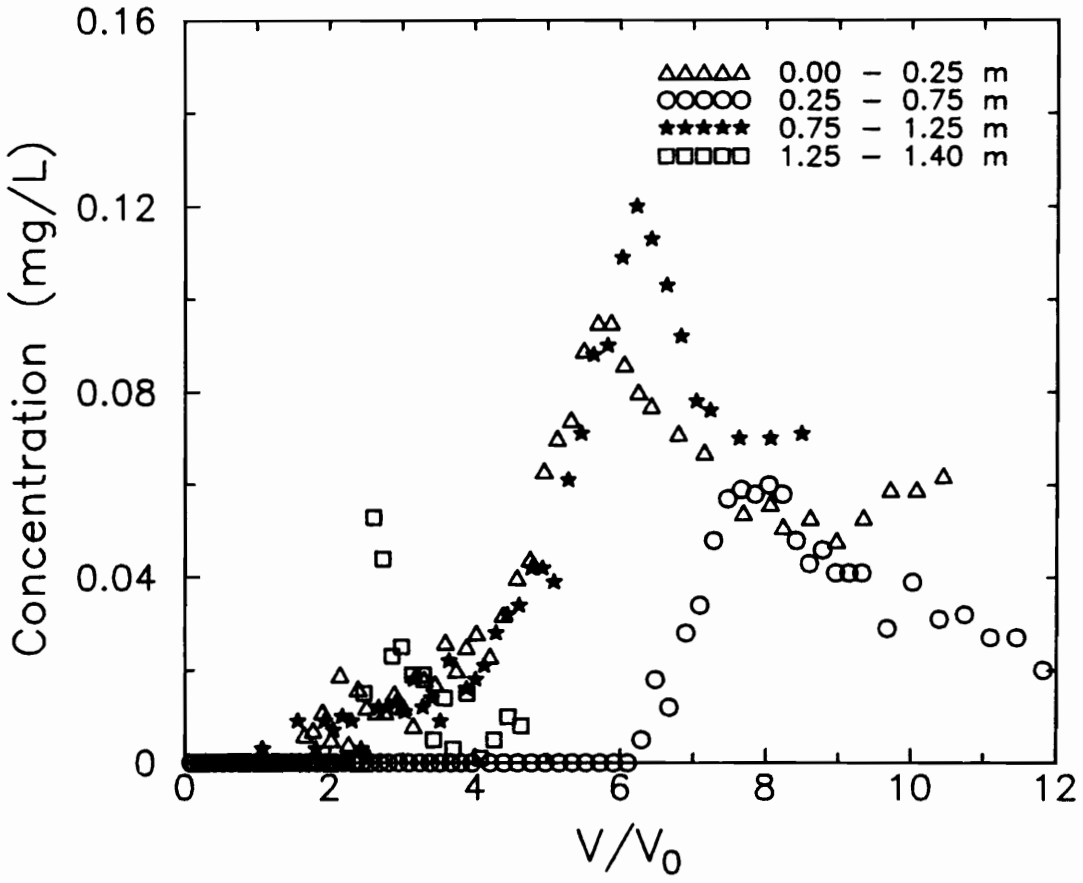

Figure 20. Column effluent concentration vs. reduced time: Cr.

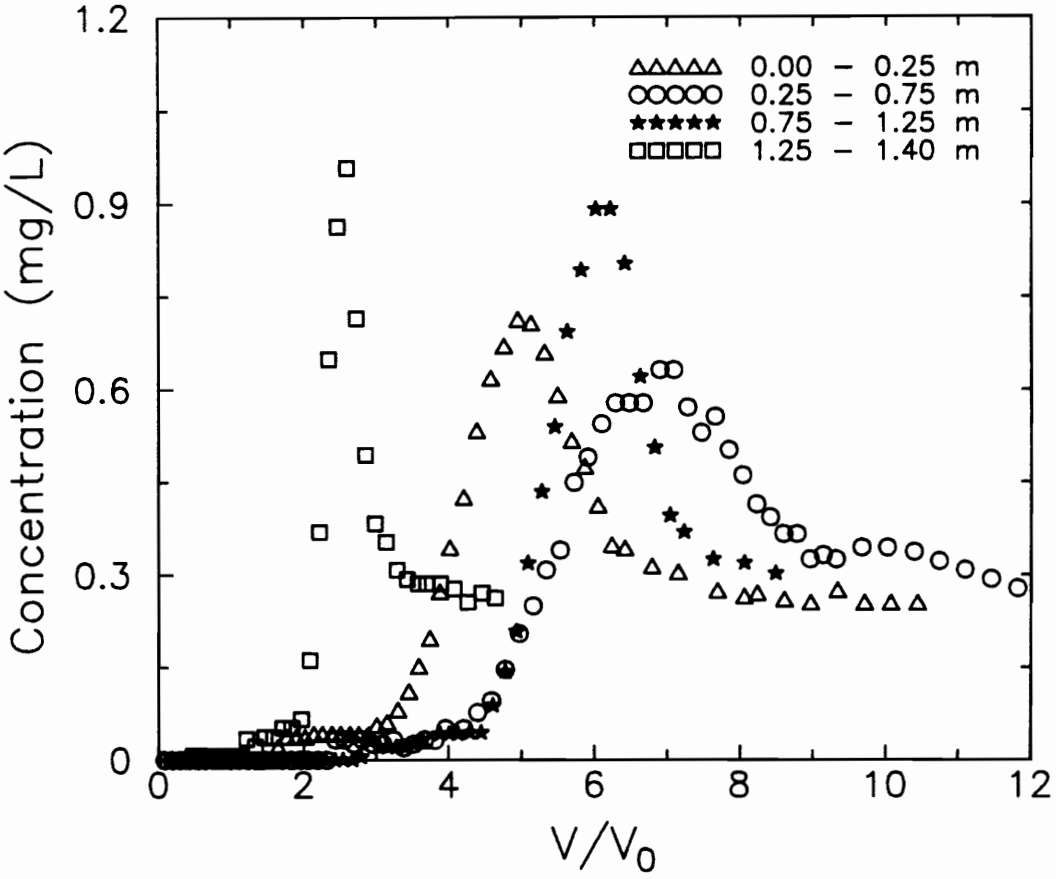

Figure 21. Column effluent concentration vs. reduced time: Cu.

sulted in longer apparent buffering at pH ≃3.5 before descending toward influent pH. Effluent Si followed this general trend (Figure 23), lending support for a desilication reaction contributing to the buffer capacity of the soils. Flux of Co through the column, which was suggested to be controlled by ion exchange, was little affected by Darcy velocity (Figure 24). This observation implies local equilibrium with respect to components partitioning between solution and soil exchange sites. Copper, whose mobility was apparently controlled by a more specific interaction with the solid phase, was sensitive to flow rate however (Figure 25). Peak Cu concentration again coincided with the decrease in pH from that of the buffer region.

Solubility Relations

A number of solid phases have been proposed to control element solubilities within acid mine drainage systems (e.g., Nordstrom, 1982) Effluent fractions were speciated with the geochemical model MINTEQA2 (Brown and Allison, 1987) to assess the potential for such phases controlling observed aqueous phase chemistry. Saturation indices (SI) defined as

$$SI = \log\left(\frac{IAP}{K_{sp}}\right) \quad (1)$$

where IAP is the ion activity product of a solution and K_{sp} is the solubility product for a given mineral phase, for selected solid phases as a function of V/V_0 for the aquifer material are illustrated, though very similar trends were observed for the other materials as well.

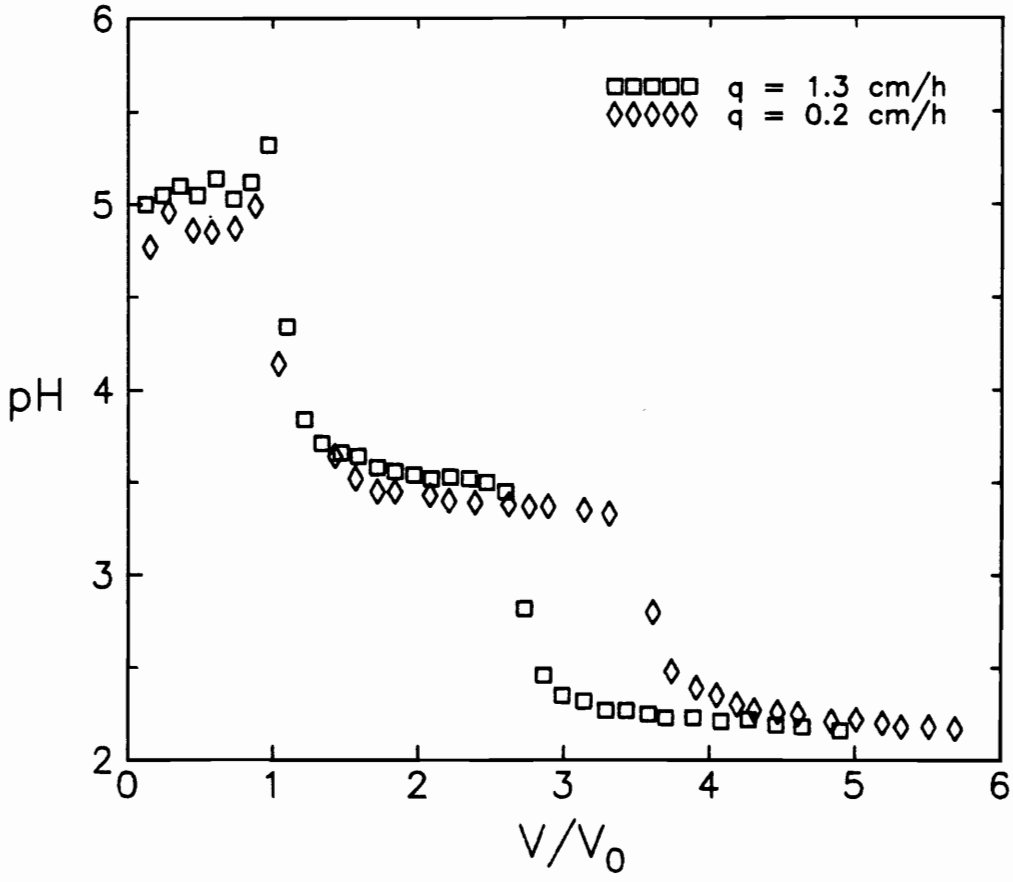

Figure 22. Column effluent concentration vs. reduced time as a function of Darcy velocity (1.25 - 1.40 m material): pH.

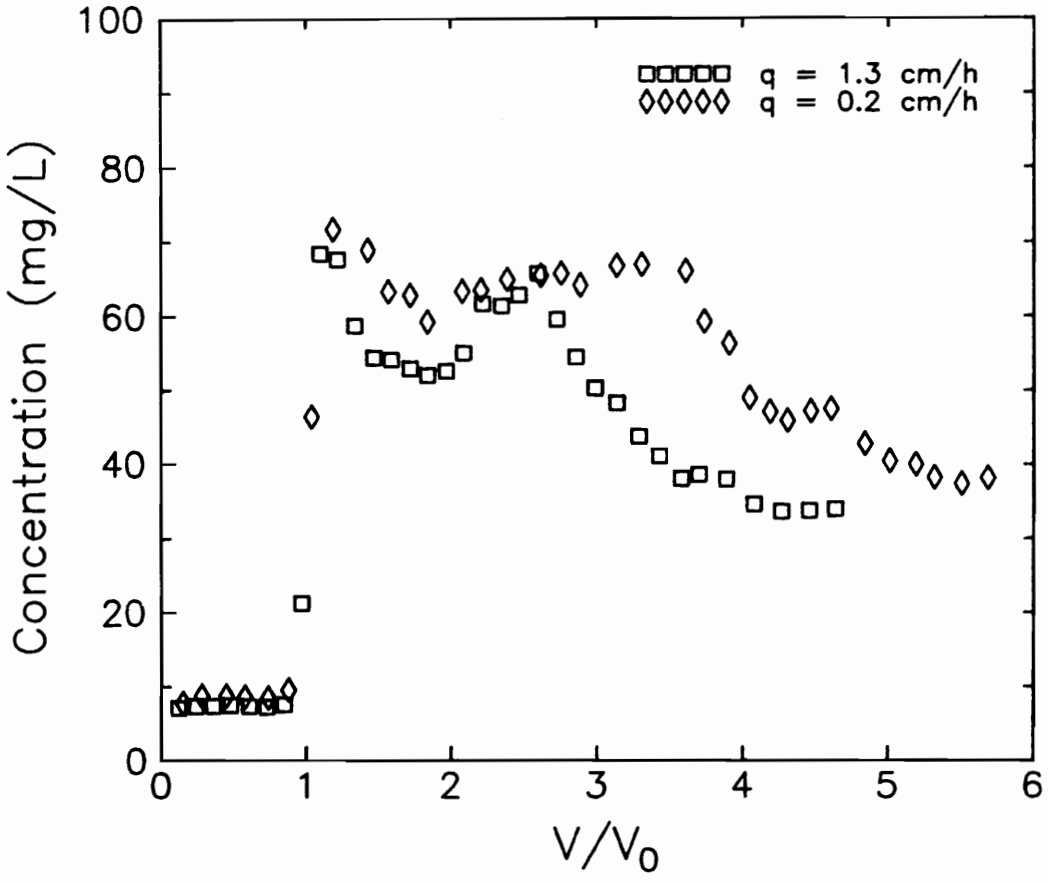

Figure 23. Column effluent concentration vs. reduced time as a function of Darcy velocity (1.25 - 1.40 m material): Si.

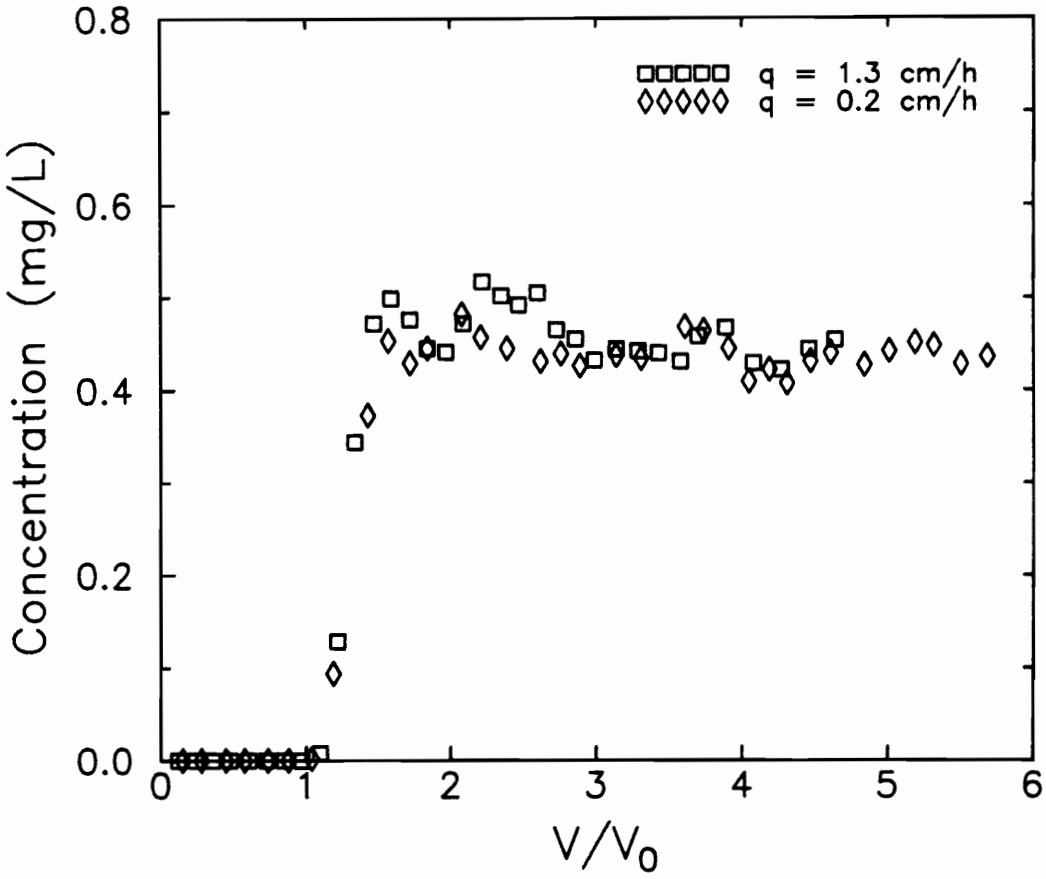

Figure 24. Column effluent concentration vs. reduced time as a function of Darcy velocity (1.25 - 1.40 m material): Co.

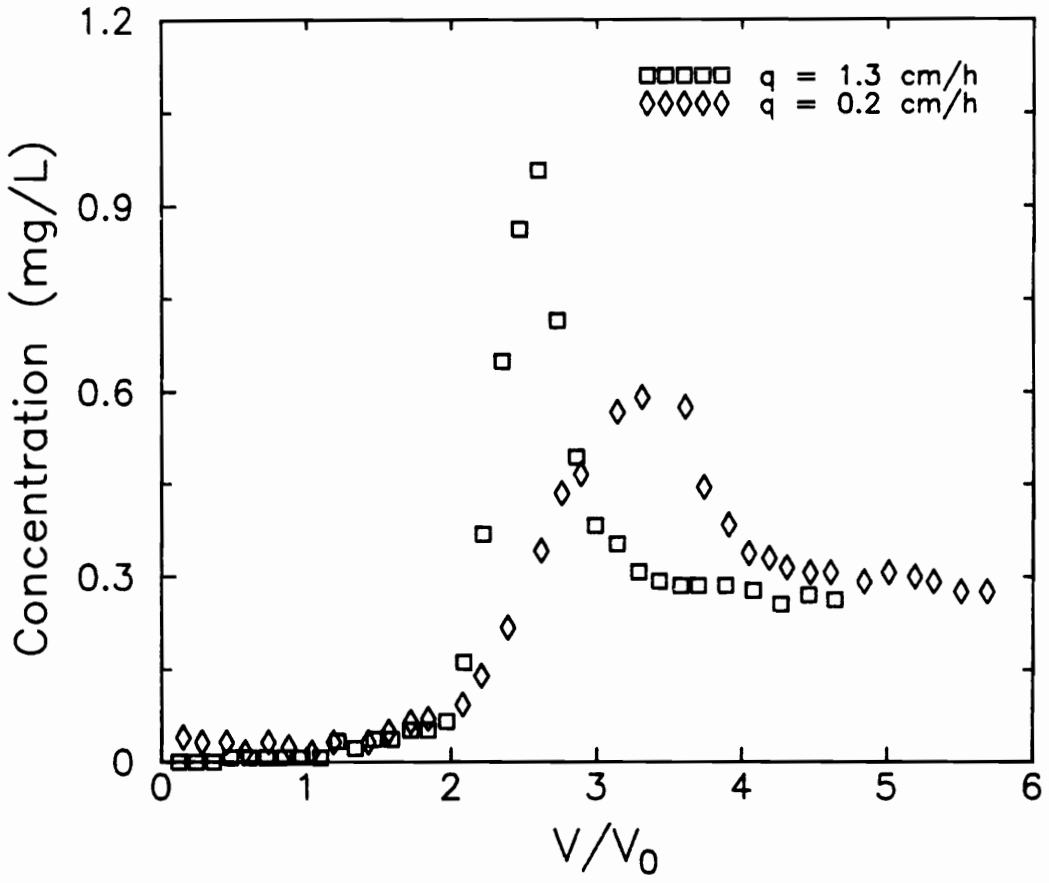

Figure 25. Column effluent concentration vs. reduced time as a function of Darcy velocity (1.25 - 1.40 m material): Cu.

Aluminum solubility most closely followed that of jurbanite, $AlOHSO_4$ (Figure 26). Both amorphous $Al(OH)_3$ and K-alum were undersaturated over the entire course of the leaching process. Jurbanite and alunite ($KAl_3(SO_4)_2(OH)_6$) were supersaturated until $V/V_0 \simeq 2.7$, the pore volume in which the soil buffer was exhausted and the pH began to decrease (Figure 3). Van Breeman (1973) suggested that $AlOHSO_4$ governs Al solubility for a range of acid sulfate soils. Nordstrom (1982) outlined the solubility relations for Al in the presence of SO_4^{2-} at low to moderate pH and reported that jurbanite solubility was in good agreement with the data of van Breeman (1973) and proposed that jurbanite controls the solubility of Al in many acid sulfate soils and acid mine drainage systems. Nordstrom and Ball (1986) noted more recently, however, at pH < 4.6, Al in surface acid drainage waters was generally transported conservatively and that apparent conformance with solubility limits was coincidental. Similar observations by Filipek et al. (1987) suggests that similarities between dissolved Al concentrations and jurbanite solubility may be misleading.

Iron was below detection limits within the effluent at early V/V_0 and as a result saturation indices are not available until $\simeq 2.5$ pore volumes. Unlike Al, in which saturation indices generally decreased below 0 at $V/V_0 > 2.5$-3 (Figure 26), the decrease in pH and appearance of Fe in the effluent yielded positive saturation indices for a number of Fe oxyhydroxide and basic sulfate phases (Figure 27). The column effluent was undersaturated only with respect to the highly soluble ferrihydrite. Results indicate that Fe concentrations in the column effluent most closely follow that predicted by assuming Na-jarosite controls Fe solubility. Variously substituted jarosites have been previously postulated to control Fe solubility within acid sulfate soils and acid mine drainage systems (Nordstrom, 1982), though significant supersaturation of acid mine

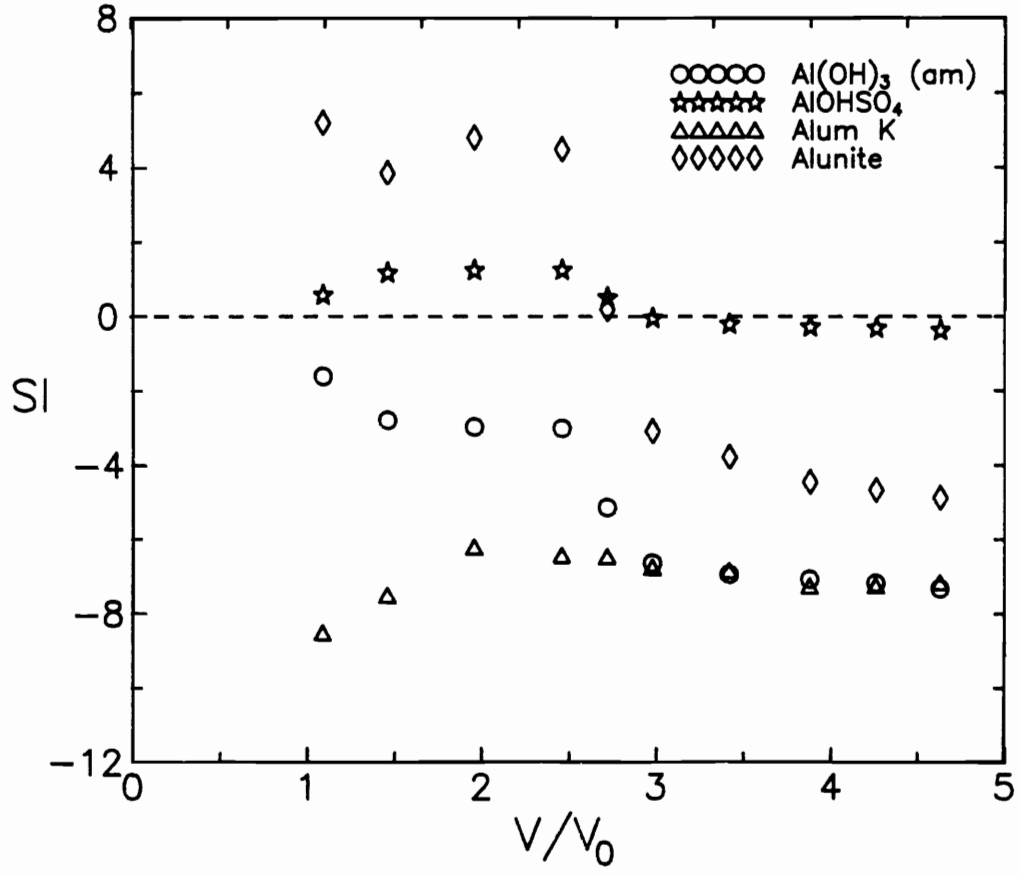

Figure 26. Saturation indices for selected aluminum minerals vs. reduced time (1.25 - 1.40 m material).

waters with respect to jarosite mineral phases has also been reported (Chapman et al., 1983; Filipek et al., 1987).

A number of solid phases proposed to control trace metal solubilities in soils (Lindsay, 1976) were also evaluated. No evidence for precipitation-dissolution reactions controlling metal mobility was found. For example, cupric ferrite, which has been suggested to control Cu solubility in soils, was undersaturated over the course of the leaching process, and thus does not explain the breakthrough behavior noted (Figure 21). Filipek et al. (1987) also reported that Cu and Zn were undersaturated with respect to all potential mineral phases for an acid drainage-surface water confluence.

Solubility calculations for selected Si-bearing minerals demonstrate that aqueous Si concentrations follow very closely that based on an amorphous SiO_2 phase (Figure 28). Transition from supersaturation to undersaturation for the phyllosilicates, as noted for the Al phases (Figure 26), occurs when the effluent pH descends below $\simeq$3.5 (Figure 28). Thus, both the kaolinite and mica within the samples (Table III) can be expected to undergo dissolution under prolonged leaching and, as noted by Barnhisel and Rotromel (1974) and Filipek et al. (1987), provide Si and other mineral structural components to solution.

As mineral dissolution is generally a slow process, being surface controlled under most conditions (Berner, 1978), the influence of flow rate on observed saturation indices was also evaluated. Saturation indices as a function of q for the phases which were found to most closely follow observed aqueous chemistries are shown in Figure 29. No discernible influence on the saturation index for the SiO_2 (am) phase was noted. Slight deviations for jurbanite and Na-jarosite at $V/V_0 > 2.5$ (Figure 29) result

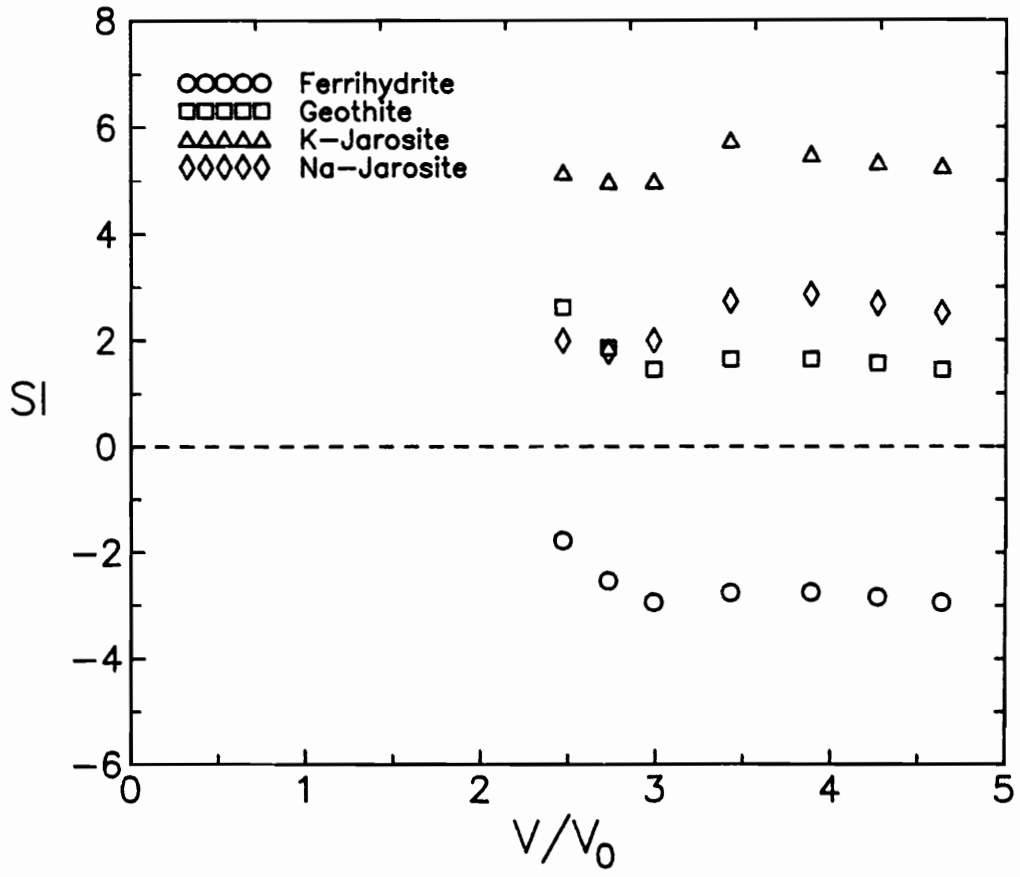

Figure 27. Saturation indices for selected iron minerals vs. reduced time (1.25 - 1.40 m material).

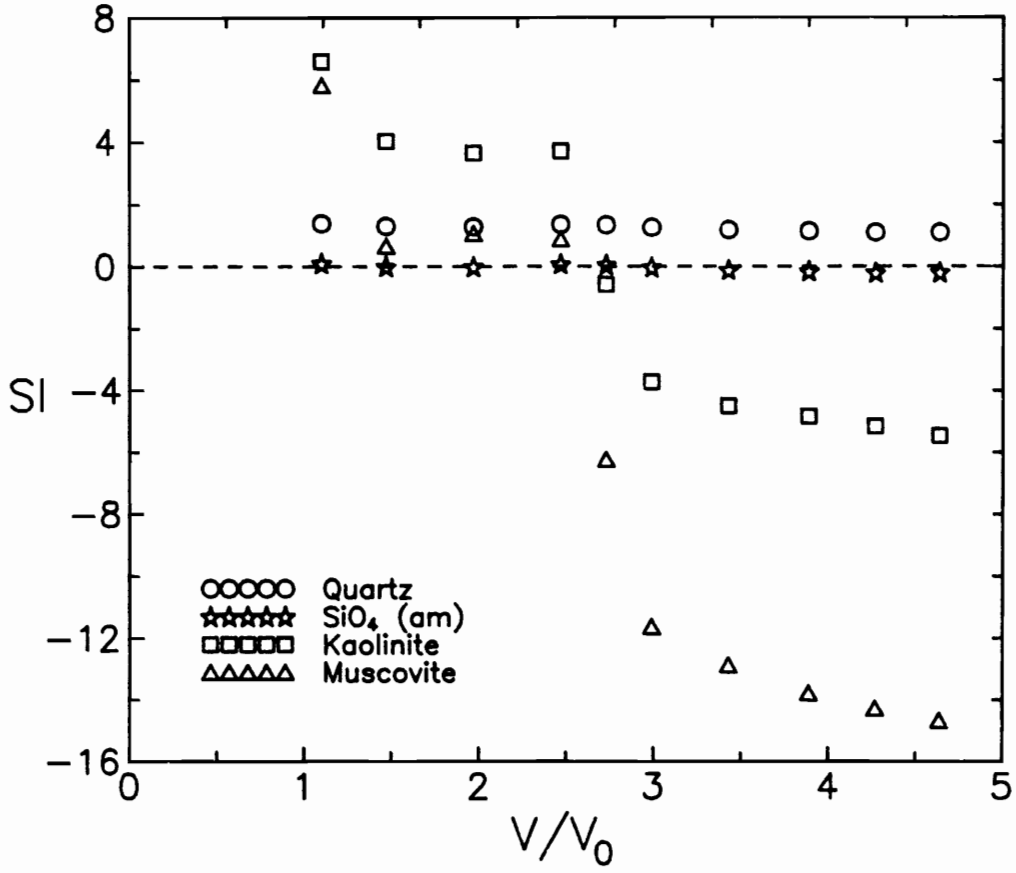

Figure 28. Saturation indices for selected silicate minerals vs. reduced time (1.25 - 1.40 m material).

principally from the difference in effluent pH for the two Darcy velocities (Figure 22). It thus appears that deviations from local thermodynamic equilbrium are not significantly influenced by reduction in Darcy velocity from 1.3 to 0.2 cm/h.

Simple Modeling of Transport

The classical convection-dispersion equation (CDE), routinely used to model solute transport in column experiments, was evaluated for its applicability to modeling component breakthrough, employed here in the form:

$$R\frac{\partial c}{\partial t} = D\frac{\partial^2 c}{\partial x^2} - V\frac{\partial c}{\partial x} \qquad (2)$$

where c is concentration (M/L^3), t is time (T), x is distance (L), D is the hydrodynamic dispersion coefficient (L^2/T), V is the pore water velocity (L/T), and R is the retardation coefficient. The retardation coefficient, R, is equal to $1 + \rho K/\theta$, with ρ the bulk density (M/L^3), K a linear partition coefficient describing distribution between sorbed and solution phases (L^3/M), and θ the volumetric water content (L^3/L^3). Central to the CDE is that of linear partitioning between sorbed and solution phases, and on that basis, the simple CDE is theoretically an oversimplification of the chemistry controlling component mobility during this investigation. Widely available codes which expressly accommodate ion exchange, specific adsorption, and precipitation-dissolution reactions are generaly lacking, in part due to the tremendous computational effort (Yeh and Tripathi, 1989).

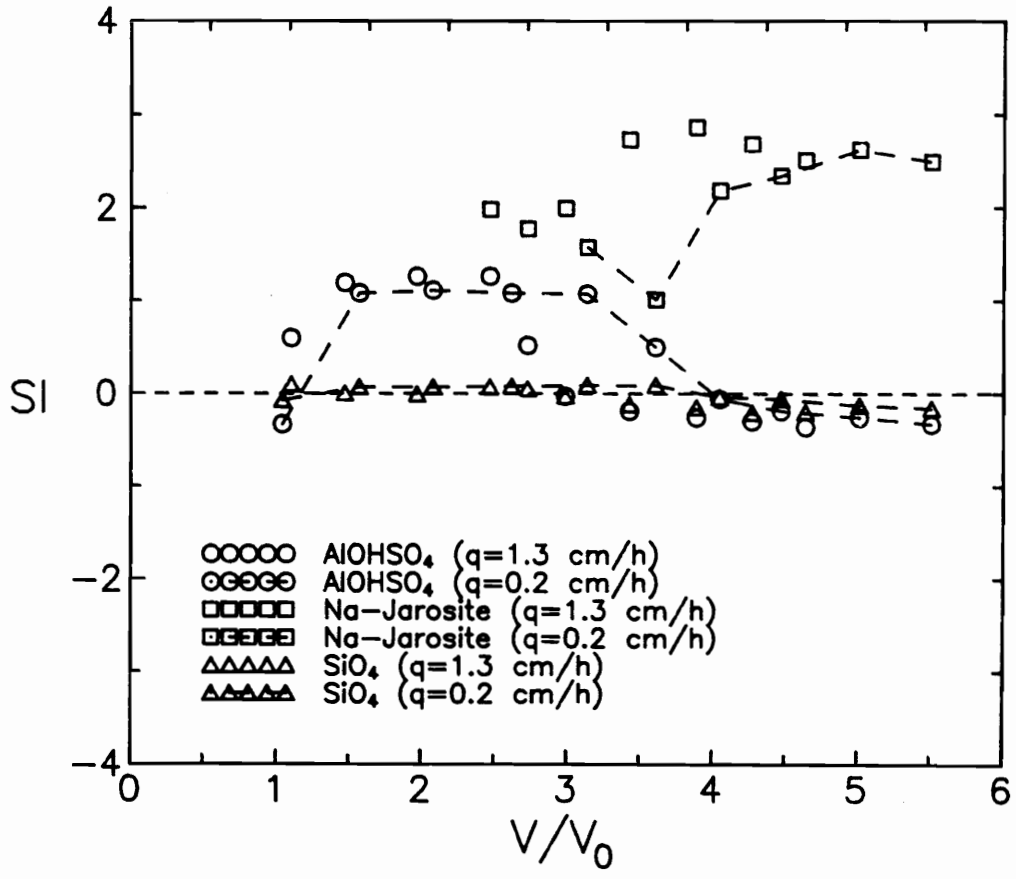

Figure 29. Saturation indices for selected minerals vs. reduced time as a function of Darcy velocity (1.25 - 1.40 m material).

Application of the simple CDE was first evaluated using a pulse of non-reactive solute (Br^-). Generally good agreement between observed (points) and fitted (line) breakthrough of Br^- was noted (Figure 30). The relative symmetry and lack of significant tailing at longer pore volumes for the Br^- indicates that the simple one-region CDE adequately describes the flow within the columns (Parker and van Genuchten, 1984). Fitted dispersion coefficients were then used as input for simulation of runoff breakthrough curves. Moderate agreement between observed (points) and predicted (lines) SO_4^{2-} breakthrough for the aquifer (1.25-140 m) and subsoil (0.25-0.75 m) materials was obtained (Figure 31), yielding fitted R's of 1.3 and 2.0, respectively. The model tended to overpredict SO_4^{2-} concentration after the initial rise in concentrations, particularly for the subsoil material, which indicates that in addition to a retardation reaction (i.e., $R > 1$), SO_4^{2-} is also participating in a reaction which is maintaining a solution concentration below the predicted C/C_0 value of 1. In general, however, the shape of the predicted breakthrough curve follows that observed (Figure 31). This relative agreement was not noted for the other elements (e.g., Figure 32). Elements in which some initial reactive mass resides within the soil exhibit pronounced waves in the breakthrough curves, as previously noted. Ion exchange, specific adsorption, and/or precipitation-dissolution reactions which result from the percolation of runoff through the soils tend to mobilize some fraction of that reactive mass and thus serve as sources not explicitly considered in the CDE. Even components in which negligible initial reactive mass exist, as in the case of a number of transition metals (Table 5), exhibit peak concentrations in column effluent in excess of influent concentration (e.g., Figure 16). Thus the transport of reversibly sorbing components also results in this general phenomenon (Clancy and Jennings, 1988).

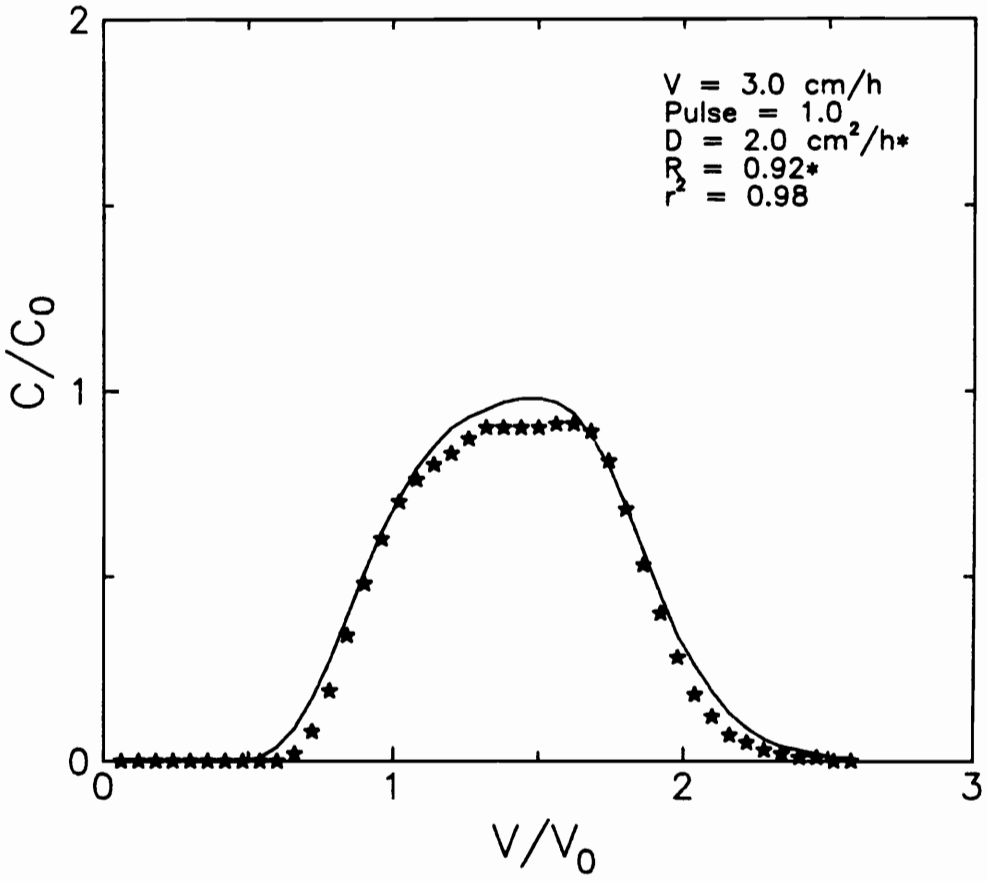

Figure 30. Observed (points) and fitted (line) bromide breakthrough curve (0.25 - 0.75 m material).

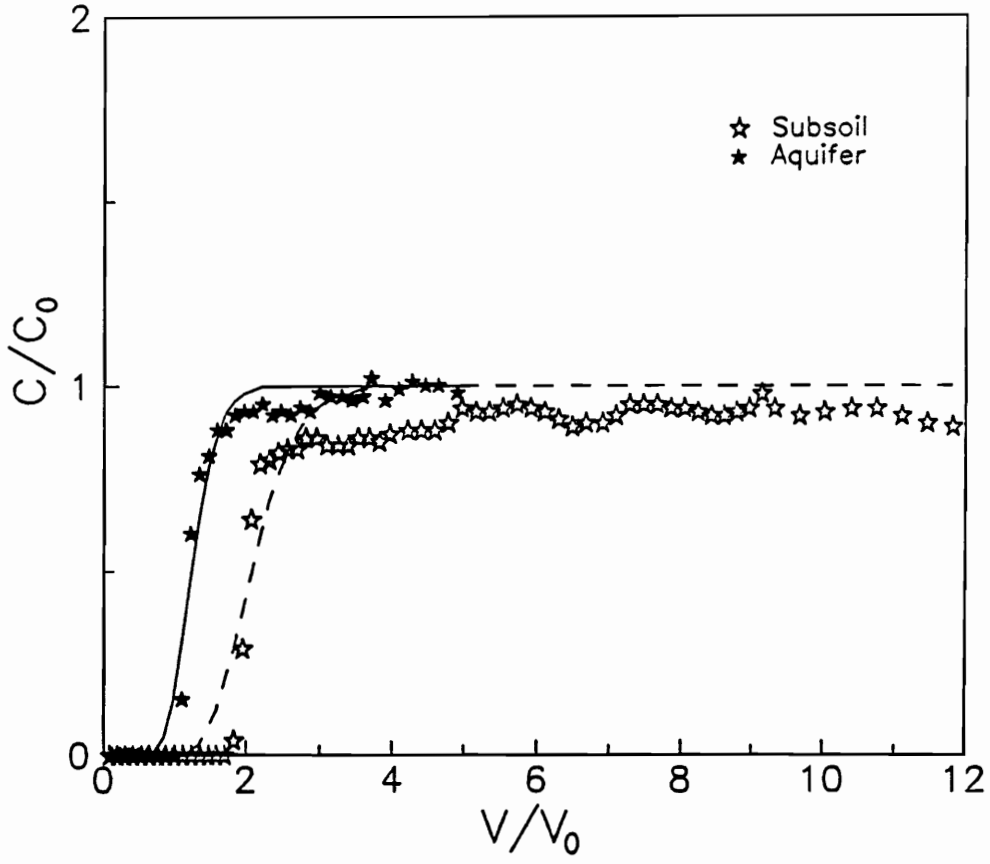

Figure 31. Observed (points) and predicted (lines) sulfate breakthrough curves for the 0.25 - 0.75 m (subsoil) and 1.25 - 1.40 m (aquifer) materials.

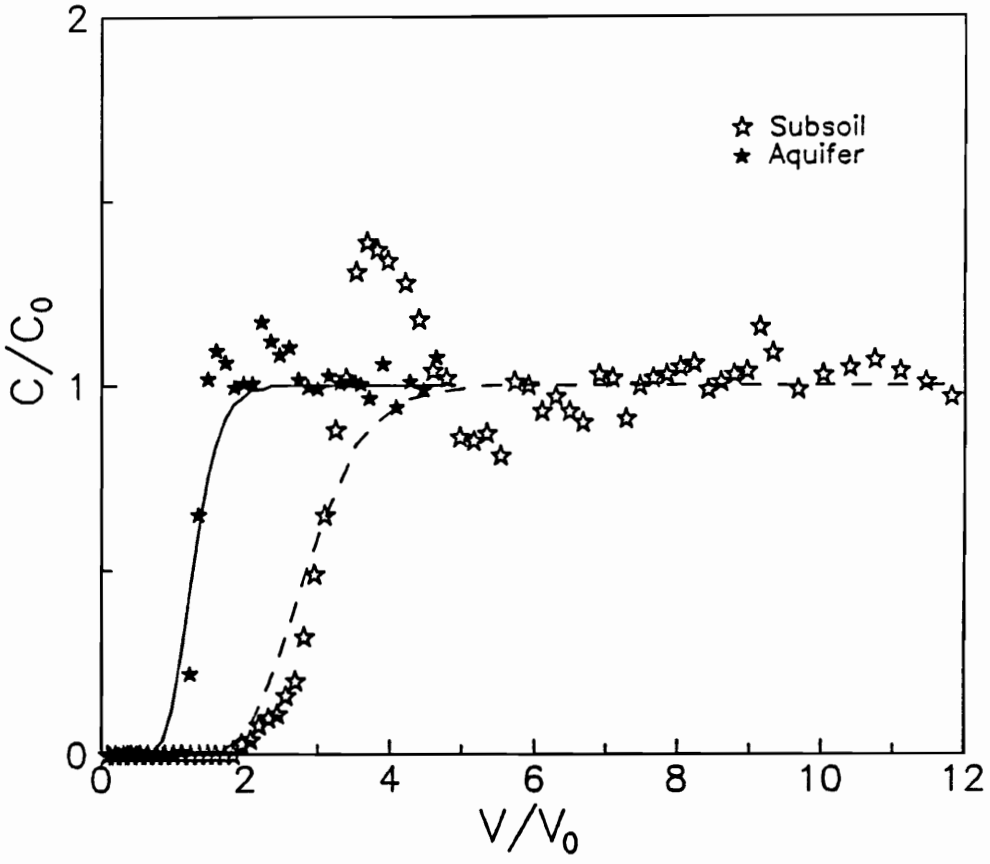

Figure 32. Observed (points) and predicted (lines) Ni breakthrough curves for the 0.25 - 0.75 m (suboil) and 1.25 - 1.40 m (aquifer) materials.

Implications for groundwater systems

A general implication of the observed transport of components within coal pile runoff, and more generally acid mine drainage, is that waves of component concentrations well in excess of that of the runoff can be expected. Exchange or other removal processes in which the soil serves as source of components to the aqueous phase can greatly increase component concentrations. Even elements not initially present in the soil to any significant extent exhibit this wave phenomenon and are a result of chromatographic processes within the soil. Thus even if runoff itself meets applicable water quality standards, groundwater downgradient may well exceed concentration limits as the wave advances with the groundwater flow.

Conclusions

A naturally acidic Coastal Plain subsoil-aquifer unit proffered little attenuation of infiltrating acidic, metal-rich coal pile runoff. Sulfate mobility governed transport of associated elements, with initial breakthrough and reduction in effluent pH occurring between 1.3 and 3 pore volumes for the sample depths evaluated. Displacement of native soil cations resulted in peak effluent concentrations well in excess of influent concentrations. An apparent buffering reaction briefly maintained effluent pH near 3.5 before descending toward that of the influent (pH 2.13). Ion exchange was the primary mechanism controlling peak concentrations within the column effluents for Al, Be, Ca, Co, Cu, Na, Ni, Mg, Mn, Sr, and Zn. More specific interactions with the solid phase

apparently regulated Li, K, Cr, and Cu transport, and precipitation-dissolution reactions controlled Fe and Si mobility.

References

Allison, L. E. 1965. Organic carbon. In C. A. Black et al. (ed.) Methods of soil analysis, Part 2. Agron. 9:1367-1378. Am. Soc. of Agron., Madison, WI.

American Public Health Association. 1976. Standard methods for the examination of water and wastewater. 14th ed. APHA/AWWA/WPCF. Washington, DC.

Anderson, M. A., P. M. Bertsch, and W. P. Miller. 1988. The distribution of lithium in selected soils and surface waters of the southeastern U.S.A. Appl. Geochem. **3:** 205-212.

Anderson, M. A., P. M. Bertsch, and W. P. Miller. 1990. Beryllium in selected southeastern soils. J. Environ. Qual. **19:** 347-348.

Aylmore, L. A. G., M. Karim, and J. P. Quirk. 1967. Adsorption and desorption of sulfate ions by soil constituents. Soil Sci. **103:** 10-15.

Baes, C. F., Jr., and R. E. Mesmer. 1976. The hydrolysis of cations. John Wiley and Sons, New York.

Barnhisel, R.I., and A. L. Rotromel. 1974. Weathering of clay minerals by simulated acid coal spoil-bank solutions. Soil Sci. **118:** 22-27.

Benjamin, M. M., and J. O. Leckie. 1981. Multiple-site adsorption of Cd, Cu, Zn, and Pb on amorphous iron oxyhydroxide. J. Coll. Interface Sci. **79:** 209-221.

Berner, R. A. 1978. Rate control of mineral dissolution under earth surface conditions. Am. J. Sci. **278:** 1235-1252.

Blake, G. R., and K. H. Hartge. 1986. Bulk density. In A. Klute (ed.) Methods of soil analysis, Part 1. Agron. **9:** 363-382. Am. Soc. of Agron., Madison, WI.

Bohn, H. L., B. L. McNeal, and G. A. O'Connor. 1985. Soil chemistry. John Wiley & Sons, New York, NY.

Brady, K. S., J. M. Bigham, W. F. Jaynes, and T. J. Logan. 1986. Influence of sulfate on Fe-oxide formation: comparisons with a stream receiving acid mine drainage. Clays Clay Miner. **34:** 266-274.

Brown, D. S., and J. D. Allison. 1987. MINTEQA2, an equilibrium metal speciation model. EPA/600/3-87/012.

Cartwright, K., R. A. Griffin, and R. H. Gilkeson. 1977. Migration of landfill leachate through glacial tills. Ground Water **15:** 294-305.

Chapman, B. M., D. R. Jones, and R. F. Jung. 1983. Processes controlling metal ion attenuation in acid mine drainage streams. Geochim. Cosmochim. Acta **47:** 1957-1973.

Clancy, K. M., and A. A. Jennings. 1988. Experimental verification of multicomponent groundwater contamination predictions. Water Resour. Res. **24:** 307-316.

Danielson, R. E., and P. L. Sutherland. 1986. Porosity. In A. Klute (ed.) Methods of soil analysis, Part 1. Agron. **9:** 443-461. Am. Soc. of Agron., Madison, WI.

Davis, E. C., and W. J. Boegly. 1981. A review of water quality issues associated with coal storage. J. Environ. Qual. **10:** 127-133.

Forbes, E. A., A. M. Posner, and J. P. Quirk. 1976. The specific adsorption of divalent Cd, Co, Cu, Pb, and Zn on goethite. J. Soil Sci. **27:** 1654-1666.

Foster, P., D. T. E. Hunt, and A. W. Morris. 1978. Metals in an acid mine stream and estuary. Sci. Total Environ. **9:** 75-86.

Filipek, L. H., D. K. Nordstrom, and W. H. Ficklin. 1987. Interaction of acid mine drainage with waters and sediments of West Squaw Creek in the West Shasta Mining District, California. Environ. Sci. Technol. **21:** 388-396.

Lindsay, W. L. 1976. Chemical equilibria in soils. John Wiley and Sons, New York.

Jackson, M. L., C. H. Lim, and L. W. Zelazny. 1986. Oxides, hydroxides, and aluminosilicates. In A. Klute (ed.) Methods of soil analysis, Part 1. Agron. **9:** 101-142. Am. Soc. of Agron., Madison, WI.

Jenne, E. A. 1968. Controls on Mn, Fe, Co, Ni, Cu, and Zn concentrations in soils and waters: the significant role of hydrous Mn and Fe oxides. In R. F. Gould (ed.) Trace Inorganics in Water, Adv. Chem. Ser. **73:** 337-387, ACS, Washington, DC.

Jones, K. C. 1986. The distribution and partitioning of silver and other heavy metals in sediments associated with an acid mine drainage stream. Environ. Pollut. (Ser. B) **12:** 249-263.

McLean, E. O. 1986. Soil pH and lime requirement. In A. L. Page et al., (ed.) Methods of soil analysis, Part 2. Agron. **9:** 199-224, Am. Soc. of Agron., Madison, WI.

Miller, W. P., and D. M. Miller. 1987. A micropipette method for soil mechanical analysis. Commun. Soil Sci. Plant Anal. **18:** 1-15.

Nordstrom, D. K., E. A. Jenne, and J. W. Ball. 1979. Redox equilibria of iron in acid mine waters. In E. A. Jenne (ed.) Chemical modeling of aqueous systems: Speciation, sorption, solubility, and kinetics. ACS Symp. Ser. **93:** 51-79. ACS, Washington, DC.

Nordstrom, D. K. 1982a. Aqueous pyrite oxidation and the consequent formation of secondary iron minerals. In J. A. Kittrick, D. S. Fanning, and L. R. Hossuer (ed.) Acid Sulfate Weathering. Soil Sci. Soc. of Am. Spec. Publ. **10:** 37-56. Soil Sci. Soc. of Am., Madison, WI.

Nordstrom, D. K. 1982b. The effect of sulfate on aluminum concentrations in natural waters: Some stability relations in the system $Al_2O_3 - SO_3 - H_2O$ at 298 K. Geochim. Cosmochim. Acta **46:** 681-692.

Norrish, K., and R. M. Taylor. 1961. The isomorphous replacement of iron by aluminum in soil goethites. J. Soil Sci. **12:** 294-299.

Parker, J. C., and M. Th. van Genucthen. 1984. Determining transport parameters from laboratory and field tracer experiments. Virginia Ag. Exp. Sta. Bull. 84-3.

Rajan, S. S. S. 1978. Sulfate adsorbed on hydrous alumina, ligands displaced, and changes in surface charge. Soil Sci. Soc. Am. J. **42:** 39-44.

Rich, C. I., and R. I. Barnhisel. 1977. Preparation of clay samples for x-ray diffraction analysis. p. 797-808. In J. B. Dixon and S. B. Weed (ed.) Minerals in soil environments. Soil Sci. Soc. Am., Madison, WI.

Robinson, G. D. 1981. Adsorption of Cu, Zn, and Pb near sulfide deposits by hydrous manganese-iron oxide coatings on stream alluvium. Chem. Geol. **33:** 65-79.

Sigg, L., and W. Stumm. 1980. The interaction of anions and weak acids with the hydrous goethite (α –FeOOH) surface. Coll. Surf. **2:** 101-117.

Singer, P. C., and W. Stumm. 1970. Acidic mine drainage: the rate-determining step. Science **167:** 1121-1123.

Singh, B. R. 1984. Sulfate sorption by acid forest soils: 3. Desorption of sulfate from adsorbed surfaces as a function of time, desorbing ion, pH, and amount of adsorption. Soil Sci. **138:** 346-353.

Swift, M. C. 1985. Effects of coal pile runoff on stream quality and macroinvertebrate communities. Water Resour. Bull. **21:** 449-457.

Sposito, G. The surface chemistry of soils. Oxford Univ. Press, New York.

Theobald, P. K., H. W. Lakin, and D. B. Hawkins. 1963. The precipitation of aluminum, iron, and manganese at the junction of Deer Creek with the Snake River in Summit county, Colorado. Geochim. Cosmochim. Acta **27:** 121-132.

van Breeman, N. 1973. Dissolved aluminum in acid sulfate soils and in acid mine waters. Soil Sci. Soc. Am. Proc. **37:** 694-697.

Wangen, L. E., and J. M. Williams. 1982. Control by alkaline neutralization of trace elements in acidic coal cleaning waste leachates. J. Water Pollut. Contr. Fed. **54:** 1302-1310.

Wangen, L. E., and M. M. Jones. 1984. The attenuation of chemical elements in acidic leachates from coal mineral wastes by soils. Environ. Geol. Water. Sci. **6:** 161-170.

Whittig, L. D., and W. R. Allardice. 1986. X-ray diffraction techniques. In A. Klute (ed.) Methods of soil analysis, Part 1. Agron. **9:** 331-362. Am. Soc. of Agron., Madison, WI.

Yeh, G. T., and V. S. Tripathi. 1989. A critical evaluation of recent developments in hydrogeochemical transport models of reactive multichemical components. Water Resour. Res. **25:** 93-108.

Chapter IV

Element Partitioning and Surface Chemical and Mineralogical Alterations

Abstract

Element partitioning results via sequential extraction procedures were generally in good agreement with mass balance calculations and corroborated inferences made about element mobility from breakthrough data. Iron accumulated within the soil column and was associated chiefly with the Ox-extractable phase. Aluminum was partitioned between the water, NH_4Cl exchangeable, and Ox extractable phases, with the water phase increasing and the Ox phase decreasing with increasing leaching. Silicon tended to follow Al to some extent, with Ox-extractable Si decreasing with increasing leaching. Calcium, Mg, Sr, Co, Zn, and Ni were associated with the exchange phase early during the leaching process, then partitioned between the

aqueous and exchange phases, supporting the notion that ion exchange was the dominant mechanism governing mobility for these elements. Manganese followed the other divalent metal ions with the exception that a limited quantity was found associated with the Ox-extractable phase. Copper and Cr departed significantly from the other first row transition metals in that their mobility appeared to be governed by coprecipitation reactions with Fe. Prolonged leaching also resulted in a net export of Al and Si fro the soil, gibbsite formation, destabilization of interstratified mica-vermiculite, increased 10 Å material, and apparent destabilization of crystalline iron phases to an Ox-extractable phase.

Introduction

In Chapter III, I presented results from experiments in which a number of different samples from a subsoil-aquifer unit were leached with acidic coal pile runoff under constant saturated flow conditions. Breakthrough data indicated a highly coupled series of chemical reactions controlled element mobility. Initial breakthrough of acidity and metals was regulated by sulfate mobility via the necessary condition of electroneutrality in solution. Apparent buffering at pH $\simeq$3.5 was observed for all the samples, the extent of which was a unique function of cation exchange capacity (CEC), mineralogy, and oxide content. Exchange of native Al, Ca, and Mg, and to a lesser extent Na and K, resulted in early breakthrough times (Na > K > Mg > Ca > Al) and assymetrical breakthrough curves. Lithium (Li) was observed to be fixed to some extent within the soil prior to breakthrough. Beryllium (Be), cobalt (Co), nickel (Ni),

manganese (Mn), and zinc (Zn) movement through the samples were relatively rapid and governed by ion exchange. Chromium (Cr) and Cu underwent apparent reversible sorption reactions. Iron (Fe) was retained by the soil until its buffer capacity was exhausted and the pH declined to pH near 2.3. Speciation of column effluent indicated supersaturation with respect a series of jarosites. Aluminum solubility most closely followed that of jurbanite. Net export of both aluminum (Al) and silicon (Si) from the samples was noted, suggesting dissolution of labile aluminosilicate phases and/or dissolution of phyllosilicate edges.

In Chapter IV, I report findings on observed partitioning of major and trace elements and on surface chemical and mineralogical alterations to the subsoil upon leaching with the coal pile runoff.

Materials and Methods

Sample Preparation

A series of columns were prepared using the 0.25 - 0.75 m sample depth as previously reported (Chapter III). Columns were leached with 1 - 8, 12, and 60 pore volumes of the runoff. After leaching, the soils were extruded and homogenized.

Element Partitioning

The partitioning of elements between the water-soluble, *M* NH_4Cl- and ammonium oxalate-extractable (Ox) fractions was evaluated. Water-soluble contents were determined from breakthrough curves. One and 1/2 g equivalent dry weight samples were extracted twice with 7.5 mL *M* NH_4Cl and the supernatants combined, followed by a 10 mL de-ionized water wash which was discarded. The previously extracted soils were then equilibrated with 30 mL ammonium oxalate reagent for 4 h in the dark (Jackson et al., 1986). Coefficients of variation (CV) for replicated extractions ranged from 2.9 to 12.2 %, with an average CV of 8.9 %.

Mineralogy

Clay mineralogy was determined on the 0, 4, 8, 12, and 60 pore volume samples as previously reported (Chapter III). In addition, oxide mineralogy was determined on samples in which Fe was not removed. Random powder mounts were prepared from the silt + clay fraction. For these determinations, the Diano diffractometer was slowed to a step speed of 0.05 ° 2θ/s. A background diffractogram of a DCB-treated silt + clay sample was then subtracted from the oxide patterns.

Infrared Analysis

Fourier-transform infrared analyses of silt + clay fractions of soils leached with runoff were performed with a Digilab FTS-45 unit using diffuse reflectance (DRIFTS). Sixty-four scans were co-added, at 4 cm^{-1} resolution.

Electrophoretic Mobility

Approximately 10 g samples from soils leached with 0, 4, 8, 12, and 60 pore volumes of runoff from above were equilibrated with 30 mL *M* of $NaClO_4$, centrifuged, and the supernatant discarded. The process was repeated an additional 4 times, followed by 2 washes with 0.01 *M* $NaClO_4$. Samples were resusupended in a third portion and wet sieved to remove >53 μm particles. The silt + clay suspensions which passed the sieve were collected and 0.25 mL of those suspensions were then pipetted into 30 mL polycarbonate Oak Ridge tubes. Twenty mL 0.01 *M* $NaClO_4$ adjusted to pH 3, 4, 5, 7, and 9 with O.1 *M* $HClO_4$ or NaOH was added, equilibrated for 15 min, centrifuged and discarded. Two additional treatments followed. The pH of an aliquot of the final wash was recorded before the sedimented material was resuspended (final suspension concentration $\simeq$0.5 mg/mL).

The above treated suspensions were then analyzed for eletrophoretic mobilities with a Malvern Zetasizer II. The Zetasizer II uses photon correlation spectroscopy with data acquisition and handling performed by a dedicated microcomputer. Cell chambers were filled with a solution equivalent in salt concentration and pH to that of the sample suspensions. Triplicate mobility determinations with a 30 s count time and applied voltage and current of $\simeq$80 mV and 3 mA, respectively, were made.

Mass Balance

To properly account for components retained by the soil columns at any time t, a mass balance about the column was calculated (Figure 33). The total volume of the column, V_T (L^3) was determined ($\simeq$127cm^3). A total reactive mass of a component i, $M_{i,T}$ (M) was defined as:

$$M_{i,T} = M_{i,aq} + M_{i,ex} + M_{i,ox} \tag{3}$$

where $M_{i,aq}$ is the total mass of component i in the aqueous phase, $M_{i,ex}$ is the total mass of component i on the exchange phase, and $M_{i,ox}$ is the total mass of component i which is extractable via the 4-h ammonium-oxalate in the dark procedure. Runoff of concentration $C_{i,in}$ for each component (Chapter III, Table 1) was supplied to the columns at constant volumetric flow Q_{in} (L^3/T) (for this investigation, Q_{in} $\simeq$6.8 cm^3/h). Column effluent at a flow of Q_{out} (L_3/T) and concentration $C_{i,out}$ (M/L^3) was collected as a function of time. The change in total component mass within the column over time may, since V_T is constant, be expressed by the ordinary differential equation:

$$\frac{dM_{i,T}}{dt} = V_T \frac{dC_{i,T}}{dt} \tag{4}$$

which, under steady saturated flow where $Q_{in} = Q_{out} = Q$, reduces to

$$\frac{dM_{i,T}}{dt} = Q(C_{i,in} - C_{i,out}) \tag{5}$$

Solutions to Eqn. 3 for the components evaluated were compared then to that component mass which was recovered by selective dissolution procedures.

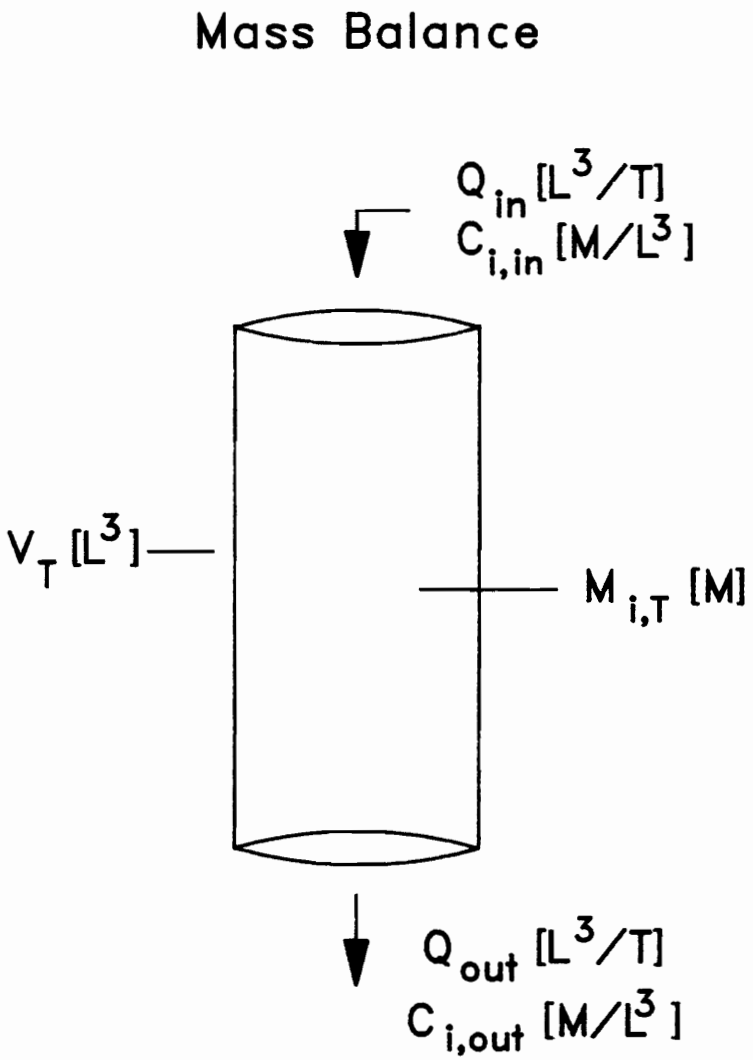

Figure 33. Mass balance about column.

Results

Element Partitioning

The distribution of elements between the water-soluble, *M* NH_4Cl exchangeable, and Ox-extractable fractions was found to vary for different components and as a function of runoff volume leached.

Major Elements

There was some modest amount of SO_4^{2-} initially present on the soil and recoverable in the NH_4Cl-extractable fraction (Figure 34). Infiltration and movement of runoff through the soil column resulted in increasing total SO_4^{2-} in good agreement with mass balance calculations (Figure 34). Extraction results indicate the SO_4^{2-} partitions principally to the NH_4Cl-extractable fraction, with some residing within the aqueous and also the Ox-extractable phases (Figure 34). Total sorbed SO_4^{2-} ($\sum$ *M* NH_4Cl- and Ox-extractable SO_4^{2-}) measured near 1000 μg/g soil with nearly 80 % recoverable in the NH_4Cl . Singh (1984) reported a similar magnitude of SO_4^{2-} sorption to an Fe podzol near pH 3.5 ($\simeq$1000 μg/g), noting increased sorption with decreasing pH, though found only $\simeq$20 % was desorbed with 0.01 *M* $Ca(NO_3)_2$. The difference in desorption efficiencies between the neutral salt extractants likely resulted from the significantly higher (50x) salt concentration used in this evaluation. Additionally, a monotonic increase in Ox-extractable sulfate with increasing V/V_0 was noted.

Iron was found to reside essentially entirely within the Ox-fraction prior to addition of runoff, with Ox-extractable Fe increasing steadily with increasing pore volumes

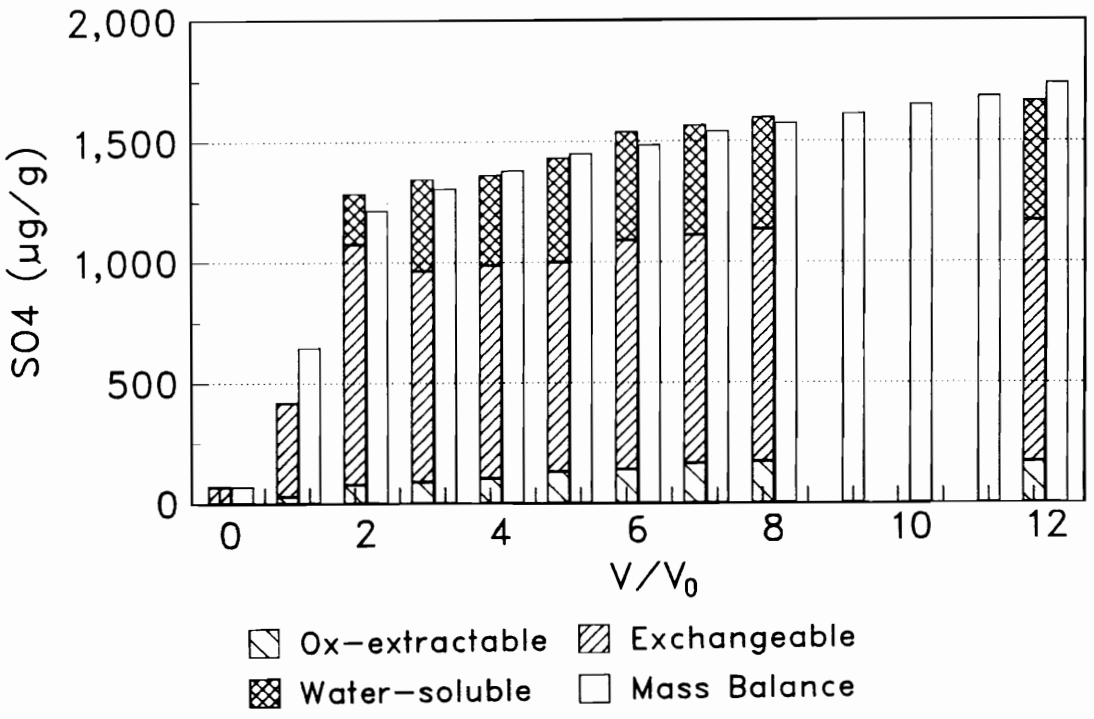

Figure 34. Mass balance and element partitioning results (0.25 - 0.75 m material): sulfate.

(Figure 35). Partitioning of limited quantities of Fe first to the exchange phase, at pH ≃3.5, and then subsequently to a water-soluble phase as the pH dropped near 2 (12 pore volumes) was also observed. The increase in Ox-extractable Fe between 0 and 8 pore volumes can be directly related to the retention of Fe noted previously from breakthrough curves (Figure 7, 0.25-0.75 m) and as illustrated in Figure 18, in good agreement with mass retained via mass balance calculations. Mass balance calculations did underestimate the extractable total reactive Fe for the sample subjected to 12 pore volumes however (Figure 35). It appears that as the soil buffer capacity was exhausted and the pH dropped to near 2, additional native crystalline Fe phases were destabilized and thus extractable in the Ox-treatment.

The steady increase in both Ox-extractable Fe (Figure 35) and SO_4^{2-} (up to $V/V_0 \simeq 8$) (Figure 34) implies an association between these two components in a poorly ordered soil phase. As previously discussed, Fe solubility within acid mine drainage-type systems is often considered to be controlled by a jarosite phase (Nordstrom, 1982a), with column effluent shown to be supersaturated with respect to such phases (Figure 27). The ratio between the increased Ox-extractable Fe ($Ox - Fe - Ox - Fe_{initial}$) (Figure 35) and SO_4^{2-} (Figure 34) in fact remained fairly constant up to 7 pore volumes with a mean Fe/SO_4^{2-} mole ratio of 2 (Figure 36). Filipek et al. (1987) reported a mean Fe/S mole ratio of 3 for precipitates within and acid drainage-impacted surface water. One notes that this is higher than that for a jarosite phase, which would possess an Fe/SO_4^{2-} ratio of 1.5 (Nordstrom, 1982). Evidence supporting the notion of destabilization of a native crystalline Fe phase upon prolonged leaching is also provided (Figure 36). That is, if precipitation of Fe and SO_4^{2-} from the runoff was the principal source of increased Ox-extractable Fe and SO_4^{2-}, then one would expect a continued ≃constant Fe/SO_4^{2-} ratio. Column effluent pH decreased upon prolonged leaching

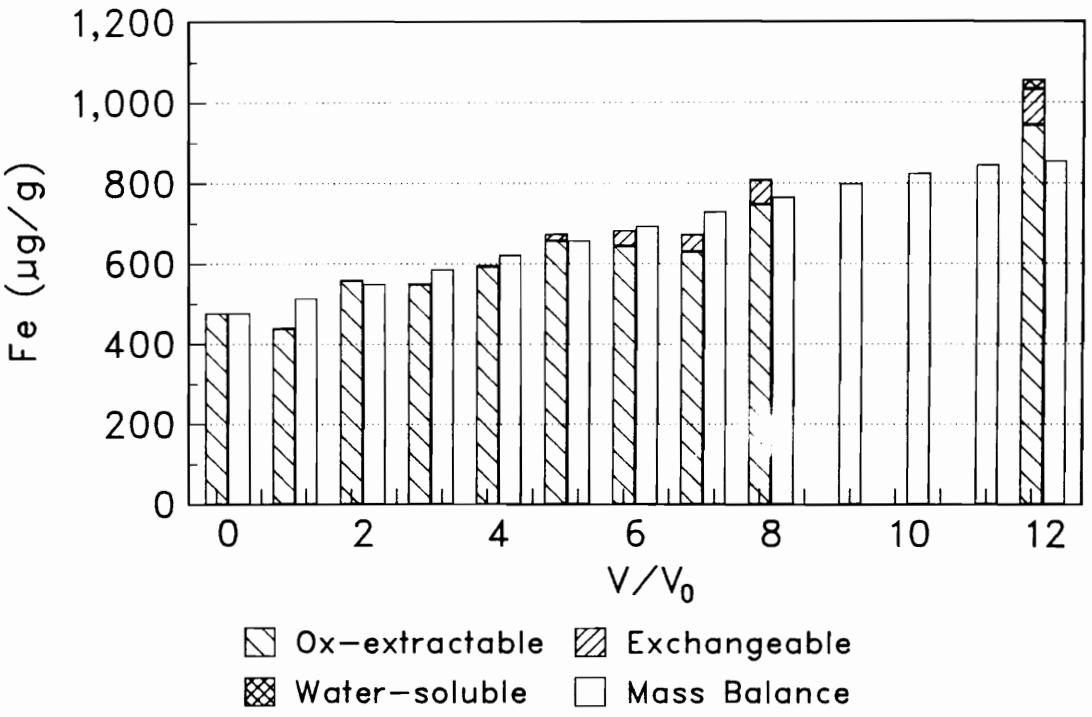

Figure 35. Mass balance and element partitioning results (0.25 - 0.75 m material): Fe.

(e.g., $V/V_0 > 8$) and approached that of the influent (Figure 3, 0.25-0.75 m). This increased H^+ activity necessarily reduces OH^- activity in solution; thus hydroxyl content of a precipitated Fe phase should decrease, rather than increase, as might be inferred from the observed increased Fe/SO_4^{2-} ratio (Figure 36). It is also interesting to note that the Fe/SO_4^{2-} mole ratio of 2 (or alternately, a SO_4^{2-}/Fe equivalent ratio of 0.33) from the Ox-pool is in accord with calculations from breakthrough curves indicating an OH/Fe ratio of $\simeq$2 for hydrolyzed Fe phases (Chapter III).

Aluminum was distributed between the exchangeable and Ox-extractable pools prior to addition of leachate as illustrated (Figure 37). A maximum in exchangeable Al was noted after $\simeq$3 pore volumes were supplied, preceding the wave of increased Al in fractions collected at subsequent pore volumes from the leaching experiments (Figure 6, 0.25-0.75 m), with some water soluble Al also detectable after 2 pore volumes (corresponding to the reduction in effluent pH to $\simeq$3.5) (Figure 37). A gradual reduction in Ox-extractable Al with increasing pore volumes was also noted, implying dissolution of a native poorly crystalline phase.

Silicon resided chiefly within the Ox and, to a lesser extent, exchangeable pools, though some Si was in solution (and shown in Figure 28 to be in equilibrium with an amorphous SiO_2 phase) prior to leaching (Figure 38). Maximum water-soluble Si occurred at 2 pore volumes (Figure 38). Leaching of the sample resulted in a gradual dimunition in Ox-extractable Si to a minimum at 6 pore volumes which was followed by increasing Ox-extractable Si. Mass balance calculations indicate a net export of Si out of the system, completely exhausting the total initial reactive mass specified (Figure 38). Deviation between observed and predicted total reactive Si indicates that an additional phase not initially accounted for is capable of transforming to these

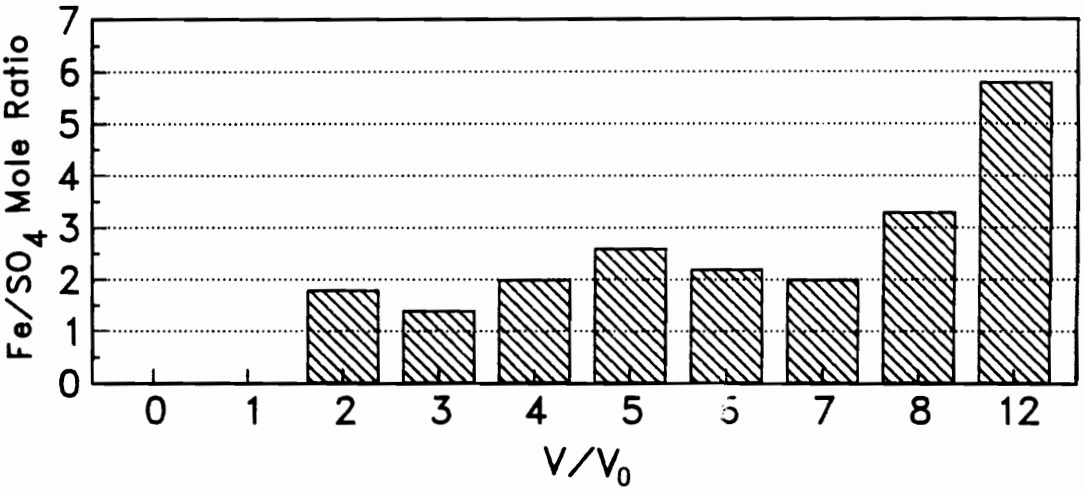

Figure 36. Ratio of additional Ox-extractable Fe to Ox-extractable sulfate as a function of influent pore volume (0.25 - 0.75 m material).

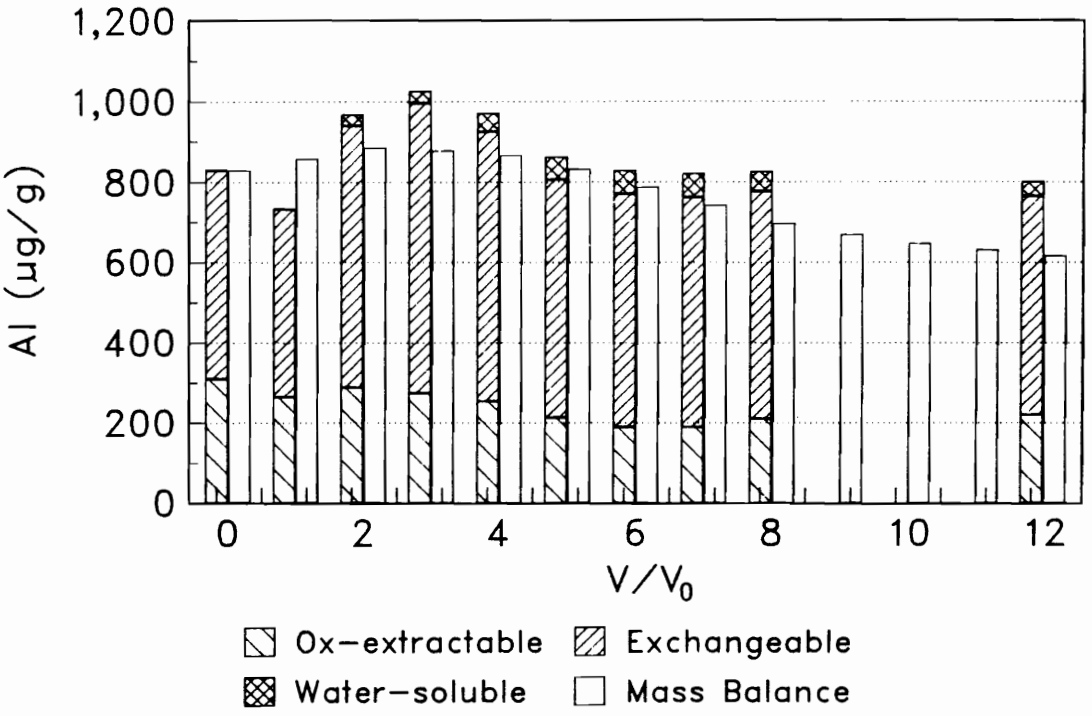

Figure 37. Mass balance and element partitioning results (0.25 - 0.75 m material): Al.

more labile phases. Desilication and formation of oxidic components is well-documented within soils subjected to naturally acidic conditions (e.g., spodic horizons formed under coniferous vegetation) as well as clays and sediments subjected to acid mine water (Barnhisel and Rotromel, 1974; Filipek et al., 1987).

Alkali Metals

Potassium was associated principally with the exchange phase, with a small fraction also found in the aqueous and the Ox-phases (Figure 39). Soil K increased to a maximum around 2-3 pore volumes, then decreased rapidly as K concentrations in the effluent increased to its peak concentration at V/V_0 of 5 (Figure 39). As final K content was signficantly less than that initially associated with the soil, there was a net export of K out of the column.

Lithium was initially present on the soil exchange phase and in very low concentrations. Infiltration of runoff resulted in storage and a peak Li content at 2 pore volumes, which one again notes is immediately prior to the appearance of Li in the column effluent (Figure 10, 0.25-0.75 m). Mass balance calculations tended to over-predict somewhat the total Li within the system, with Li found only in the aqueous phase at later pore volumes. Trace amounts of Li have previously been observed to undergo fixation reactions in selected soils and clay minerals (Anderson et al., 1989; Davey and Wheeler, 1980), with sorbed Li not readily displaced with common soil extractants (Anderson et al., 1989). It seems plausible that the discrepancy between mass balance and extraction results may be a result of fixation of Li to sites inaccessible by the NH_4Cl (Anderson et al., 1989) and Ox extractants.

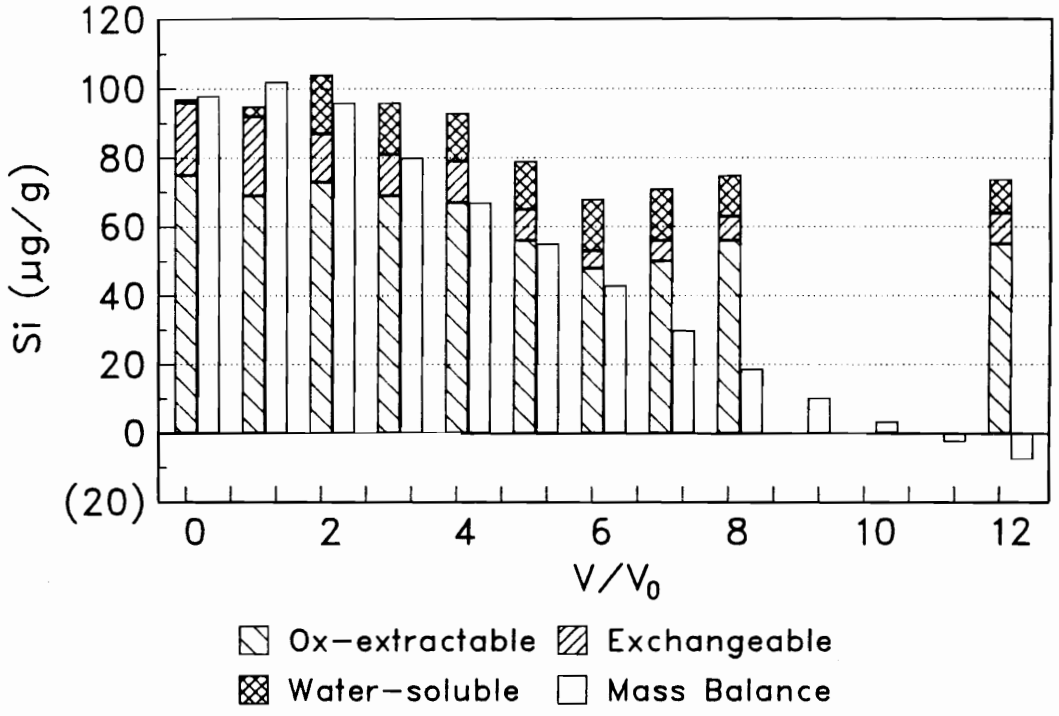

Figure 38. Mass balance and element partitioning results (0.25 - 0.75 m material): Si.

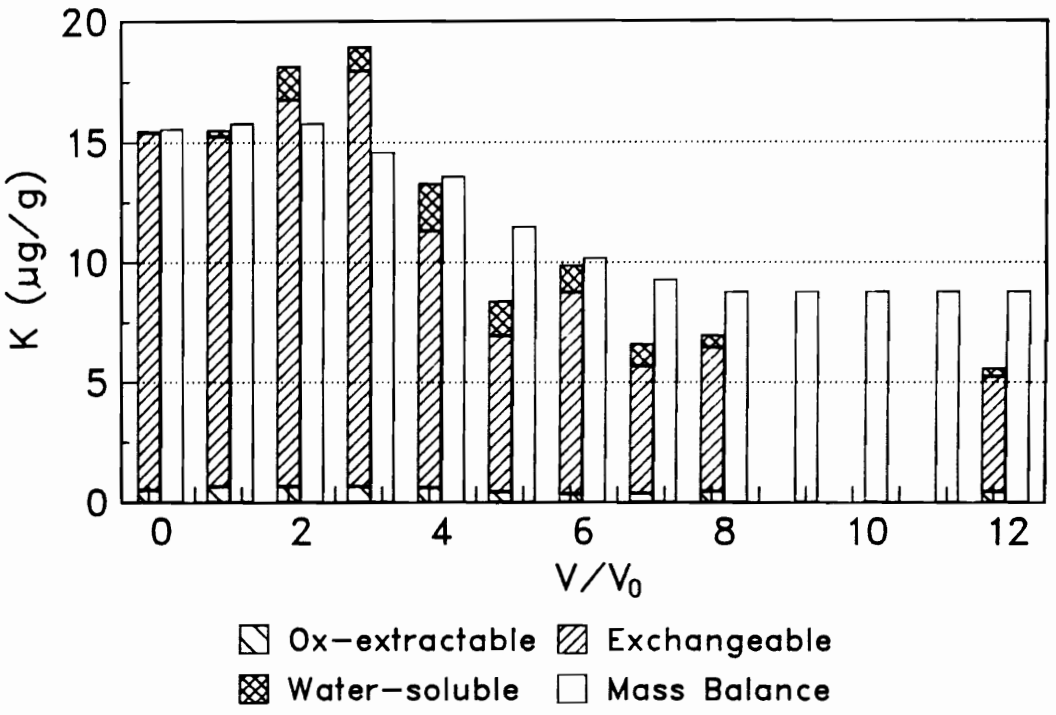

Figure 39. Mass balance and element partitioning results (0.25 - 0.75 m material): K.

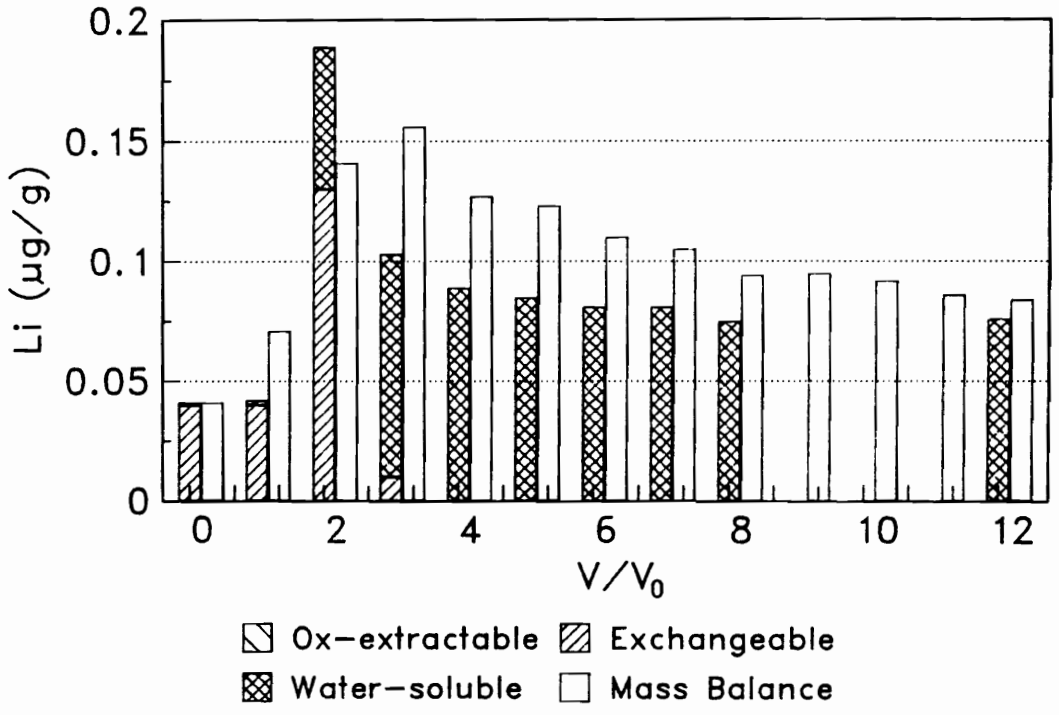

Figure 40. Mass balance and element partitioning results (0.25 - 0.75 m material): Li.

Like Li, there was a net storage of Na, with peak column content at 2 pore volumes (Figure 41). In this instance, however, mass balance calculations tended to underestimate total Na content. This discrepancy implies that an additional source of Na, not originally accounted for, exists within the soil. Though no feldspars were detectable via XRD (Table 4), dissolution of Na-feldspars may be a potential Na source.

Alkaline Earth Metals

Trace exchangeable Be was found prior to addition of leachate, within the range reported by Anderson et al. (1990) for southeastern U.S. soils (Figure 42). Mass balance calculations were in relative agreement with extraction results up to 3 pore volumes, after which significant overestimation of Be was noted (Figure 42). Hydrolysis of Be would not be expected over the pH at which its loss is observed ($\simeq$3.5 and below) (Baes and Mesmer, 1976), though coprecipitation to a recalcitrant phase may be an important reaction contributing to the observed discrepancy between observed and theoretical results.

Calcium was found only in the exchangeable pool prior to leaching, with this pool increasing dramatically after flux of two pore volumes into the column (Figure 43) and which preceded the peak breakthrough concentration between 3 and 4 pore volumes (Figure 13, 0.25-0.75 m).

Similarly, negligible Mg was identified within the water and Ox-phases prior to leaching (Figure 44). Unlike Ca, exchangeable Mg content decreased slightly at 2 pore volumes, and instead partitioned considerably more mass to the mobile aqueous phase (Figure 44). The difference in observed breakthrough of Ca and Mg can be related to the considerably higher exchangeable Mg content of the soil rela-

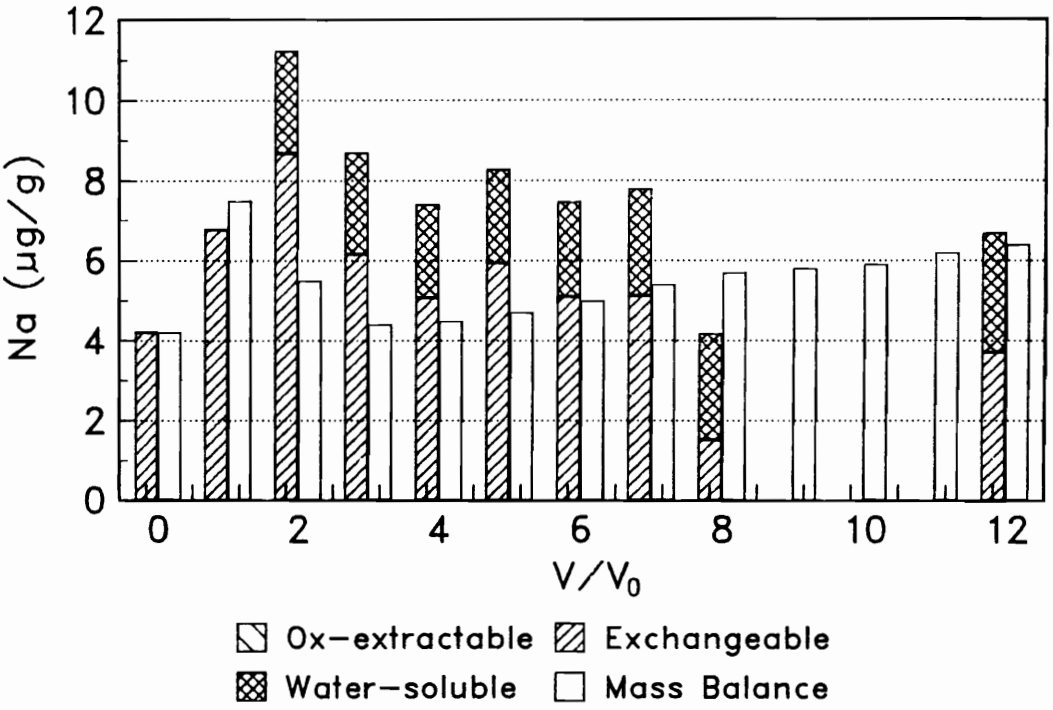

Figure 41. Mass balance and element partitioning results (0.25 - 0.75 m material): Na.

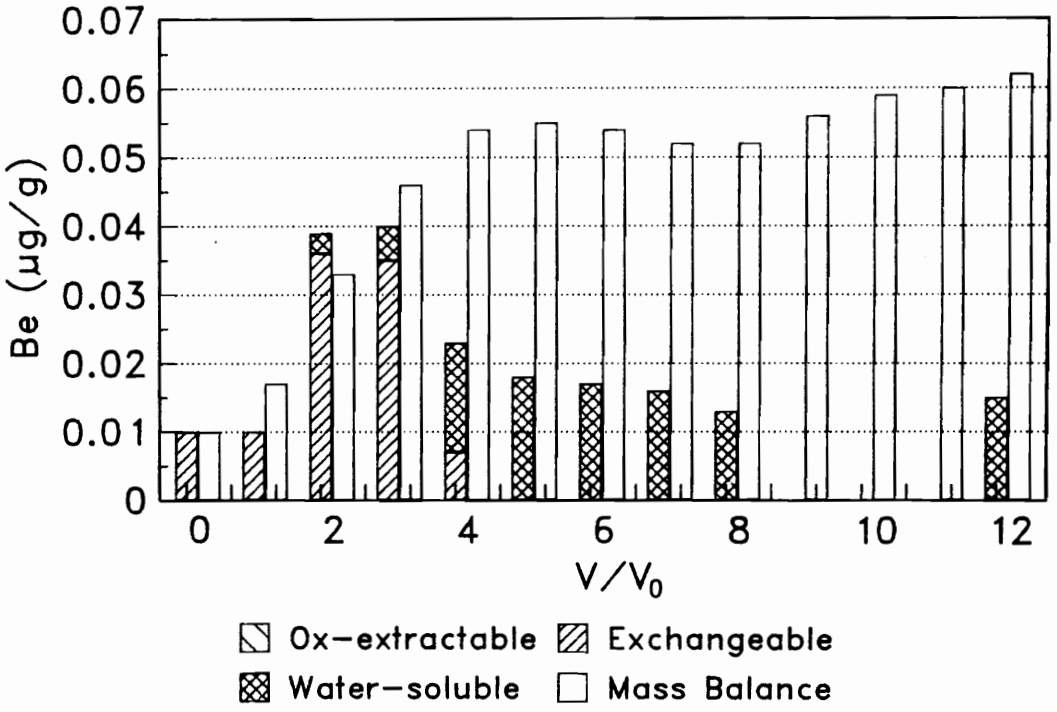

Figure 42. Mass balance and element partitioning results (0.25 - 0.75 m material): Be.

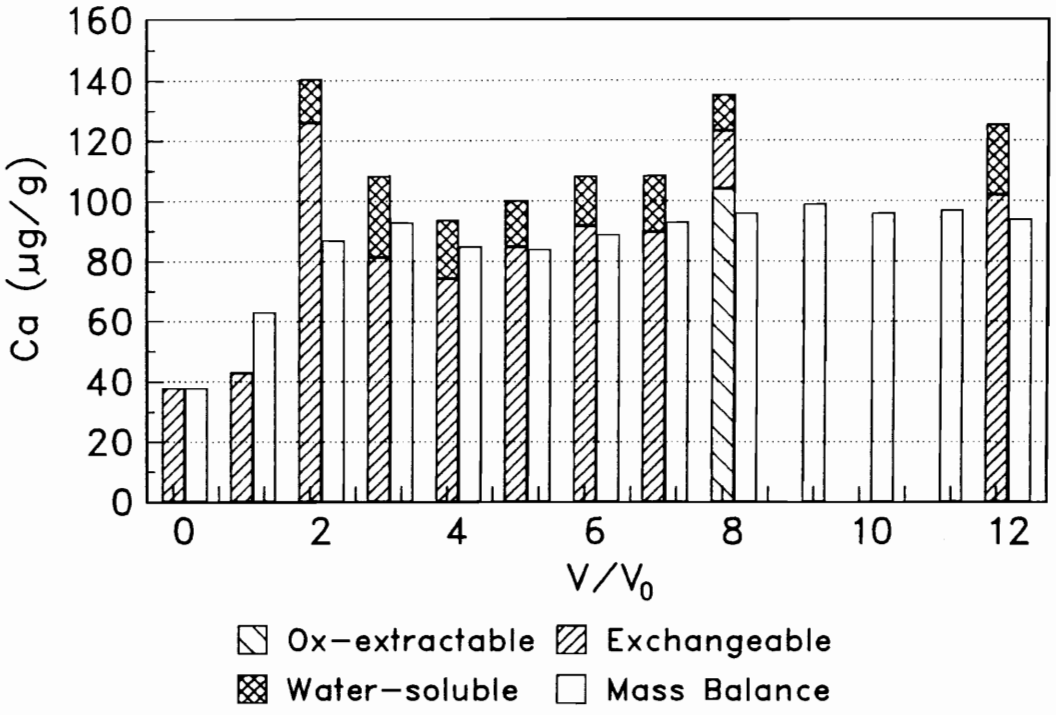

Figure 43. Mass balance and element partitioning results (0.25 - 0.75 m material): Ca.

tive to Ca. The advance of protons, sulfate, and other elements at ≃2 pore volumes resulted in net efflux from the soil exchange phase. One additionally notes a minimum in exchangeable Mg at 3 pore volumes (Figure 44), coincident with the highest exchangeable Al content (Figure 37). As Al and Mg constitute the major exchange phase components within the native soil, the two appear to be competing directly for available exchange sites.

As indicated in Table 5 of Chapter III, evidence for a minor amount of Sr within the soil was provided. The native subsoil here evaluated was found to contain ≃ 1 μg/g soil, essentially all residing on the soil exchange phase (Figure 45). Akin to Ca, an increase in exchange phase content occurred at 2 pore volumes, as well as the partitioning of limited mass to the mobile phase. Also similar to the other alkaline earth metals, a mininum in exchangeable Sr occurred at approximately 4 pore volumes, coincident with ≃peak exchange phase Al. All the alkaline earth metals tended to rebound only slowly after their approximate minimum near 4 pore volumes, which also coincides with the gradual decrease in exchange phase Al (Figure 37). Thus selectivity for these divalent cations increased as the favored trivalent Al was eluted from the soil surface. Good general agreement between mass balance calculations and extraction results were noted for Ca, Mg, and Sr (Figures 43-45).

Transition Metals

A number of first row transition metals exhibitted very similar breakthrough behavior, with peak effluent concentrations of Co, Mn, Ni, and Zn near 4 pore volumes (Figures 46-49). No detectable Co, Ni, and Zn was identified in any of the three pools prior to leaching with the coal pile runoff (Figures 46,48, and 49, respectively). Exchangeable forms were noted after 1 pore volume for Zn and Ni, with additional exchangeable and

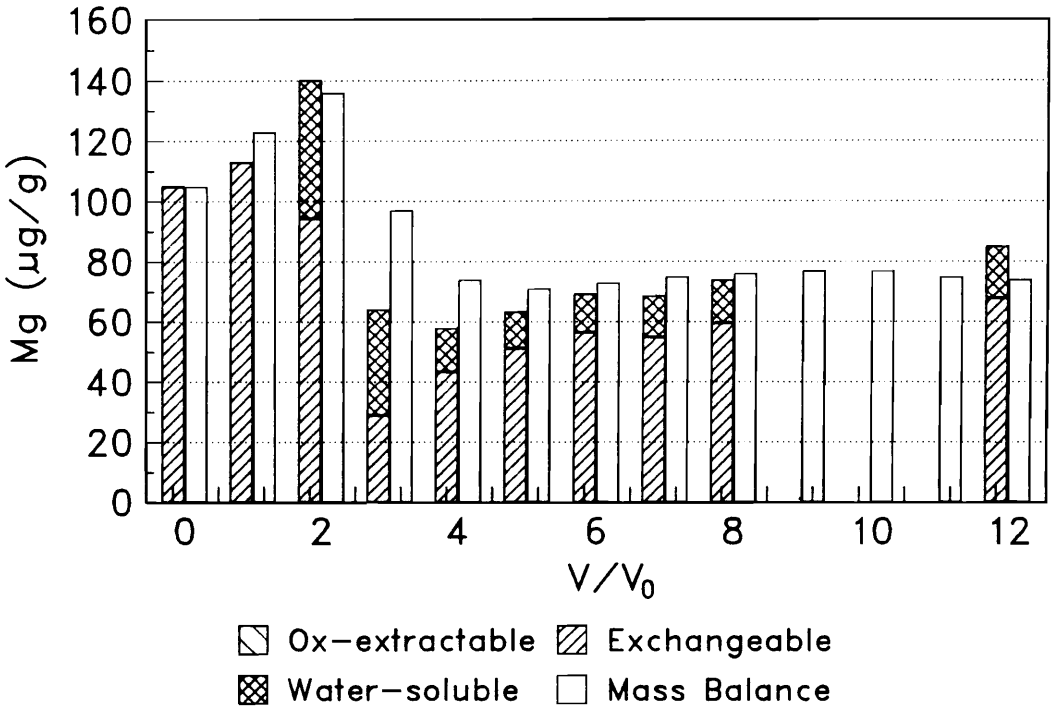

Figure 44. Mass balance and element partitioning results (0.25 - 0.75 m material): Mg.

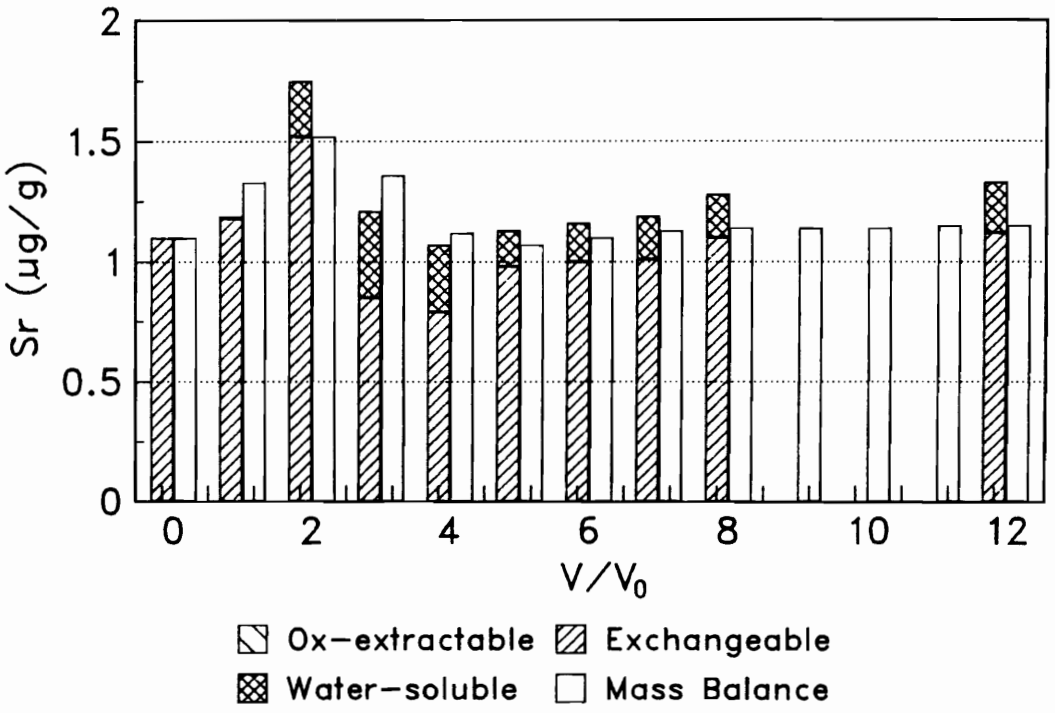

Figure 45. Mass balance and element partitioning results (0.25 - 0.75 m material): Sr.

also soluble metal contents occurring upon extraction after 2 pore volumes. Exchangeable Ni and Zn both tended to decrease somewhat between 3 and 4 pore volumes (coincident with maximal exchangeable Al) before ascending again (Figures 48 and 49, respectively). Cobalt exhibited somewhat different behavior in that it tended to increase generally with increasing leaching volumes (Figure 46). Manganese was found in relatively trace quantities prior to leaching, including an Ox-extractable phase (Figure 47). A maximum in exchange phase Mn occurred at two pore volumes (Figure 47), with a minimum coincident again with peak effluent Mn concentration from the breakthrough experiments (Figure 17, 0.25-0.75 m) and maximum exchange phase Al (Figure 37). No evidence for accumulation in or mobilization from the Ox-phase was apparent. Thus, under the conditions evaluated here, specific interactions with hydrous oxides and coprecipitation with nascent solid phases are of secondary importance in regulating Co, Mn, Ni, and Zn mobility. Rather simple partitioning between aqueous and exchange phases constitute the principal reactions governing transport within acid runoff percolating through acid subsoils.

Limited Cr was found associated with the Ox-extractable phase for all treatments, including the native condition (Figure 50). Chromium partitioning was limited to this phase until the 7th pore volume, where Cr was found in both the exchange and water-soluble phases (Figure 50) which coincides with the onset of significant elution of Cr from the soil column (Figure 20, 0.25-0.75 m). This partitioning behavior contrasts that for the previous transition metals and implies a coprecipitation reaction controls Cr mobility. The low concentrations of Cr in the runoff (10 μg/L) resulted in negligible loading to the soil, thus the results are subject to limitations imposed by the extraction procedure and analytical methods.

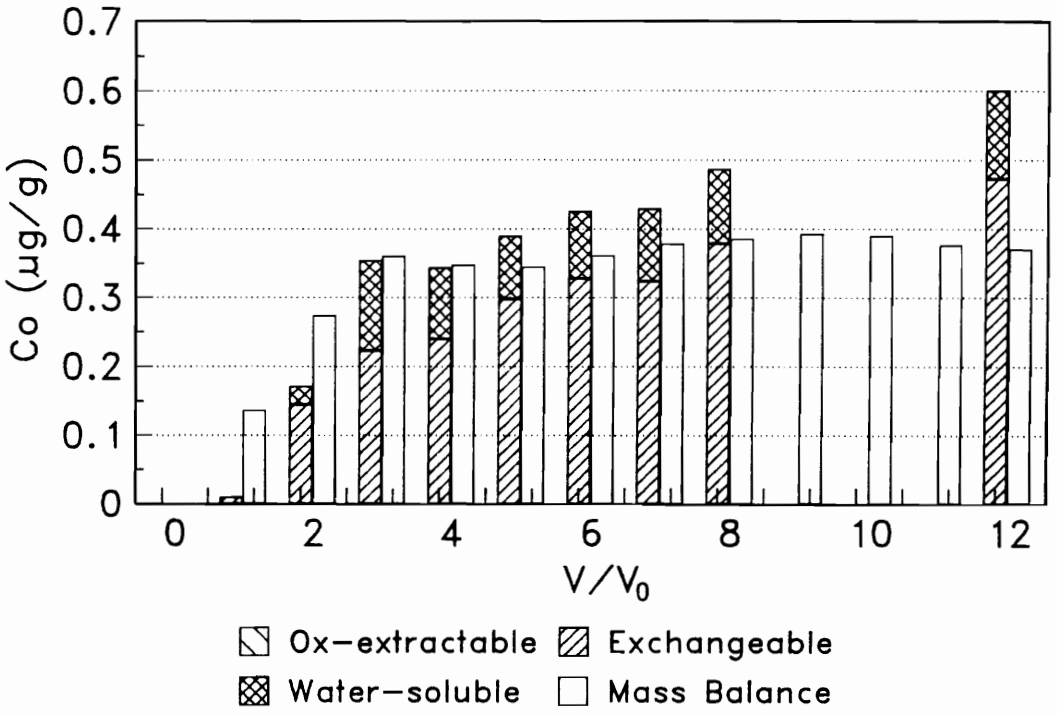

Figure 46. Mass balance and element partitioning results (0.25 - 0.75 m material): Co.

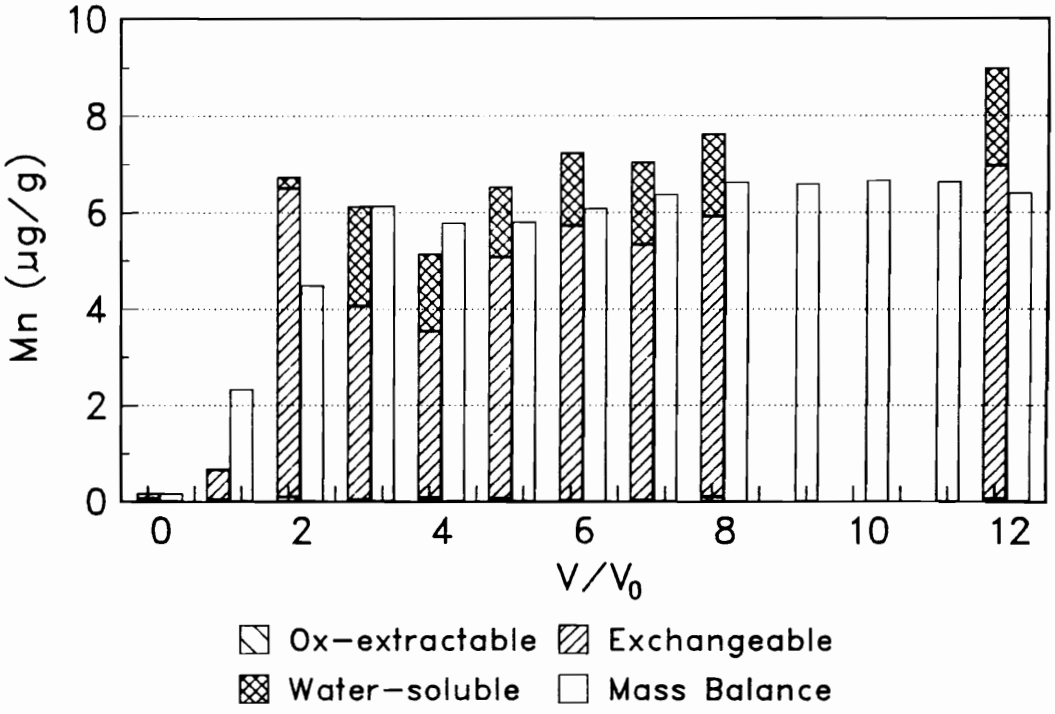

Figure 47. Mass balance and element partitioning results (0.25 - 0.75 m material): Mn.

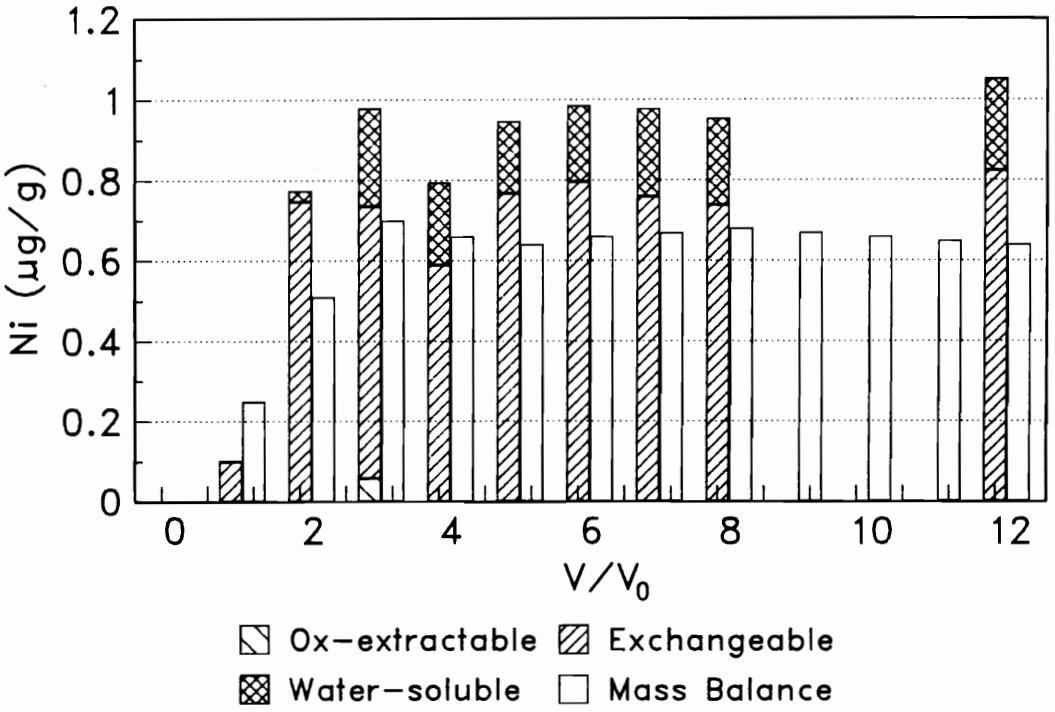

Figure 48. Mass balance and element partitioning results (0.25 - 0.75 m material): Ni.

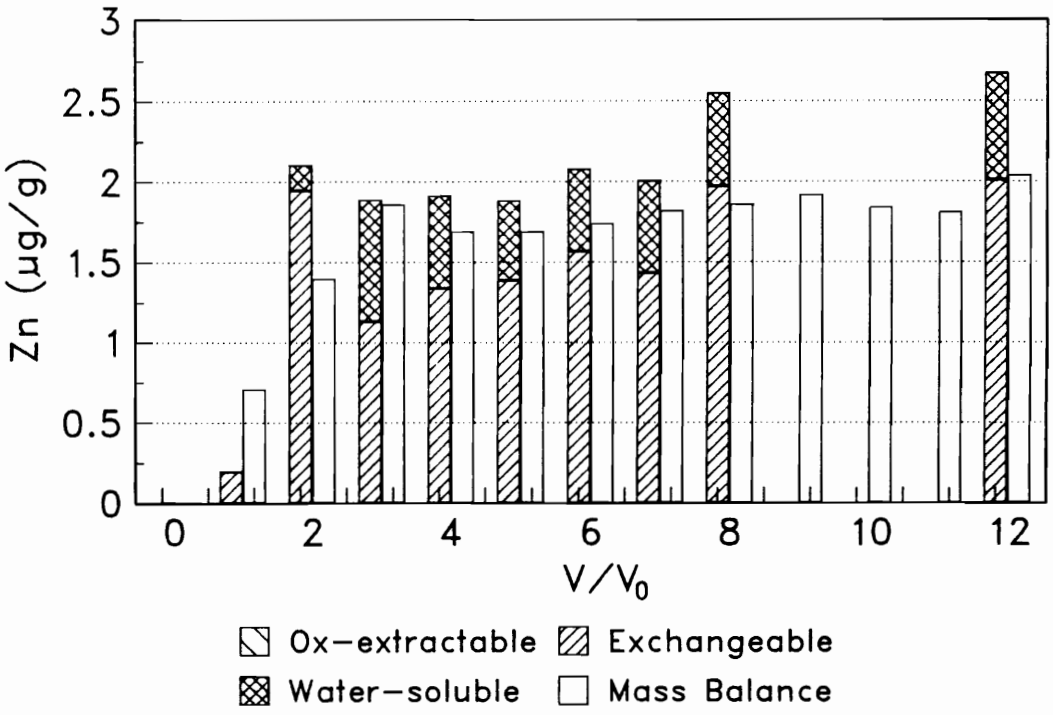

Figure 49. Mass balance and element partitioning results (0.25 - 0.75 m material): Zn.

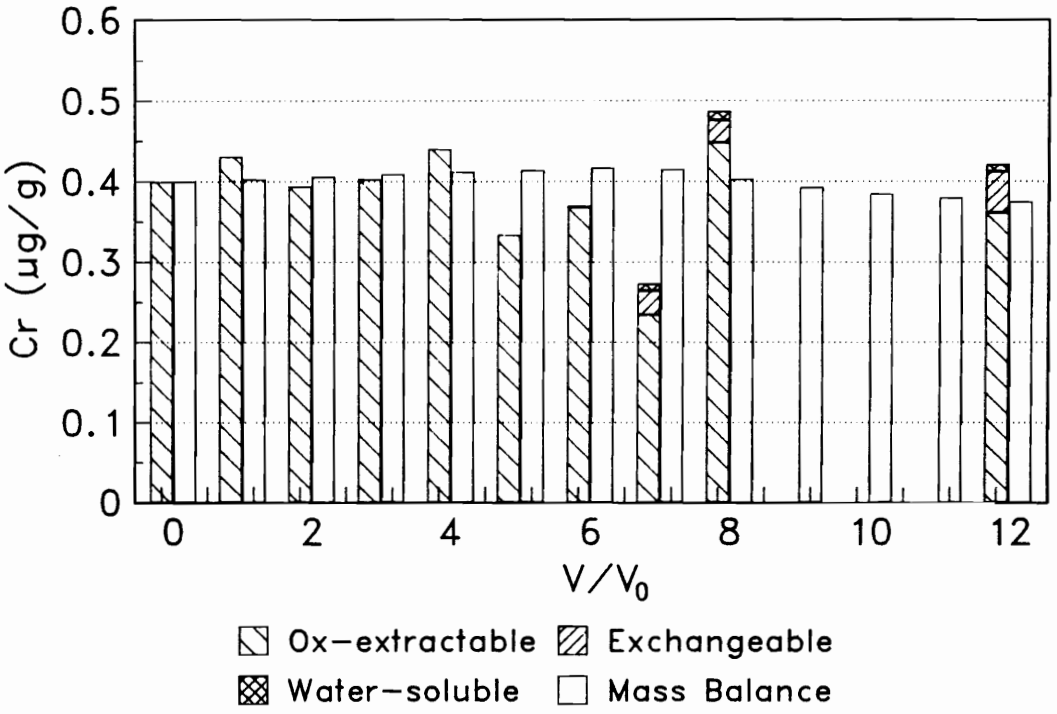

Figure 50. Mass balance and element partitioning results (0.25 - 0.75 m material): Cr.

Copper partitioning results were somewhat odd. The native soil was found to contain some exchangeable Cu, which decreased rapidly upon leaching (Figure 51). It was proposed that Cu in the coal pile runoff was coprecipitating with Fe or participating in first specific adsorption then subsequent desorption (Chapter III). A lack of recoverable Cu after 2 pore volumes (the onset of coal pile runoff in the column effluent) was noted until 6 pore volumes.

Clay Mineralogy

The potential for alterations in phyllosilicate mineralogy upon leaching with the runoff was evaluated through XRD analyses. Clay fractions from samples leached with 0, 4, 8, 12, and 60 pore volumes were x-rayed after Fe removal. Despite relatively high inputs of acidity, only subtle alterations were noted. For example, diffractograms of KCl, 25 °C-treated clays showed no discernible differences in the dominant 7.2 Å 001 and 3.6 Å 002 reflections of kaolinite (Figure 52). Some slight reduction in the broad low angle reflection between 14 and 20 Å reflection and a concomitant increase in the 10 Å reflection was noted, however (Figure 52), suggesting degradation of a weakly ordered interstratified mica-vermiculite mineral upon prolonged leaching.

Analyses of samples by DSC provided evidence for slight reduction in the area of the kaolinite endotherm at ≃480 °C, and for the 60 pore volume sample, a subtle endotherm near 300 °C, characteristic for gibbsite, and a broad albeit modest endotherm on the low temperature side of the kaolinite endotherm (Figure 53). Gibbsite is a common weathering product resulting from desilication of phyllosilicates subjected to acidic conditions. Low temperatue shoulders on the

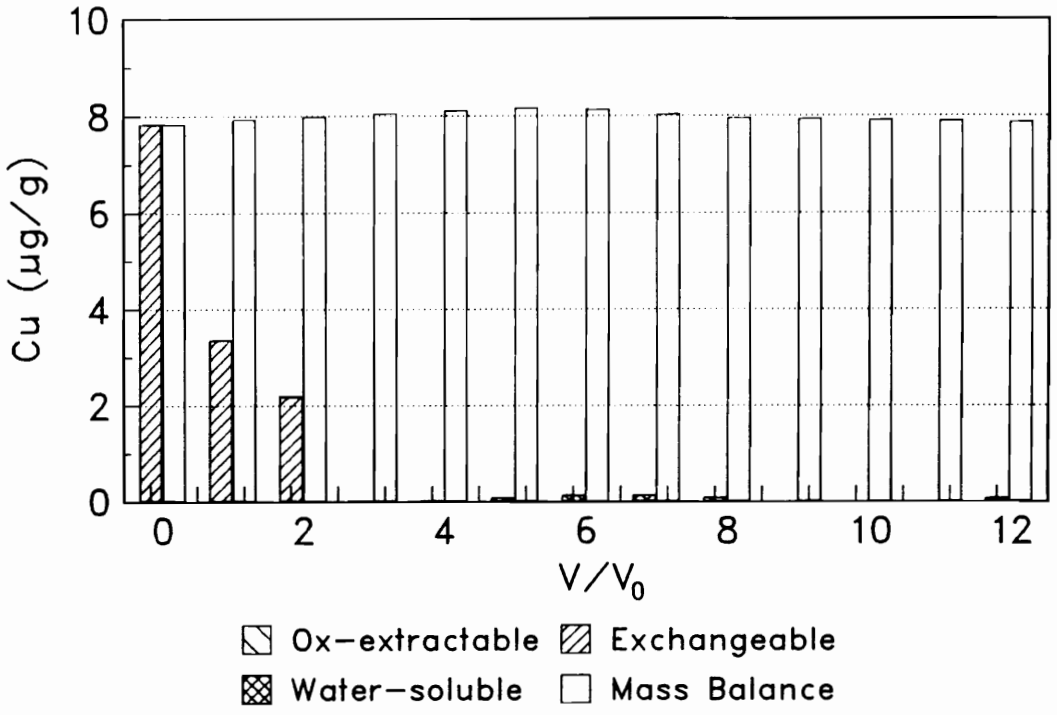

Figure 51. Mass balance and element partitioning results (0.25 - 0.75 m material): Cu.

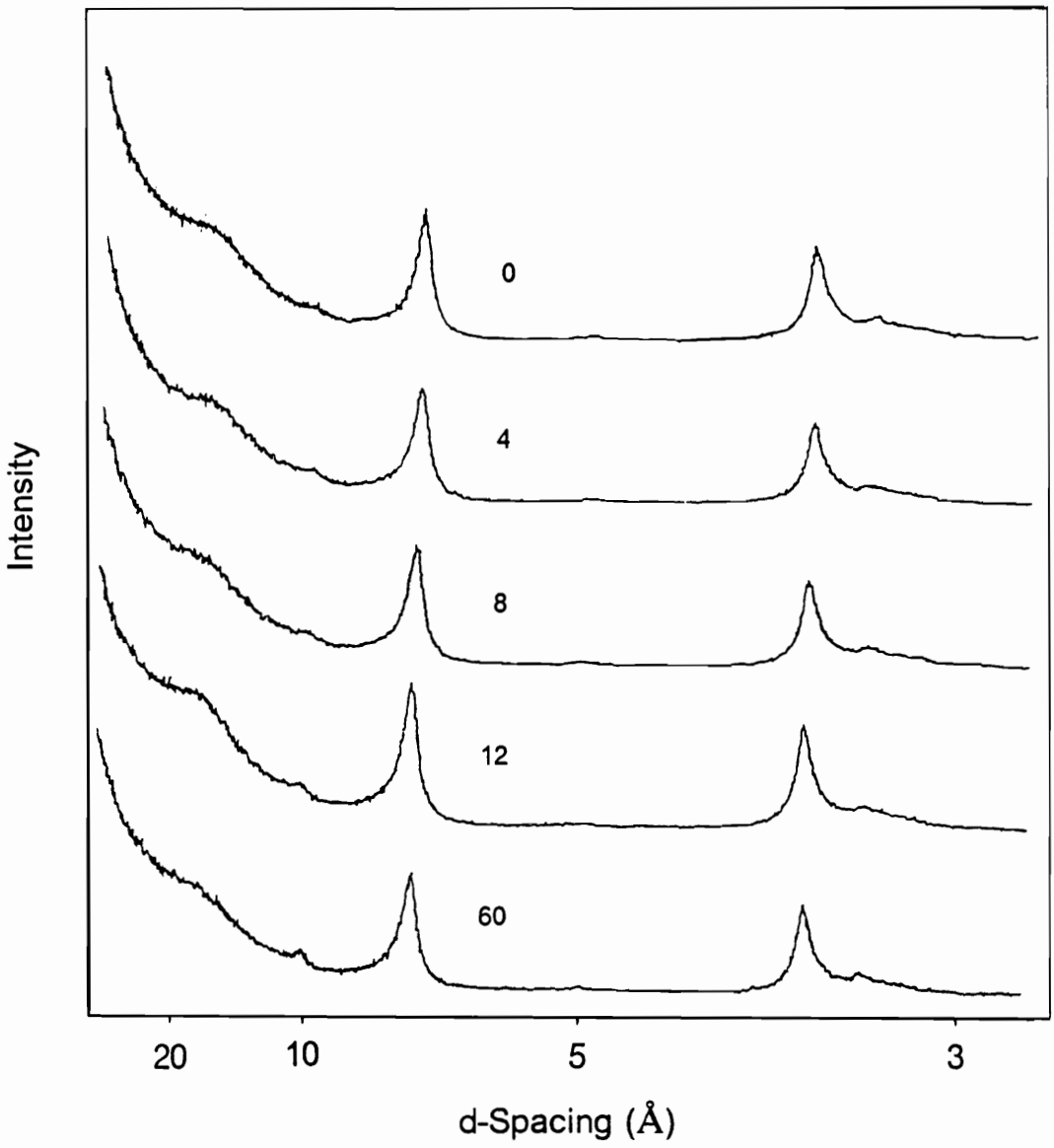

Figure 52. X-ray diffractograms of clay fraction of 0.25 - 0.75 m material after leaching with 0, 4, 8, 12, and 60 pore volumes of runoff (K-sat, 25 °C).

kaolinite endotherm are often associated with hydroxy-interlayer Al. The reduction in the skewness of the shoulder with increasing pore volumes and emergence of a better defined endotherm at 60 pore volumes suggests gradual dissolution of hydroxy-interlayer Al and the formation of a better defined interlayer phase.

The mineralogy of the oxide phases was evaluated via differential XRD (i.e., subtraction of patterns of DCB-treated samples from that of untreated samples). Evidence for goethite (4.188, 2.566, 2.502, 1.818, and 1.515 Å reflections) and hematite (1.688 and 1.476 Å reflections) was found for the samples. No changes in the diffractograms with increasing pore volumes, and a general lack of characteristic peaks, including the strong jarosite reflection at 3.03 Å suggests an absence of basic Al and Fe sulfate phases forming during the leaching process, though analytical limitations on detection of small amounts of these phases precludes firm support for or against their existence.

Infrared Analysis

Infrared analysis of the samples tended to yield very similar spectra as well (Figure 54). The well-defined peaks at 3700, 3625, 1100, 1010, and 910 cm^{-1} are all diagnostic for kaolinite (Farmer and Palmieri, 1975), and tend to dominate the spectra. The broad absorbance band centered near 3300 cm^{-1} and that near 1640 cm^{-1} correspond to water, likely retained by swelling 2:1 minerals within the samples. Characteristic jarosite and sulfate absorbances at 1175, 1110, and 1020 cm^{-1} (Omori and Kerr, 1963) are absent.

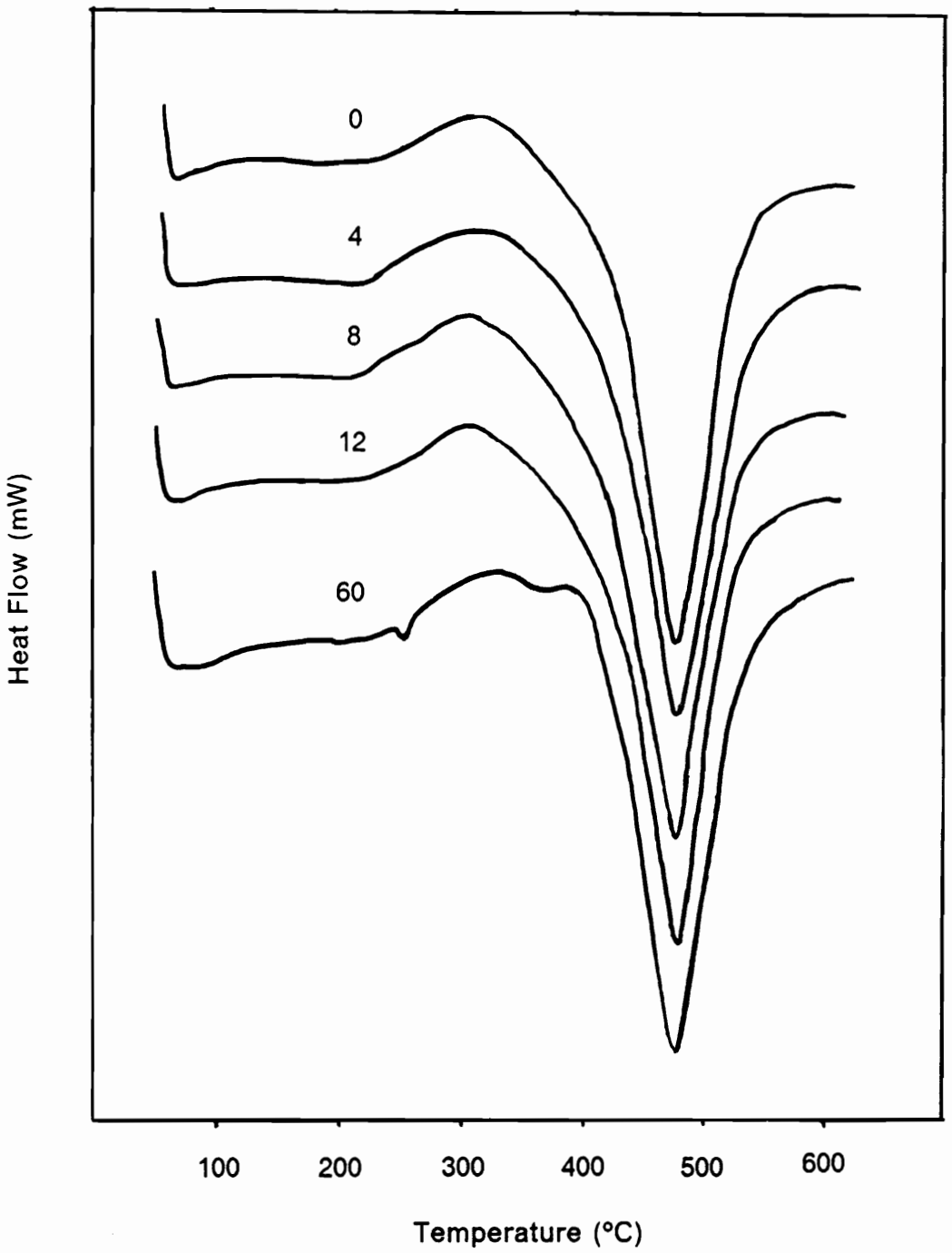

Figure 53. Thermograms of clay fraction of 0.25 - 0.75 m material after leaching with 0, 4, 8, 12, and 60 pore volumes of runoff.

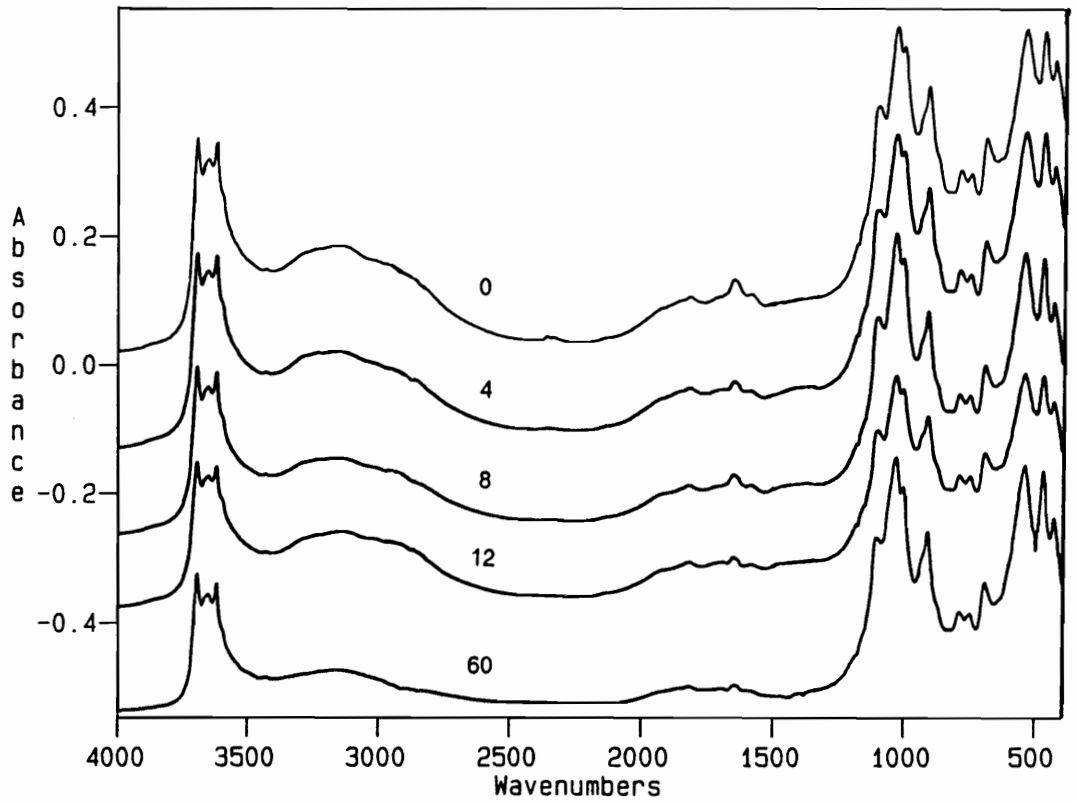

Figure 54. Infrared spectra of silt+clay fraction of 0.25 - 0.75 m material after leaching with 0, 4, 8, 12, and 60 pore volumes of runoff.

Electrophoretic Mobilities

Electrophoretic mobility of samples increased with increased leaching for any given suspension pH and increased with increasing suspension pH (Figure 55). The high mobilities even at low pH support the mineralogical data indicating appreciable constant charge mineral content (Harsh et al., 1988). The contribution of variable charge minerals (e.g., the kaolinite and oxyhydroxides) is also significant, as can be seen by the steep increase in mobility upon increasing suspension pH (Figure 55) (Williams and Williams, 1978). One does notice a somewhat flatter pH response with increasing pore volumes as well as the previously noted overall higher negative mobility (Figure 55). Additional charge was apparently generated via specific adsorption of sulfate to oxide phases (Hansmann and Anderson, 1985; Rajan, 1978) and a net increase in constant charge via dissolution of native constant charge-blocking oxidic phases (in excess of the potential blocking of sites by the noted precipitation of Fe phases within the soil columns).

Conclusions

Element partitioning results via selective dissolution procedures were generally in good agreement with mass balance calculations and corroborate inferences made about element mobility from breakthrough data. Iron was observed to accumulate within the soil column and was associated chiefly with the Ox-extractable phase. Aluminum was partitioned between the water, NH_4Cl exchangeable, and Ox

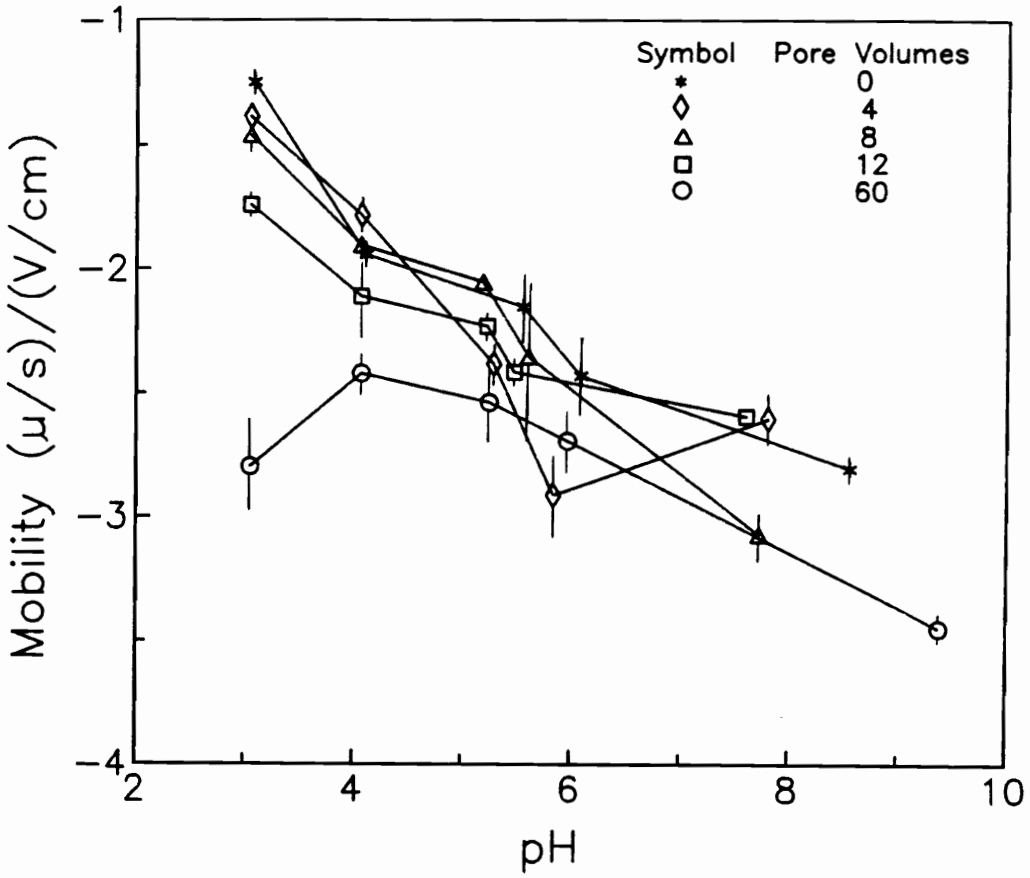

Figure 55. Electrophoretic mobility of silt+clay fraction of 0.25 - 0.75 m material after leaching with 0, 4, 8, 12, and 60 pore volumes of runoff.

extractable phases, with the water phase increasing and the Ox phase decreasing with increaing leaching. Silicon tended to follow Al to some extent, with Ox-extractable Si decreasing with increasing leaching. Calcium, Mg, Sr, Co, Zn, and Ni were associated with the exchange phase early during the leaching process, then partitioned fairly consistently between the water and exchange phases, supporting the notion that ion exchange was the dominant mechanism governing mobility for these elements. Manganese followed the other divalent metal ions with the exception that a limited quantity was found associated with the Ox-extractable phase. Copper and Cr departed significantly from the other first row transition metals in that their mobility appeared to be governed by specific adsorption/desorption reactions. Sustained leaching had little discernible effect on gross phyllosilicate mineralogy, though formation of gibbsite and limited destabiliization of interstratified mica-vermiculite was demonstrated after 60 pore volumes had been supplied to the column. Oxide mineralogy was fairly uniform, with goethite and hematite both present within the soils. Evidence for distinct basic Al or Fe sulfate phases formed during leaching was generally lacking. Electrophoretic mobility increased (become more negative) with increased leaching, due in part to specific adsorption of sulfate and consequent generation of additional negative charge within the soil, and by dissolution of native charge-blocking oxidic phases.

References

Anderson, M. A., P. M. Bertsch, and W. P. Miller. 1989. Exchange and apparent fixation of Li in selected soils and clay minerals. Soil Sci. **148:** 46-52.

Baes, C. F., Jr., and R. E. Mesmer. 1976. The hydrolysis of cations. John Wiley and Sons, New York.

Barnhisel, R.I., and A. L. Rotromel. 1974. Weathering of clay minerals by simulated acid coal spoil-bank solutions. Soil Sci. **118:** 22-27.

Davey, B. G., and R. C. Wheeler. 1980. Some aspects of the chemistry of lithium in soils. Plant Soil **57:** 49-60.

Farmer, V. C., and F. Palmieri. 1975. The characterization of soil minerals by infrared spectroscopy. In J. E. Gieseking (ed.) Soil components. Vol. 2 - Inorganic components. Springer-Verlag, New York. pp.573-670.

Filipek, L. H., D. K. Nordstrom, and W. H. Ficklin. 1987. Interaction of acid mine drainage with waters and sediments of West Squaw Creek in the West Shasta Mining District, California. Environ. Sci. Technol. **21:** 388-396.

Hansmann, D. D., and M. A. Anderson. 1985. Using electrophoresis in modeling sulfate, selenite, and phosphate adsorption onto goethite. Environ. Sci. Technol. **19:** 544-551.

Harsh, J. B., H. E. Doner, and D. W. Fuerstenau. 1988. Electrophoretic mobility of hydroxy-aluminum and sodium-hectorite in aqueous solutions. Soil Sci. Soc. Am. J. **52:** 1589-1592.

Jackson, M. L., C. H. Lim, and L. W. Zelazny. 1986. Oxides, hydroxides, and aluminosilicates. In A. Klute (ed.) Methods of soil analysis. Part 1. Agron. **9:** 545-567, Am. Soc. Agron., Madison, WI.

Lindsay, W. L. 1976. Chemical equilibria in soils. John Wiley and Sons, New York.

Nordstrom, D. K. 1982a. Aqueous pyrite oxidation and the consequent formation of secondary iron minerals. In J. A. Kittrick, D. S. Fanning, and L. R. Hossner (ed.) Acid sulfate weathering. Soil Sci. Soc. of Am. Spec. Publ. **10:** 37-56. Soil Sci. Soc. of Am., Madison, WI.

Omori, K., and P. F. Kerr. 1963. Infrared studies of saline sulfate minerals. Geol. Soc. Am. Bull. **74:** 709-734.

Rajan, S. S. S. 1978. Sulfate adsorbed on hydrous alumina, ligands displaced, and changes in surface charge. Soil Sci. Soc. Am. J. **42:** 39-44.

Singh, B. R. 1984. Sulfate sorption by acid forest soils: 3. Desorption of sulfate from adsorbed surfaces as a function of time, desorbing ion, pH, and amount of adsorption. Soil Sci. **138:** 346-353.

Williams, D. J. A., and K. P. Williams. 1978. Electrophoresis and zeta potential of kaolinite. J. Coll. Interface Sci. **65:** 79-87.

Chapter V

Summary and Conclusions

Runoff from a coal stockpile on the Department of Energy's Savannah River Site has contaminated an underlying shallow water table aquifer. This dissertation is an attempt to understand the geochemical processes occurring as this acidic, metal-rich plume migrates through the subsurface. Toward that end, samples of uncontaminated subsoil and aquifer materials were leached with runoff under steady saturated flow, effluent collected, and element flux determined. Observed component transport was then related to soil chemical and mineralogical properties and reactions governing mobility proposed. Mass balance calculations, selective dissolution techniques, and mineralogical and surface chemical analyses were used to better identify the important geochemical processes affecting multicomponent transport.

The naturally acidic Coastal Plain subsoil and aquifer materials provided little attenuation, with peak element concentrations often moving at 0.25 to 1 times the rate of water flow. The appearance of elements in the effluent was related to sulfate mobility.

Ion exchange controlled peak Be, Ca, Co, Mg, Mn, Ni, Sr, and Zn effluent concentrations, whereas precipitation and coprecipitation was important to Fe and Cr and Cu mobilities, respectively. Solubility relations were of limited utility in describing element fluxes, however. Prolonged leaching also resulted in a net export of Si and Al from the columns. Observation of a gibbsite endotherm from DSC analysis of clay from soil leached with 60 pore volumes provides additional independent evidence for a desilication reaction. X-ray diffraction also indicated destabilization of interstratified mica-vermiculite and increased 10 Å material upon prolonged leaching with the acidic runoff. Reduction in Darcy velocity form 1.3 to 0.2 cm/h had little influence on relative transport of components affected by ion exchange, though did influence components regulated by precipitation reactions.

These observations have a number of implications for soil and groundwater systems subject to infiltrating runoff from coal stockpiles and more generally from acid mine drainage. First of all, naturally acidic, non-carbonaceous soils offer little resistance to subsurface migration of acidic, metal-rich runoff. As a result, coal stockpiles situated on such materials pose a serious threat to underlying groundwater systems. Industries located on the Atlantic Coastal Plain, which is generally naturally acidic, coarse textured and therefore capable of relatively rapidly conducting water, and with often relatively shallow aquifer systems, in particular are prone to degrading local water quality. The occurrence of both high industrial activity and urban populations over much of this physiographic province implies potentially severe local environmental problems.

Demonstrated chromatographic and precipitation-dissolution waves attendant with infiltration and migration of runoff within subsurface materials further exacerbates

potential water quality problems. That is, mobilization of native soil components via exchange, desorption, and dissolution, and chromatographic effects, all contribute to the development and movement of waves of components in concentrations greatly exceeding initial source concentrations. Discharge of effluent meeting appropriate water quality criteria may thus produce downgradient concentrations greatly exceeding standards and source concentrations. This phenomenon poses difficult legal ramifications and also emphasizes the need for continued research evaluating multicomponent transport processes.

Vita

of

Michael Alan Anderson

Michael Alan Anderson was born September 18, 1960 (two months early and four and one-half minutes before Mark David Anderson, with whom he bears a strong resemblance) in Aurora, Illinois. He graduated from Illinois Benedictine College in Lisle, Illinois in May of 1982 with a B.S. in Biology. He then ventured to the balmy clime of northern Minnesota, where, in June of 1984, he was conferred a Master of Arts degree in Environmental Studies (based largely on his insistence with regular augering through 1+ m of ice) in June of 1984. He then happily scampered due west to begin a temporary appointment as a Hydrologist with the Bureau of Land Management in Coeur d'Alene, Idaho. Upon completion of his duties with the BLM, he departed for Aiken, SC to accept a position as a Research Technician in Environmental Chemistry at the University of Georgia's Savannah River Ecology Laboratory under Dr. Paul M. Bertsch. Somehow he ended up here (Virginia Tech).